2018

Heteromerization of G Protein-Coupled Receptors in Human Vascular Smooth Muscle Cells: Identification of Hetero-Oligomeric Receptor Complexes between α1-Adrenergic Receptors, Arginine Vasopressin Recptor 1a, Chemokine (c-X-C Motif) Receptor Type 4, and Atypical Chemokine Receptor 3.

Lauren J. Albee
Loyola University Chicago, lalbee@luc.edu

LOYOLA UNIVERSITY CHICAGO

HETEROMERIZATION OF G PROTEIN-COUPLED RECEPTORS IN HUMAN VASCULAR SMOOTH MUSCLE CELLS: IDENTIFICATION OF HETERO-OLIGOMERIC RECEPTOR COMPLEXES BETWEEN α_1-ADRENERGIC RECEPTORS, ARGININE VASOPRESSIN RECPTOR 1A, CHEMOKINE (C-X-C MOTIF) RECEPTOR TYPE 4, AND ATYPICAL CHEMOKINE RECEPTOR 3.

A DISSERTATION SUBMITTED TO
THE FACULTY OF THE GRADUATE SCHOOL
IN CANDIDACY FOR THE DEGREE OF
DOCTOR OF PHILOSOPHY

INTEGRATIVE CELL BIOLOGY

BY
LAUREN JEAN ALBEE
CHICAGO, IL
MAY 2018

ACKNOWLEDGEMENTS

I would like to first thank my PhD mentor, Dr. Matthias Majetschak, for providing me with a wonderful opportunity to study vascular physiology. Working in his laboratory, I have expanded my knowledge base and gained confidence in my abilities as a scientist; for that I am extremely grateful. The Majetschak laboratory has become a home away from home and that is due in large part to the amazing individuals I have had the privilege of working with. Heather LaPorte started out as my lab manager and quickly became one of my closest friends.

The members of the Burn and Shock Trauma Institute, both past and present, have been crucial in helping me develop as a scientist and a person. Walking the halls, there was always a friendly face or someone to share frustrations with. All of you made coming to work a pleasant experience.

I would like to thank the Graduate School community for all the support. Ann Kennedy was essential to helping me stay sane and be organized. Leanne Cribbs does an amazing job mentoring all of the graduate students from orientation until the day we graduate.

Finally, I would like to thank my committee members for their guidance over the past few years: Drs. Mashkoor Choudhry, John Callaci, Gregory Mignery, and Kuzahi Muthumalaiappan. To have met and learned so much from such a diverse group of individuals has truly been a privilege.

TABLE OF CONTENTS

LIST OF FIGURES

LIST OF TABLES

LIST OF ABBREVIATIONS

α-AR	Alpha Adrenergic Receptor
ACKR3	Atypical Chemokine Receptor Type 3
AT	Angiotensin Receptor
ATP	Adenosine Triphosphate
aVP	Arginine Vasopressin
AVPR	Arginine Vasopressin Receptor
AxR	Adenosine Receptor
B2	Bradykinin Receptor
BRET	Bioluminescence Resonance Energy Transfer
cAMP	Cyclic Adenosine Monophosphate
CCR	C-C Chemokine Receptor
CXCL	C-X-C Chemokine Ligand
CXCR	C-X-C Chemokine Receptor
DAG	Diacylglycerol
DxR	Dopamine Receptor
FRET	Fluorescence Resonance Energy Transfer
GDP	Guanine Diphosphate
GPCR	G Protein-Coupled Receptor

GRK	G Protein-Coupled Receptor Kinase
GTP	Guanine Triphosphate
HA	Hemagglutinin
hVSMC	human Vascular Smooth Muscle Cells
IP_3	Inositol Trisphosphate
MAP	Mitogen Activated Protein
MTx	Melatonin Receptor
OR	Opioid Receptor
PE	Phenylephrine
PLA	Proximity Ligation Assays

CHAPTER 1

INTRODUCTION AND LITERATURE REVIEW

Cardiovascular Diseases

Cardiovascular diseases are the number one global killer, claiming more lives than all types of cancer combined [1]. Cardiovascular diseases pose a significant socioeconomic threat to the developed world. An estimated $316 billion is spent annually in the US for treatment and lost productivity related to cardiovascular diseases. Currently, global spending for cardiovascular diseases is over $870 billion and projected to exceed $1045 billion by 2030 [1].

Adequate control of vascular function is crucial for normal blood pressure regulation. Many cardiovascular diseases affect vascular reactivity, leading to abnormally high or low blood pressure [2]. One in three Americans are currently living with hypertension and less than half of these individuals are managing their hypertension [1,2]. Hypertension is a key risk factor for development of a multitude of other pathological conditions [1,2]. Conversely, severe hypotension and shock affect the critically ill. The inability to maintain sufficient systemic vascular resistance and blood pressure frequently occurs in critically ill patients and is associated with high mortality rates due to cardiovascular collapse [3]. Vasodilatory shock and vascular refractoriness account for over 200,000 deaths annually in the USA [3]. The mechanisms underlying impaired vascular reactivity

are poorly understood. Thus, a better understanding of the molecular mechanisms that govern vascular reactivity are key to the development of improved treatments options. Over 45% of all drugs on the market target G protein-coupled receptors (GPCRs) [4-8]. An estimated 200 cardiovascular GPCRs exist within the human receptorome, and medications targeting the adrenergic, vasopressin, and angiotensin GPCRs account for the majority of all prescriptions for cardiovascular disease management [5,9]. GPCRs have been extensively studied, yet we are only just beginning to uncover the molecular mechanisms governing their behavior.

G Protein-Coupled Receptors

GPCRs are a highly conserved family of receptors representing the largest and most diverse family of receptors in eukaryotes [10,11]. These cell surface receptors are composed of an extracellular N-terminus, seven transmembrane spanning alpha helices, and an intracellular C-terminus (Fig. 1) [7,10-14]. Following completion of the

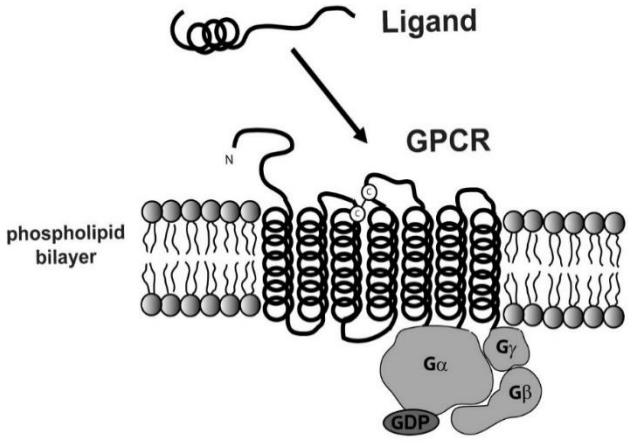

Figure 1. Schematic drawing of a G protein-coupled receptor within the plasma membrane. The N-terminus is extracellular, followed by seven transmembrane α-helices, with an intracellular C-terminus. Heterotrimeric G proteins couple to the third intracellular loop and C-terminus. Ligands interact with the extracellular loops [16].

human genome project, over 800 GPCR sequences were identified and many classification systems arose [15,16].

The most widespread classification system for GPCRs is the class or clan system, based on sequence homology [16]. This A-F system is designed to cover all GPCRs, those from both vertebrates and non-vertebrates [15]. One significant challenge in presenting a unifying classification system is the disparity in sequences between mammalian and invertebrate receptors [15]. With the rapid accumulation of sequencing data, a database has been developed for GPCRs [15]. Here all GPCRs are divided into six groups, taking into account phylogenetic origin and functional role: rhodopsin-like, equivalent to class A receptors, further subdivided into α,β,γ,δ groups; secretin-like, equivalent to class B receptors; metabotropic glutamate, equivalent to class C; fungal pheromone, equivalent to class D; cyclic adenosine monophosphate (cAMP), similar to class E; and frizzled-like, akin to class F [15,16]. Class A or rhodopsin-like receptors comprise those most studied, therefore these are principal drug targets [6,8,15].

Heterotrimeric G Proteins.

GPCRs couple to heterotrimeric G proteins (Gα, Gβ/Gγ subunits) to elicit a response by transmitting extracellular signals into intracellular signaling cascades to target downstream effectors [6,7,10-13,17-19]. Upon activation by a ligand, the GPCR undergoes a conformational switch, thus activating the G proteins by allowing for the exchange of guanine diphosphate (GDP) to guanine triphosphate (GTP) that is associated with the Gα subunit [7,10,11,13]. This guanine nucleotide exchange factor activity induces dissociation of the heterotrimeric complex from the receptor [13]. Furthermore, the

subunits dissociate and activate downstream targets, thus initiating a unique signaling cascade [13]. Following the signal propagation, the GTP associated with the Gα subunit becomes hydrolyzed to GDP, allowing for re-association with the Gβ/Gγ dimer and the unoccupied receptor, thereby reverting back to an inactivated state (Fig. 2) [12].

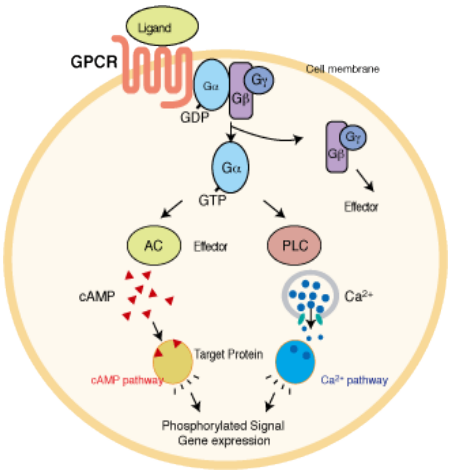

Figure 2. Diagrammatic representation of activation of GPCRs. Upon ligand binding, a conformational change allows the exchange of GDP for GTP, thus allowing G proteins subunits to dissociate, trigger effectors, thus initiating signaling cascades to allow for transmission of extracellular signals intracellularly [16].

Gα proteins have been classified into four main families, $G\alpha_i/G\alpha_o$, $G\alpha_q$, $G\alpha_s$, and $G\alpha_{12}$, based on sequence similarity of the Gα subunit [12,13]. Each of these families of Gα proteins initiates differing downstream signaling pathways. Additionally, some GPCRs have been known to couple to two or more distinct Gα proteins, thereby allowing for fine tuning of the effector response [20]. Primary Gα effectors of the $G\alpha_i/G\alpha_o$ family lead to inhibition of adenylyl cyclase [21-24]. Additionally, the Gβ/Gγ subunit opens K^+ channels and can lead to modulation of Ca^{2+} channels [25]. Examples of these receptors include chemokine receptors, α_2-adrenergic receptor (AR), muscarinic receptors, serotonin receptors, and dopamine receptors amongst others [21-24].

Signaling cascades initiated by the activation of GPCRs coupled to $G\alpha_s$ activate adenylyl cyclase, thus catalyzing the conversion of adenosine triphosphate (ATP) to cAMP. cAMP then acts as a second messenger initiating a plethora of intracellular events. Members of this family include β-AR, serotonin receptors, dopamine receptors, histamine receptors [26-30]. Conversely, activation of $G\alpha_i$ proteins can lead to inhibition of adenylyl cyclase activity [31-33].

Furthermore, $G\alpha_q$ activates phospholipase C. Signaling via the phospholipase C cascade is one mechanism to induce smooth muscle contraction [33,34]. These $G\alpha_q$ receptors include arginine vasopressin receptors (AVPR), α_1-AR, members of the muscarinic and serotonin receptor family, and histamine receptors among others [33,35-37]. The GTP-bound $G\alpha_q$ subunit activates phospholipase C, which catalyzes the cleavage of phosphatidylinositol 4,5-bisphosphate into inositol 1,4,5-trisphosphate (IP_3) and diacyl glycerol (DAG) [33,35-37]. Both IP_3 and DAG act as second messengers ultimately leading to Ca^{2+} release and protein kinase C activation, respectively (Fig. 3) [33-38].

Finally, free Gβ/Gγ subunits can act as signaling molecules independent of Gα [25]. Gβ/Gγ from histamine receptors can activate the phospholipase A_2 pathway. Additionally, Gβ/Gγ have been determined to enhance the activity of Kv7 channels [25].

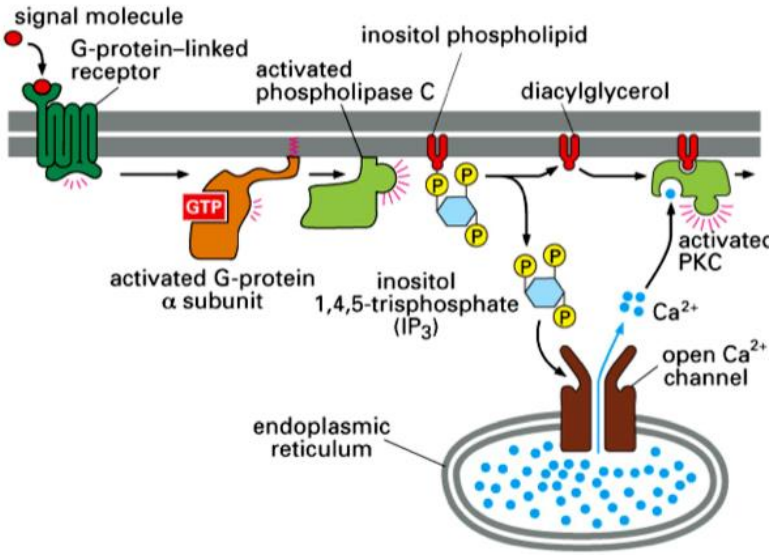

Figure 3. Inositol trisphosphate production. Upon PE or aVP binding, α_1-AR or AVPR1A respectively, initiate a downstream signaling cascade leading to production of inositol trisphosphate (IP_3) and ultimately intracellular Ca^{2+} release via the activation of phospholipase C [149]

β-arrestin.

GPCRs can transmit extracellular signals not only through activation of the heterotrimeric G proteins, but also through β-arrestin pathways. Arrestins are a small family of proteins crucial for regulating signal transduction of GPCRs. Initially arrestins were solely thought to be the mechanism to terminate signaling of GPCRs via mediating endocytosis of the receptor [39-42]. Upon ligand binding the heterotrimeric G proteins initiate a signaling cascade, often leading to activation of GPCR kinases (GRKs). GRKs in turn, phosphorylate the GPCR, which acts as a docking site for β-arrestins (Fig. 4) [40,42-45]. β-arrestins can then either act as a scaffold for clatherin-mediated endocytosis or they can act as a scaffold for alternate signaling pathways, such as the mitogen activated protein (MAP) kinase [39,40,42,45,46]. Furthermore, β-arrestin binding to the GPCR

occludes the binding site for G proteins, thereby desensitizing the receptor [41,44,47-49]. Additionally, β-arrestins lead to desensitization by interfacing with second messenger degrading enzymes [41,44,47-49]. Signaling via the β-arrestin complex has been attributed to apoptosis, metastasis, chemotaxis, and protein translation, all occurring via activation of the GPCR, which in turn initiates MAP kinase pathways [41-43,45,47,48,50,51].

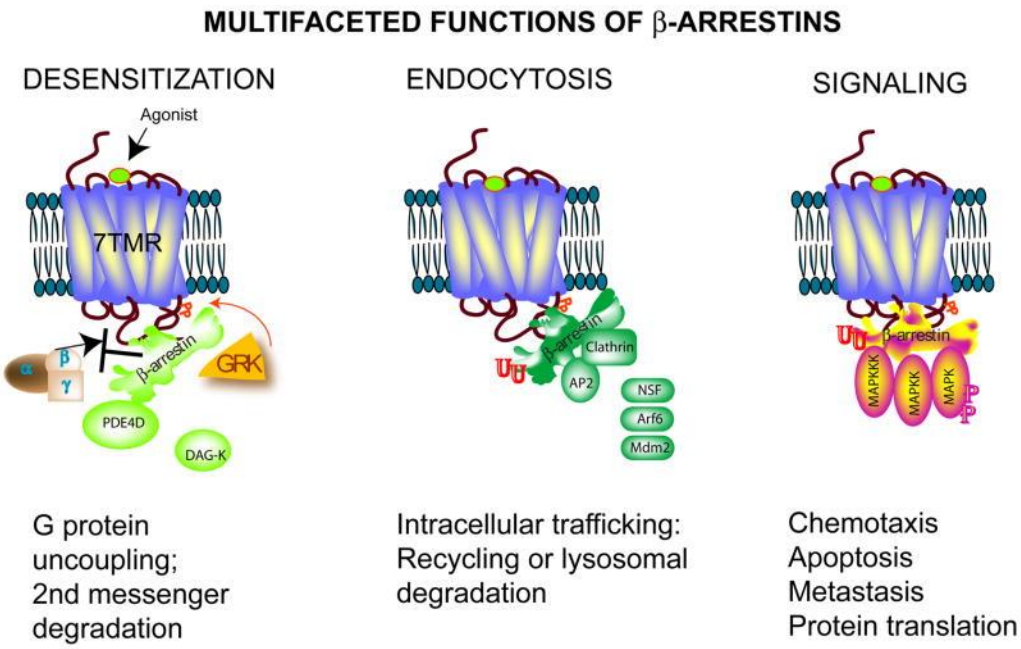

Figure 4. Roles of β-arrestin signaling. β-arrestins function to terminate G protein-mediated signaling via uncoupling the heterotrimeric G proteins from the receptor or to induce endocytosis of the GPCR. Additionally, GPCRs can signal via G protein independent mechanisms [44].

GPCR Ligands.

Due to their ubiquitous nature and seemingly limitless therapeutic potential, GPCR-targeted drug-based discovery became a lucrative area of research. Natural ligands for GPCRs are physically and chemically diverse. These can include, photons, odorants, ions, both peptide and non-peptide hormones, chemokines, neurotransmitters,

metabolic intermediaries among others [52]. Classically, synthetic GPCR ligands were developed based on their ability to act as an agonist, to simply enhance the natural response of the receptor, or to act as an antagonist, inhibiting deleterious functions [9,18,53,54]. As more studies uncovered the complexity of GPCRs, drugging the GPCR-ome evolved from development and identification of simple agonists and antagonists to creation of biased ligands [8,9,55]. Classic models of receptor pharmacology assume that ligands elicit effects through a single signaling cascade [18,46,56]. Thus, one can utilize a single functional assay to identify the nature of the ligand: full agonist, neutral antagonist, partial agonist, or inverse agonist [4,8,23,57]. Multiple signaling pathways from a single receptor indicate that a ligand may act as a full agonist for one pathway and as a partial agonist for a differing pathway. This phenomenon was coined biased agonism [9,55,58]. Some of the earliest evidence for biased agonism was reported for α_2-AR agonists leading to varied efficacies for $G\alpha_s$ and $G\alpha_i$ effectors [9]. The potential for refined pharmacological approaches exists by exploiting one desired signaling pathway and inhibiting non-desired effects.

Biased ligands can act orthosterically, interacting at the same site as the endogenous agonist, or allosterically, binding elsewhere on the receptor to modulate function (Fig. 5) [53,59,60]. Many of the biased ligands described to date act orthosterically [9], however anything that would affect the conformation of the receptor could impact the ability of a particular ligand to elicit a response. Classically, description of the functional selectivity of a particular ligand assumes that the receptors are functioning as independent units or protomers. Yet a multitude of evidence within the past two decades indicates that

GPCRs do not exist and function as individual protomers, rather many function in large dynamic, oligomeric receptor complexes [13,36,61-64]. This heteromerization of GPCRs has profound effects on the development of biased ligands and our understanding of GPCR pharmacology.

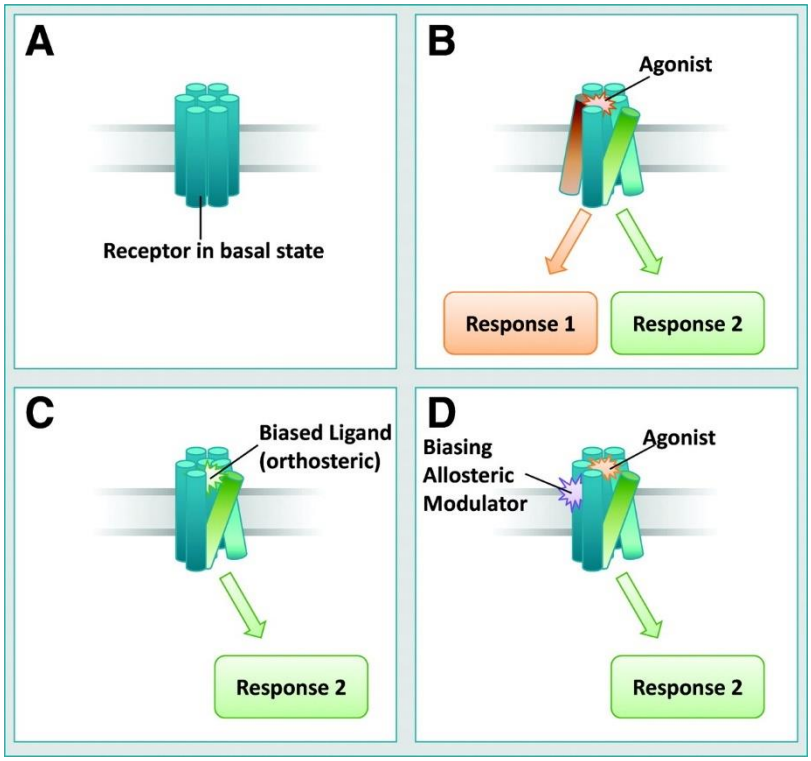

Figure 5. Mechanism of biased ligands. Schematic representation of biased ligands and how binding of an agonist differs from that of a biased agonist binding in the orthosteric site and how allosteric modulators affect agonist function [57].

GPCR Heteromerization

Receptor cross-talk was previously believed to be two or more independent GPCRs communicating via convergence of downstream effector molecules [18,65-68]. However, since the discovery of heteromerization an alternative mechanism may explain receptor cross-talk. Cross-talk between receptors could be convergence of signaling cascades or

it could be due to direct physical interaction of two or more GPCRs. Consonant with this line of reasoning, several studies determined the repercussions of GPCR heteromerization [18,61,62,69]. Five main roles of GPCR heteromerization are described below (Fig. 6).

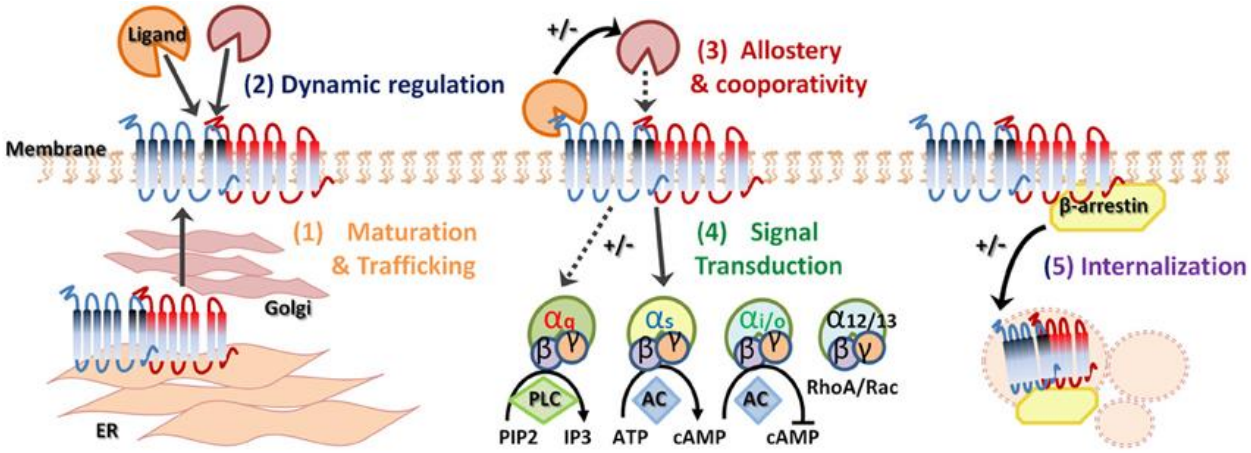

Figure 6. Roles of GPCR heteromerization. GPCR heteromerization has been implicated in many processes. Some receptors require dimer formation for proper maturation and trafficking to the plasma membrane. Heteromerization of GPCRs affects receptor function through dynamic regulation, cooperativity, allosteric modulation, convergence of signaling pathways, and through internalization [161].

Maturation and Trafficking.

GPCR complex formation has been attributed to appropriate folding, maturation, and trafficking to the plasma membrane. Exit of GPCRs from the endoplasmic reticulum is a key step in the oligomerization process. Incorrectly folded proteins are retained and degraded, however, if a retention signal is masked by interactions with a receptor partner, then a misfolded receptor may be trafficked to cell surface [69]. The chemokine (C-X-C motif) receptor (CXCR) type 1:CXCR2 heterodimer formation is required for

appropriate targeting to the plasma membrane [70]. Additionally, several other studies have demonstrated that GPCRs dimerize within the endoplasmic reticulum [71-73].

Dynamic Regulation.

The occupied vs unoccupied conformational state of the receptor may play an important role in oligomerization. The binding of agonist to one receptor may facilitate or inhibit interactions at differing transmembrane interfaces [36,62,74]. A multitude of studies suggest that dynamic regulation is an intrinsic property of a given heteromer, dependent upon the macro-molecular environment. Some studies indicate that ligand binding enhances dimer formation, whilst others hamper this process [71,73,75-77].

Allostery and Cooperativity.

Once receptors reach the plasma membrane and interact with an available receptor partner, the potential for varied pharmacological profiles drastically increases. Both negative, C-C chemokine receptor (CCR) 2:CCR5 [78], and positive, β_1-AR:β_2-AR [79], cooperative binding have been described. When the δ and κ opioid receptors (OR) were co-expressed, a low affinity for either selective agonist was observed, However, a significant increase in affinity was observed with a combination of both ligands, indicating positive cooperativity [64]. GPCR heteromerization has profound impact on the bias of ligands [9,59,60,74]. Heteromerization between seemingly unrelated receptors would yield an unprecedented level of diversity in pharmacological potential. GPCR oligomerization could allow for new opportunities for the generation of selective ligands that would target the heteromer and not the individual protomer. Evaluating all the

possible combinations would be a daunting task, thus the need to detect endogenous, functionally relevant heteromers is imminent.

Signal Transduction.

Many GPCRs have the capacity to signal through both G-protein dependent and β-arrestin pathways [13,36,45,51]. Co-expression of receptors often is accompanied by changes in the biochemical fingerprint, which is likely due to receptor heteromerization [18,22,26,27,53,55,56,64-67,69,78,80,81]. Heteromerization can allow for potentiation of signaling as our laboratory observed with CXCR4:α_1-AR heteromers [82-84]. Similar findings were demonstrated with the δOR:κOR [64], CCR2:CCR5 [78], and the angiotensin receptor (AT1):bradykinin receptor (B2) [85]. Conversely, heteromerization can also lead to ablation of signaling as is the case with the adenosine (A1) and dopamine (D1) receptors [22,26,27]. Furthermore, changes in the binding of Gα protein subfamilies has also been reported [20,31,61,86]. Loss of $G\alpha_i$ coupling was confirmed when the μOR and δOR were co-expressed [31]. Although all the aforementioned heteromers were confirmed via co-immunoprecipitation, proximity, or resonance energy transfer (RET)-based approaches, cross-talk due to downstream convergence of effectors cannot be excluded.

Internalization.

Multiple lines of evidence suggest that heteromerization could affect agonist-induced receptor endocytosis [27,77,87,88]. Stimulation of one receptor may be sufficient to cause internalization of both receptors. Examples include α_{1a}-AR:α_{1b}-AR [87] and the A2A:D2 [27]. Conversely, heteromerization may also help to stabilize receptors. Activation of the κOR

antagonized endocytosis of both the δOR [64] and β_2-AR [88]. Receptor co-internalization may also occur through convergence of β-arrestin signaling cascades [89,90].

Methods to Detect Heteromers.

The majority of studies investigating receptor heteromerization observed co-expressed receptors. Determination of protein-protein interactions in native cells has often been achieved through co-immunoprecipitation experiments [91]. Exploitation of fluorescently tagged fusion proteins for use in fluorescence RET (FRET) or bioluminescence RET (BRET) -based approaches is invaluable in expression-based systems, however RET-based approaches have limited applications with endogenously expressed proteins [91]. The advent of proximity ligation assays (PLA) has enabled the visualization of protein-protein interactions at single molecule resolution [92]. PLA involves staining cells or tissues with primary antibodies, then probing with species specific secondary antibodies conjugated to a short oligonucleotide sequence to create a DNA template. Rolling circle amplification then allows fluorescent probes to hybridize to the DNA, thus one can view a single protein or protein-protein interaction as an individual “spot” under a fluorescent microscope. Signal number, not the intensity of the signals, are quantified and presented as PLA signals per cell.

Validation of Heteromers in Native Tissues.

It has been suggested that three criteria must be met in order to accept that a heteromeric receptor complex exists in native tissues: 1. receptor partners should co-localize and physically interact; 2. heteromers should exhibit properties distinct from

individual protomers; and 3. heteromer disruption should lead to loss of heteromer specific properties [62]. Although a multitude of receptor heteromers have been suggested based on studies in expression systems, only four of such heteromeric receptor complexes (δOR:μOR [31], A2a:D2 [27], melatonin 1 receptor (MT1):MT2 [93], $\alpha_{1A/B}$-AR:CXCR4 [84]) have been identified and validated in native tissues [62].

CXCR4

CXCR4 is a GPCR ubiquitously expressed throughout the body [80,94-96]. CXCR4 is essential for normal cardiovascular development, plays a role in neuronal guidance, and it has widespread roles in the immune system [65,80,81,97-100]. CXCR4 couples to the pertussis sensitive $G\alpha_i$ family. Upon activation by its cognate ligand, C-X-C motif ligand (CXCL) 12 (also referred to as stromal cell- derived factor (SDF)1α), CXCR4 couples to GTP bound-$G\alpha_i$ which inhibits adenylyl cyclase activity, while the Gβ/Gγ subunits activate phospholipase Cβ allowing intracellular Ca^{2+} flux [95,101]. CXCL12 is a constitutively expressed human chemokine, that also binds to and activates atypical chemokine receptor (ACKR) 3 [97,102,103]. Our laboratory discovered that extracellular ubiquitin also activates CXCR4, but not ACKR3, making it the only selective CXCR4 agonist [94,95,101,104]. CXCR4 can be inhibited by AMD3100, also referred to as Plerixafor [105,106]. AMD3100 not only inhibits CXCR4, but also enhances binding of CXCL12 to ACKR3 [105,106]. AMD3100 also acts as an ACKR3 agonist [105,106].

Inhibition of CXCR4 has proven effective for decreasing HIV infection to $CD4^+$ T-cells, as well as diminishing the invasion of metastatic cells in a variety of cancers [107,108]. However, activation of CXCR4 can also have beneficial effects. Administration of

CXCL12 has been shown to have positive outcomes for autoimmune diseases, sepsis, and stroke [109-113]. Additionally, our laboratory documented that treatment with extracellular ubiquitin stabilized hemodynamics, decreased resuscitation fluid requirements, and protected organ integrity in multiple models of shock [94,104,114]. This apparent dichotomy in CXCR4 functions may be due to the influence of other receptors in heteromeric complexes.

Recently, the crystal structure of CXCR4 was resolved and CXCR4 was shown to exist as a homodimer [108,115,116]. CXCR4 has also been implicated in other heteromeric complexes. Heteromerization with β_2-AR in cardiomyocytes has been extensively studied [20,105,117,118]. The CXCR4:ACKR3 heteromer demonstrates constitutive recruitment of β-arrestin, thus enhancing cell migration [119]. CXCR4 has also been shown to interact with other chemokine receptors, CXCR3 [120], CCR2, and CCR5 [24,121]. The CXCR4:δOR heteromer displays a unique signaling pattern. When agonists for both of these receptors are administered concurrently, the combination of agonists inactivates the signaling by the heteromeric complex [122]. These studies, although useful, do not fulfill all the criteria to validate heteromers in native tissues [62], thus more work is required to understand the role of these heteromers in the regulation of CXCR4 function.

However, CXCR4 does form validated heteromers with $\alpha_{1A/B}$-AR in human vascular smooth muscle cells (hVSMC) [82-84]. CXCR4 is essential for vascular responsiveness and our laboratory demonstrated that activation of CXCR4 potentiates α_1-AR-mediated

responses [94,104,114]. As previous studies suggest, these receptors may act in concert as part of a larger multimeric complex to regulate vascular function [82,83,114,123].

ACKR3

ACKR3, also referred to as CXCR7 or RDC-1 was initially categorized as an orphan GPCR [124]. Orphan receptors are those receptors whose endogenous ligand is unknown [57]. Upon identifying that ACKR3 binds to CXCL11 and CXCL12 [119,123], it was re-classified as a scavenger receptor for chemokine ligands [97,102,124]. Scavenger receptors are those that sequester ligand without leading to canonical signaling pathways. ACKR3 shares significant sequence homology with the C-X-C chemokine receptor family yet does not activate $G\alpha_i$ pathways [97,103,124]. Thus, it was re-classified to the atypical chemokine receptor family. Although ACKR3 does not signal through $G\alpha_i$ pathways, it does signal via the β-arrestin signaling cascade [51]. ACKR3 is the first GPCR that was identified to exhibit biased signaling [51]. ACKR3 has also been identified as a co-receptor for HIV [125].

The functions for ACKR3 are not well defined. ACKR3 was thought to modulate the signaling of CXCR4 [51]. This would occur through convergence of downstream signaling effectors, scavenging CXCL12, or through heteromerization [51]. ACKR3 and CXCR4 have been shown to form heteromeric complexes in hVSMC and also in recombinant systems [82,107,119,123]. This apparent dimerization may elicit various roles depending upon the cell type and other receptors present. Bach *et al*. [114] also identified that activation of ACKR3 antagonized α_1-AR-mediated vasoconstriction, although the mechanism remains elusive.

α_1-AR

Adrenergic receptors are GPCRs comprised of three main families, α_1-AR coupling to $G\alpha_q$ proteins, α_2-AR coupling to $G\alpha_i$, and β-AR coupling to $G\alpha_s$ [33]. Each of these families consist of subtypes, with the α_1-ARs having three distinct subtypes; A, B, D. Phenylephrine (PE) binds to α_1-AR, thus activating phospholipase C, which in turn yields IP_3 and subsequent Ca^{2+} mobilization [126-129]. α_1-ARs are primarily found within the smooth muscle of the vasculature, but are also present in areas of smooth muscle throughout the body, found within the central and peripheral nervous system, and found on cells of the immune system [130-132]. Catecholamines signal through α_1-AR in both the central and peripheral nervous systems [38,129,134]. α_1-ARs are often targeted pharmacologically to regulate hemodynamics [21,35,110,128,133,134].

α_1-AR subtypes have differing roles depending upon the location of the vascular bed [135-137]. α_{1A}-Ars are chiefly responsible for vasoconstrictive responses in the resistance vessels, whereas $\alpha_{1B/D}$-AR modulate vascular reactivity in the larger conduit vessels [33,131,138-140]. Aside from the divergent dominance in the vasculature, α_1-AR respond differently when exposed to agonist despite all being coupled to the same $G\alpha_q$ protein. α_{1B}-AR are rapidly internalized via the β-arrestin pathway when activated, yet α_{1A}-AR are more resistant to receptor-mediated endocytosis [87,141].

Although recombinant α_{1a}-AR (recombinant receptor subtypes are denoted with a lowercase letter [142]) protomers are resistant to internalization, when co-expressed with

α_{1b}-AR, both receptors are internalized, thus implying differential function of the heteromer from the individual protomer [87,129]. Recombinant α_{1d}-AR has also been shown to heteromerize with α_{1b}-AR, yet it does not interact with α_{1a}-AR [135,143]. When CXCR2 is co-expressed with α_{1a}-AR, these receptors form heteromeric complexes that lead to cross-recruitment of β-arrestin2 [144]. Whether these receptors interact in native cells remains to be determined. CXCR4 potentiates $\alpha_{1A/B}$-AR mediated effects in hVSMC through the formation of heteromeric complexes [82-84]. Additional α_1-AR heteromers likely exist based on multiple lines of evidence for receptor cross-talk with ACKR3 and arginine vasopressin receptors (AVPR) type 1A [32,35,114,127,128,136,145-153], but have yet to be identified.

AVPR1A

AVPR1A are GPCRs essential for the regulation of vascular tone [38,154]. AVPRs couple intracellularly to $G\alpha_q$, upon activation lead to accumulation of IP_3 and thus intracellular Ca^{2+} flux [33,148,155]. Among the three receptor subtypes (AVPR1A, AVPR1B and AVPR2), AVPR1A is predominantly found in the vasculature and induces vasoconstriction upon agonist binding [38,148,154]. These receptors are targeted clinically for blood pressure control in patients with hyper- and hypotension [33,38,155]. Arginine vasopressin (aVP), a nonapeptide hormone, acts as an agonist for AVPR1A within the vasculature to increase blood pressure, whereas Vaptans, non-peptide vasopressin receptor antagonists (VRAs), are used clinically to treat hyponatriema and congestive heart failure [35,156]. SR49059 is a non-peptide VRA selective for AVPR1A which reduces blood pressure [156].

AVPR1A has been shown to form heteromers in heterologous expression systems with AVPR2 and oxytocin receptors [89,155,157,158]. Chemokine receptors have been demonstrated to affect vascular reactivity through the formation of heteromeric receptor complexes with α_1-AR [83,84]. Little is known about the role of chemokine receptors on AVPR1A function [82-84,114]. Several studies suggested a link between aVP release and the inflammatory system [65,68,80,99,159,160]. CXCL12 was shown to decrease activity of aVP-releasing neurons in the supraoptic nucleus and paraventricular nucleus [65,99]. Yet, other reports indicated that CXCL12 infusion led to increased plasma aVP levels [80]. Furthermore, evidence suggests that aVP has potent anti-inflammatory effects [68,159,160]. However, to date, no information exists about the role of AVPR1A and chemokine receptors on cardiovascular function.

Cross-talk Between the Immune and Neurohormonal Vasoactive Systems

Recently, our laboratory provided evidence for cross-talk between the chemokine and neurohormonal vasoactive systems [94,104,114]. Furthermore, our laboratory identified that CXCR4 heteromerizes with α_1-AR and through this heteromeric complex, CXCR4 potentiates α_1-AR-mediated effects [83,84]. Activation of ACKR3 led to opposing effects of CXCR4 [114]. Ablation of α_1-AR-mediated vasoconstriction was observed with activation of ACKR3 in isolated mesenteric resistance arteries [114]. This cross-talk between ACKR3, CXCR4, and α_1-AR indicates these receptors are functionally connected, yet how this cross-talk is occurring remains elusive.

Heteromerization between ACKR3 and α_1-AR alone likely does not account for the cardiovascular collapse observed with concurrent activation of ACKR3 and inhibition of

CXCR4 with the synthetic peptide TC14012 [114]. In α_1-AR knockout animals, only a minimal decrease to blood pressure is observed [138]. Therefore, other vasoactive receptors that are critical for the regulation of hemodynamic responsiveness may be modulated by ACKR3. As CXCR4 sensitizes α_1-AR function via the formation of heteromeric receptor complexes [82-84] ACKR3 may also form heteromeric complexes with α_1-AR to aid in the fine tuning of blood pressure control. CXCL12 inhibits aVP-release in the central nervous system and may also affect aVP-mediated effects in the periphery [65,99]. Thus, ACKR3 and CXCR4 may also form heteromeric receptor complexes with AVPR1A.

Based on the foregoing, we hypothesize that hetero-oligomeric receptor complexes between the immune and vasoactive systems regulate vascular smooth muscle function. Here, evidence is provided for ACKR3 cross-talk with the adrenergic and vasopressin systems in hVSMC. We aimed to identify interactions of both recombinant and endogenously expressed receptors, characterize the functional relevance of ACKR3:CXCR4:α_1-AR and ACKR3:AVPR1A heteromerization, and ascertain how ACKR3-mediated β-arrestin recruitment affects the expression of alternate heteromeric receptor partners. The findings from these studies could allow for the development of novel therapeutic strategies to prevent and treat cardiovascular diseases.

These studies highlight the importance of GPCR hetero-oligomerization on receptor regulation of hVSMC function. Furthermore, as additional heteromeric complexes are discovered and characterized in both healthy and diseased states, the need for heteromer-specific drug design will sharply rise. Exposing the physiological

consequences of the pharmacological properties of heteromers will allow for a targeted approach to treat pathologic conditions.

CHAPTER 2

ANTIBODY VALIDATION

Introduction

Several previous reports indicated that commercially available antibodies directed against GPCRs may lack sufficient selectivity for the receptor targets [161-167]. Therefore, it has been proposed that anti-GPCR antibodies should be validated prior to use. Criteria have been proposed to substantiate antibody selectivity [161]. These criteria include diminished staining for the target receptor in animals where the receptor gene has been deleted or decreased staining for the target receptor following gene silencing techniques [161]. Furthermore, staining for a related receptor subtype should be unaffected by the knock-out/down approaches to determine antibody selectivity [161].

Our laboratory has routinely confirmed that commercially available antibodies against GPCRs that were utilized in recent studies displayed sufficient selectivity [84,95,168]. In this dissertation, several antibodies that have not been previously validated have been employed. Thus, to ensure rigor and reproducibility, we validated these antibodies utilizing established criteria for selectivity.

Results

To test the selectivity of goat anti-CXCR4 (Abcam, Ab1670) and rabbit anti-CXCR4 antibodies (Alomone Labs, ACR-014), hVSMC were treated with 1μM of CXCR4 siRNA or non-targeting (NT) siRNA for 72 hours. PLA was utilized to visualize changes in CXCR4 surface expression (Fig. 7). Incubation of hVSMC with CXCR4 siRNA reduced PLA signals with goat anti-CXCR4 (Abcam, Ab1670) by 79 ± 4% and PLA signals with rabbit anti-CXCR4 (Alomone Labs, ACR-014) by 75 ± 4%, as compared with cells incubated with NT siRNA.

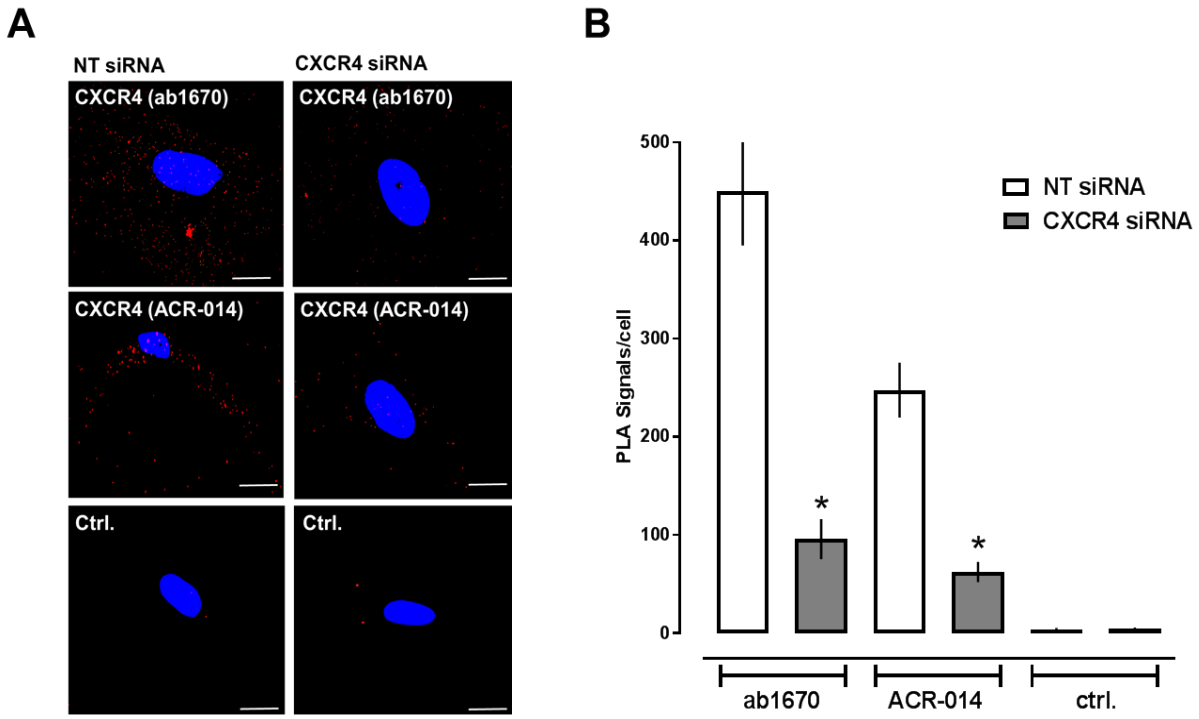

Figure 7. Validation of anti-CXCR4 antibodies. hVSMC were incubated with non-targeting (NT) or CXCR4 siRNA and then used in PLA for the detection of CXCR4 with goat anti-CXCR4 (Abcam Ab1670) and rabbit anti-CXCR4 (Alomone Labs ACR-014). **A.** Representative PLA images showing merged PLA/4′,6-diamidino-2-phenylindole dihydrochloride (DAPI) signals. Ctrl: Omission of primary antibody. Scale bars = 10 μm. **B.** Quantification of PLA signals per cell, as in A. n = 10 images per condition. Data presented as mean ± SEM, Student's t-test with post hoc, *: $p<0.05$ vs. cells incubated with NT siRNA.

Although the selectivity of the rabbit anti-AVPR1A (Bioss, BS-11598R) antibody was previously demonstrated in flow cytometry experiments [168], we confirmed the selectivity of this anti-AVPR1A antibody under the specific experimental conditions in which the antibody was being utilized in this dissertation. AVPR1A was depleted in hVSMC by incubation with 1μM AVPR1A siRNA for 72 hours, then assayed for receptor surface expression via PLA. Validation of two AVPR1A antibodies, rabbit anti-AVPR1A (Bioss, BS-11598R) and mouse anti-AVPR1A (LS Bio, C196528) was performed. Incubation of hVSMC with AVPR1A siRNA reduced PLA signals with rabbit anti-AVPR1A (Bioss, BS-

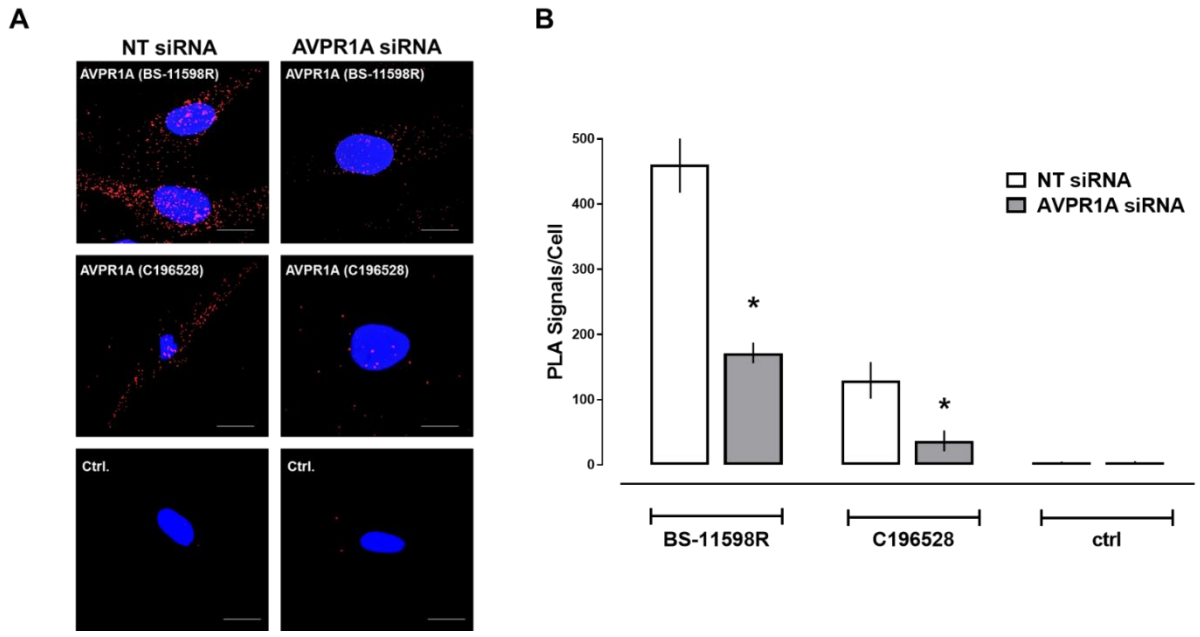

Figure 8. Validation of anti-AVPR1A antibodies. hVSMC were incubated with non-targeting (NT) or AVPR1A siRNA and then used in PLA for the detection of AVPR1A with rabbit anti-AVPR1A (Bioss, BS-11598R) and mouse anti-AVPR1A (LS Bio, C196528). **A.** Representative PLA images showing merged PLA/4′,6-diamidino-2-phenylindole dihydrochloride (DAPI) signals. Ctrl: Omission of primary antibody. Scale bars = 10 μm. **B.** Quantification of PLA signals per cell, as in A. n = 10 images per condition. Data presented as mean ± SEM, Student's t-test with post hoc, *: $p<0.05$ vs. cells incubated with NT siRNA.

11598R) by 63 ± 3% and PLA signals with mouse anti-AVPR1A (LS Bio, C196528) by 72 ± 12%, as compared with cells incubated with NT siRNA (Fig. 8).

FLAG and human influenza virus hemagglutinin (HA) antibodies were used to detect N-terminal FLAG or HA-tagged CXCR4 expression by PLA in HEK 293T cells. As these cells do not express either tag under basal conditions, the selectivity of these antibodies was confirmed via PLA in cells transfected with empty vector (pcDNA3) (Fig. 9). Strong PLA signals were detected in cells expressing recombinant FLAG-CXCR4 that were stained with anti-FLAG (Fig. 9 upper left) and also for cells expressing HA-CXCR4 stained with anti-HA (Fig. 9 upper right). Cells transfected with pcDNA3 then stained

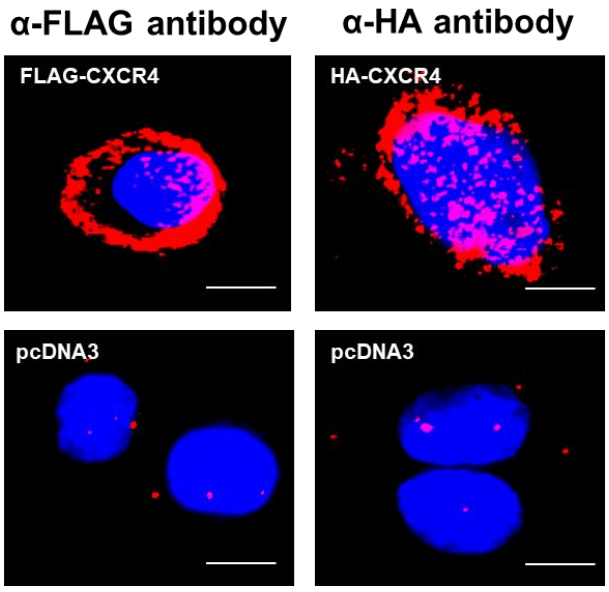

Figure 9: Validation of anti-FLAG and anti-HA antibodies. HEK 293T cells were transiently transfected with pcDNA3, FLAG-CXCR4, or HA-CXCR4, then PLA was performed with α-FLAG or α-HA antibodies to detect the tagged receptors. Representative images showing merged PLA/4′,6-diamidino-2-phenylindole dihydrochloride (DAPI) signals. Scale bars = 10 μm.

with either anti-FLAG or anti-HA (Fig. 9 lower panels) did not yield comparable signals to the cells transfected with tagged GPCRs.

Discussion

In this chapter, we employed gene silencing via RNA interference to deplete receptors from the cell surface in hVSMC and utilized cells that do not express the antibody targets to confirm antibody selectivity by PLA. The results demonstrate sufficient selectivity of the antibodies that were tested.

Previous studies suggested that approximately 70% reduction in staining of the target receptor following a knock-down approach would indicate excellent antibody selectivity [162,168]. Using this benchmark, the goat anti-CXCR4 (Abcam, Ab1670), rabbit anti-CXCR4 (Alomone Labs, ACR-014), and mouse anti-AVPR1A (LS Bio, C196528) antibodies display excellent selectivity. The rabbit anti-AVPR1A (Bioss, BS-11598R) antibody showed a 63% reduction in PLA signals following AVPR1A siRNA incubation. Although this antibody did not reach the arbitrary benchmark of 70% reduction in staining for excellent selectivity, the reduction in staining following AVPR1A siRNA provides reasonable evidence to indicate sufficient selectivity.

All antibodies utilized in this dissertation have been validated for selectivity. Furthermore, antibodies employed in this dissertation are directed against the extracellular domains, typically the N-terminus, the highly selective ligand binding domain. Table 1 lists the antibodies that were used in this dissertation and indicates the validation methodology employed.

Antibody	***Cat. No.***	***Validation Technique***
mouse anti-ACKR3	R&D systems, MAB42273	siRNA-flow cytometry [168]
rabbit anti-ACKR3	Abcam, Ab38089	siRNA-flow cytometry [168]
goat anti-CXCR4	Abcam, Ab1670	siRNA-PLA [82]
rabbit anti-CXCR4	Alomone Labs, ACR-014	siRNA-PLA [82]
mouse anti-α_{1A}-AR	Abcam, Ab87990	siRNA-flow cytometry [83]
rabbit anti-α_{1A}-AR	Abcam, Ab137123	siRNA-flow cytometry [83]
rabbit anti-α_{1B}-AR	Abcam, Ab169523	siRNA-flow cytometry [168]
goat anti-α_{1B}-AR	Santa Cruz, SC27136	siRNA-flow cytometry [83]
goat anti-α_{1D}-AR	Santa Cruz, SC27099	siRNA-flow cytometry [168]
rabbit anti-α_{2A}-AR	Abcam, A85570	siRNA-flow cytometry [168]
rabbit anti-α_{2B}-AR	Abcam, Ab151727	siRNA-flow cytometry [168]
rabbit anti-α_{2C}-AR	Abcam, Ab140702	siRNA-flow cytometry [168]
rabbit anti-β_2-AR	Abcam, Ab3442	siRNA-flow cytometry [168]
rabbit anti-AVPR1A	Bioss, BS-11598R	siRNA-PLA
mouse anti-AVPR1A	LS Bio, C196528	siRNA-PLA
mouse anti-FLAG	Sigma, F1804	PLA (no FLAG on cells)
rabbit anti-HA	Abcam, Ab9110	PLA (no HA on cells)

Table 1. Table of validated antibodies. hVSMC were utilized to validate the aforementioned antibodies either by flow cytometry or PLA after incubation with receptor specific siRNA or non-targeting (NT) siRNA or in cells not expressing target GPCR.

CHAPTER 3

α_1-ARs FUNCTION WITHIN HETERO-OLIGOMERIC RECEPTOR COMPLEXES WITH CHEMOKINE RECEPTORS ACKR3 AND CXCR4 IN VASCULAR SMOOTH MUSCLE CELLS

Introduction

Previous studies suggest that CXCR4 and ACKR3 play an integral role in blood pressure regulation in both healthy and diseased states [81,83,84,94,104,114,169,170]. Recently, our laboratory reported that CXCR4 activation potentiated α_1-AR function in vascular smooth muscle and stabilized blood pressure during the cardiovascular stress response to hemorrhagic shock; whereas ACKR3 activation antagonized α_1-AR mediated effects [114]. Furthermore, it was identified that CXCR4 actions on α_1-AR function were due to endogenously expressed CXCR4:$\alpha_{1A/B}$-AR heteromeric receptor complexes present on hVSMC [83,84]. The mechanisms governing the inhibitory effects of ACKR3 on α_1-AR are undetermined. Therefore, we evaluated whether ACKR3 heteromerization with α_1-AR may also be a mechanism for the observed cross-talk in hVSMC. Here, we provide evidence for receptor cross-talk in hVSMC, identify CXCR4:ACKR3:α_1-AR hetero-oligomeric complexes of recombinant and endogenously expressed receptors, and ascertain the functional role of the heteromers.

Results

3.1 ACKR3 Activation Inhibits $G\alpha_q$-Mediated Signaling Upon α_1-AR Activation.

ACKR3 activation was previously demonstrated to antagonize PE-induced vasoconstriction of isolated mesenteric resistance arteries. However, the effects of ACKR3 activation on α_1-AR-mediated signaling events in hVSMC are unknown. Therefore, to provide evidence for signaling cross-talk between ACKR3 and α_1-AR, downstream $G\alpha_q$-protein mediated signaling was assessed by measuring production of IP_3 upon activation of α_1-AR with PE. hVSMC were pre-treated with agonists for ACKR3, then stimulated with PE. Prior to measuring IP_3 production, we confirmed the activity of the ACKR3 agonists, CXCL11, CXCL12, and TC14012 (a synthetic peptide agonist for ACKR3 and antagonist for CXCR4),utilizing a β-arrestin 2 recruitment assay (PRESTO-Tango [171]), as ACKR3 is only known to activate β-arrestin signaling cascades [51]. The EC_{50} for β-arrestin 2 recruitment to ACKR3 was 16.5 $\pm$ 3.9 nM for CXCL11, 2.4 $\pm$ 0.3 nM for CXCL12, and 87.5 $\pm$ 19.0 nM for TC14012 (Fig. 10). These data provide evidence that natural chemokines and a synthetic agonist activate ACKR3. When hVSMC were stimulated with 1μM PE, cellular IP_3 concentrations increased 5.3-*fold*. However, pre-treatment with the ACKR3 agonists (Fig. 10) ablated the PE-induced increases in IP_3 (Fig. 11), thus indicating receptor cross-talk.

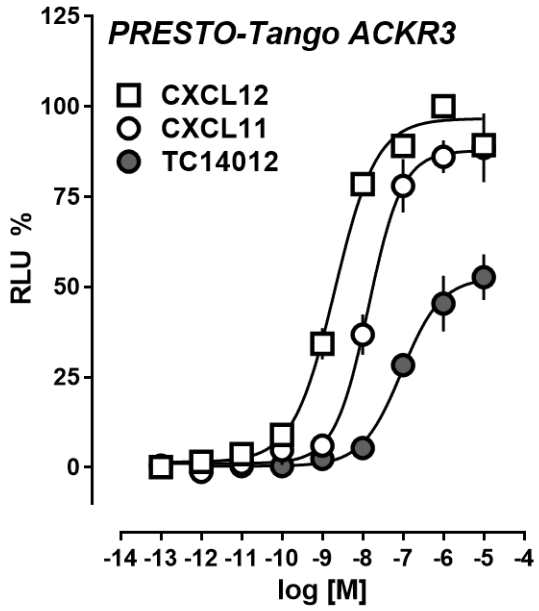

Figure 10. ACKR3 agonists recruit β-arrestin 2 to ACKR3 in HTLA cells. β-arrestin 2 recruitment assay (PRESTO-Tango) to test ACKR3 agonist activity. Cells were treated CXCL12 (open squares), CXCL11 (open circles) and TC14012 (grey circles). RLU (%): relative luminescence units in % of the RLU after treatment with 1 μM CXCL12 (=100%). Data presented as mean ± SEM, non-linear regression analysis, n=3 independent experiments per condition.

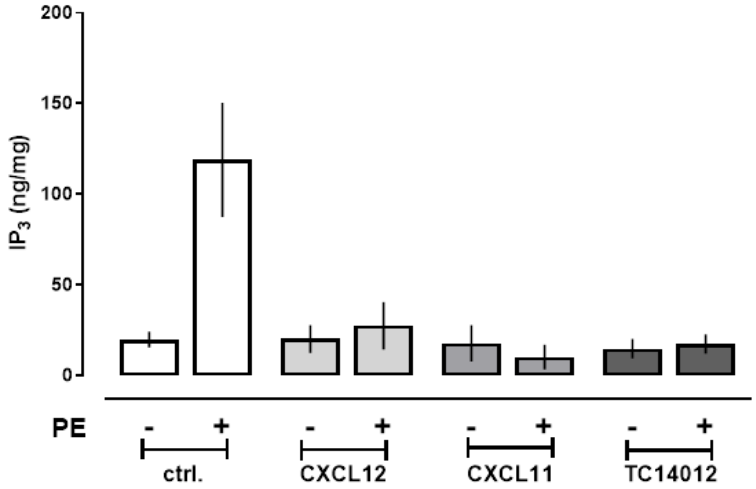

Figure 11. ACKR3 inhibits α_1-AR signaling in hVSMC. hVSMCs were treated with vehicle or ACKR3 ligands (1 μM, 15 min) and then stimulated with 1 μM phenylephrine (PE) for 5 min. IP_3 production was measured by ELISA. n=3 independent experiments. Data presented as mean ± SEM, Student's t-test with post hoc, *: $p<0.05$ vs. cells incubated with untreated.

3.2 ACKR3 Forms Heteromeric Complexes with $\alpha_{1A/B/D}$-AR.

To ascertain if ACKR3 could form heteromeric complexes with α_1-ARs, recombinant N-terminal FLAG or HA tagged receptors were expressed in human embryonic kidney (HEK) 293T cells. PLA were utilized to visualize and quantify individual receptors and receptor-receptor interactions at single molecule resolution. Interactions between ACKR3 and CXCR4 and CXCR4 and α_{1a}-AR served as positive controls, as these heteromeric complexes have been previously described in recombinant systems [83,84,119,123]. When HA-tagged ACKR3 was co-expressed with FLAG-tagged $\alpha_{1a/b/d}$-AR, positive PLA signals were observed (mean $\pm$ SEM, HA-ACKR3: FLAG-α_{1a}-AR, 87 $\pm$ 10; FLAG-α_{1b}-AR, 66 $\pm$ 9; FLAG-α_{1d}-AR, 53 $\pm$ 6, PLA signals/cell, $p < 0.05$ vs. ctrl.) (Fig.12). Comparable signals were observed for interactions with FLAG-ACKR3:HA-CXCR4 (mean $\pm$ SEM, 70 $\pm$ 10, PLA signals/cell, $p < 0.05$ vs. ctrl.) and HA-CXCR4:FLAG-α_{1a}-AR (mean $\pm$ SEM, 97 $\pm$ 28, PLA signals/cell, $p < 0.05$ vs. ctrl.) (Fig.12). As a negative control pcDNA3 transfected cells were stained with anti-HA and anti-FLAG antibodies (mean $\pm$ SEM, 13 $\pm$ 2, PLA signals/cell) (Fig.12). The individual signals and not the signal intensity were quantified as described in chapter 6.

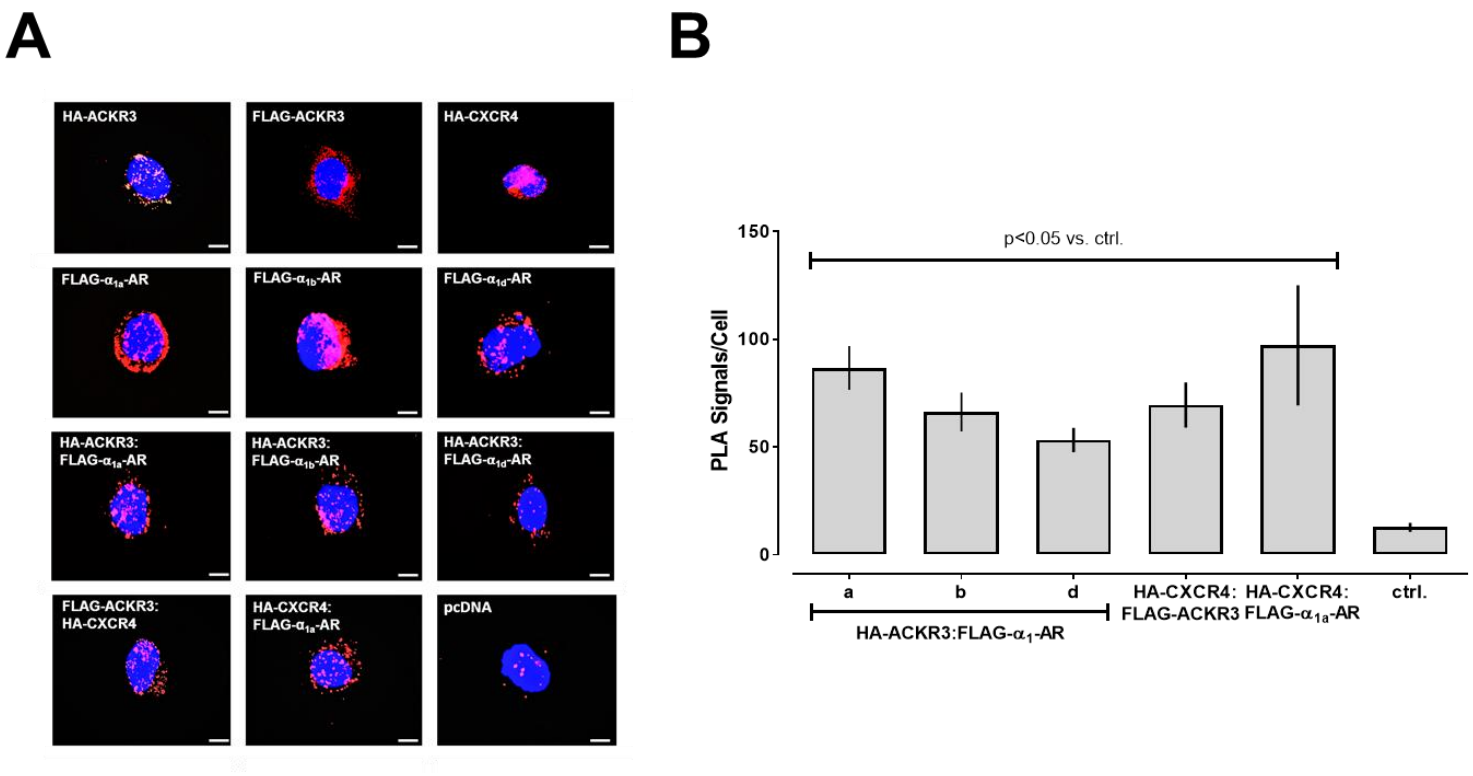

Figure 12. ACKR3 forms heteromeric complexes with $\alpha_{1a/b/d}$-AR in HEK293T cells. A. Typical PLA images for the detection of individual receptors and receptor-receptor interaction in HEK293T cells transfected with DNA encoding HA- or FLAG-tagged receptors. Ctrl: Cells transfected with pcDNA. Images show merged PLA/4′,6-diamidino-2-phenylindole dihydrochloride (DAPI) signals. Scale bars = 10 μm. **B.** Quantification of PLA signals per cell, as in C. N = 3 with n = 10 images per condition and experiment. Data presented as mean ± SEM, One way ANOVA with Dunnett's multiple comparison post hoc, $p<0.05$ vs. ctrl.

ACKR3 co-expression with $\alpha_{1a/b/d}$-AR suggests that these receptors could form heteromeric receptor complexes, therefore we assessed whether these receptors are in close proximity to form receptor-receptor interactions in hVSMC. hVSMC were stained with anti-ACKR3 in combination with anti-$\alpha_{1A/B/D}$-AR, anti-$\alpha_{2A/B/C}$-AR, or anti-CXCR4 to detect receptor-receptor interactions or with one primary antibody to visualize individual receptors (Fig. 13). Positive interactions were detected for ACKR3 with all α_1-AR subtypes and with α_{2B}-AR (mean $\pm$ SEM, ACKR3:α-AR; 1A, 32 $\pm$ 6; 1B, 37 $\pm$ 6; 1D, 18 $\pm$ 2; 2B, 30 $\pm$ 4, PLA signals/cell $p < 0.05$ vs. ctrl) (Fig.13). Interactions between ACKR3 and CXCR4 served as a positive control, whereas omission of one primary antibody was utilized as a negative control (mean $\pm$ SEM, ACKR3:CXCR4, 38 $\pm$ 6; ctrl, 3 $\pm$ 0.6, PLA signals/cell $p < 0.05$ vs. ctrl) (Fig.13).

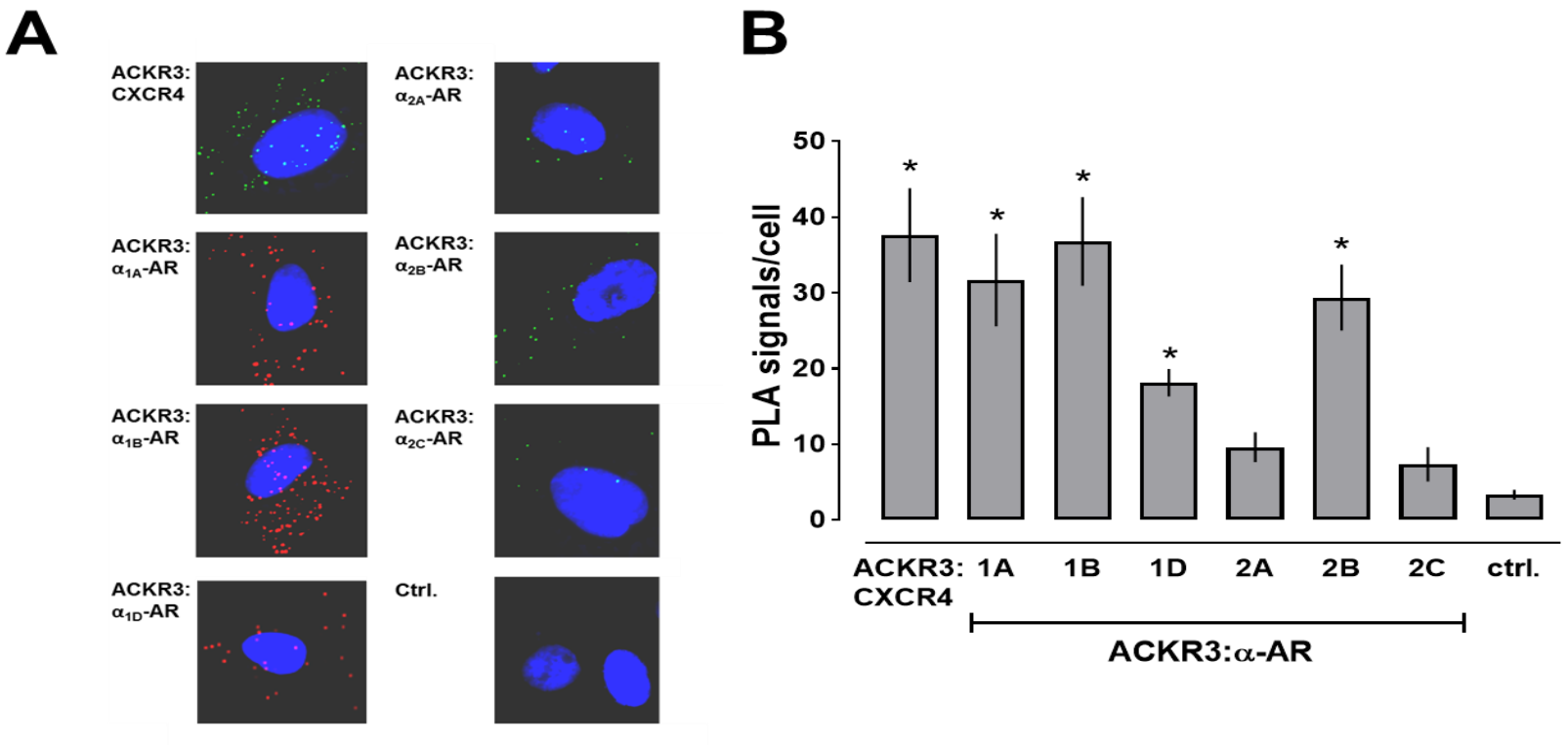

Figure 13. ACKR3 forms heteromeric complexes with $\alpha_{1A/B/D}$-AR and α_{2B}-AR in hVSMC. A. Representative PLA images for the detection of receptor-receptor interactions in hVSMC. Ctrl.: Omission of one primary antibody. Images show merged PLA/4′,6-diamidino-2-phenylindole dihydrochloride (DAPI) signals. Scale bars = 10 μm. **B.** Quantification of PLA signals for receptor-receptor interactions per cell, as in A. N = 3 with n = 10 images per condition and experiment. Data presented as mean ± SEM, One way ANOVA with Dunnett's multiple comparison post hoc, *, $p<0.05$ vs. ctrl. The differences in PLA signal color are not representative of differing conditions, simply utilized different PLA reagents.

To confirm that PLA findings correspond to direct physical interactions, ACKR3 was immunoprecipitated from hVSMC lysate and then immunoblotted for $\alpha_{1A/B/D}$-AR and $\alpha_{2B/C}$-AR (Fig.14). All α_1-AR subtypes and α_{2B}-AR could be immunoprecipitated with anti-ACKR3 in hVSMC (Fig. 14). When immunoblotting for α_{1D}-AR, a band of 50 kDa was detected in the ACKR3 immunoprecipitate, however we were unable to detect α_{1D}-AR in the hVSMC lysate (input). This can be attributed to the low density of α_{1D}-AR in hVSMC and the enrichment of α_{1D}-AR in the ACKR3 immunoprecipitate. Furthermore, the α_{1A}-AR band in the ACKR3 immunoprecipitate appeared to migrate lower (46.1 (95% confidence interval (CI)) (42.2-50.2) kDa) than in the hVSMC lysate (49 (95% CI) (44.8-53.8) kDa), which may be due to post-translational receptor modifications or partial proteolytic processing occurring during the experimental procedure. Collectively these observations suggest that ACKR3:$\alpha_{1A/B/D}$-AR heteromeric receptor complexes are constitutively expressed on hVSMC.

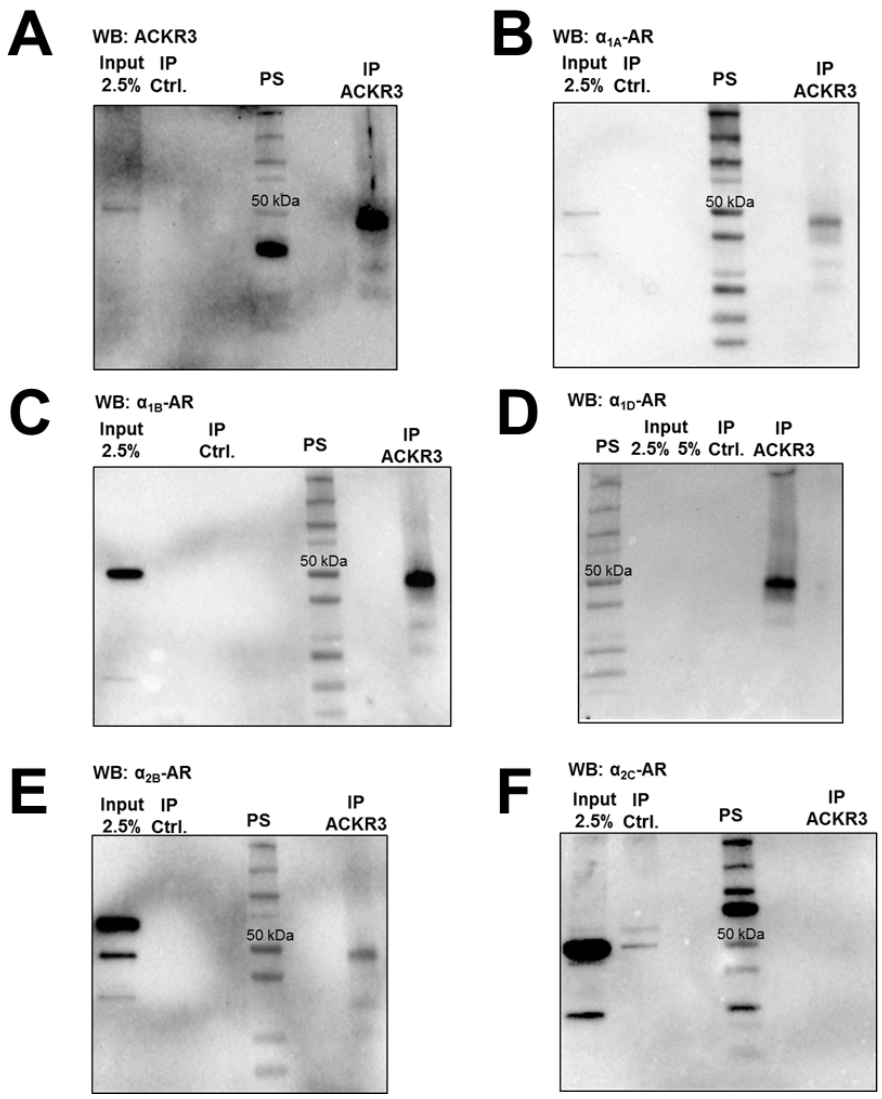

Figure 14. ACKR3 forms heteromeric complexes with $\alpha_{1A/B/D}$-AR and α_{2B}-AR in hVSMC. A-F. hVSMC were lysed and ACKR3 was immunoprecipitated (IP) followed by Western blotting (WB) to detect ACKR3 (**A**), α_{1A}-AR (**B**), α_{1B}-AR (**C**), α_{1D}-AR (**D**), α_{2B}-AR (**E**) and α_{2C}-AR (**F**) in the IP samples. IP control: precipitate after incubation of cell lysates with nonreactive or IgG_1- coupled resin. PS: protein standards. The white light images are overlaid at the corresponding position of the standard proteins (PS). Images are representative of n = 3 independent experiments.

3.3 ACKR3 Gene Silencing Inhibits α_1-AR Signaling.

To identify how heteromerization between ACKR3 and α_1-AR affects α_1-AR signaling in hVSMC, ACKR3 was depleted from the cell surface via RNA interference and changes in receptor interactions were visualized via PLA.

Representative PLA images from four independent experiments indicate that individual receptor expression was not changed, except for ACKR3 after incubation with ACKR3 siRNA (Fig. 15). ACKR3 siRNA reduced PLA signals for ACKR3 in hVSMC by more than 70% when compared with hVSMC incubated with non-targeting (NT) siRNA. Quantification of PLA signals for receptor-receptor interactions showed that ACKR3 gene silencing significantly decreased the ACKR3:α_{1B}-AR, ACKR3:α_{1D}-AR, and ACKR3:CXCR4 heteromers (52 $\pm$ 7% of NT, 72 $\pm$ 4% of NT, and 65 $\pm$ 7% of NT respectively, $p < 0.05$ vs NT). Interactions between ACKR3:α_{1A}-AR and CXCR4:α_{1A}-AR were not affected by ACKR3 siRNA treatment (17 $\pm$ 11% of NT and 14 $\pm$ 11% of NT respectively, $p > 0.05$ vs NT) (Fig. 15).

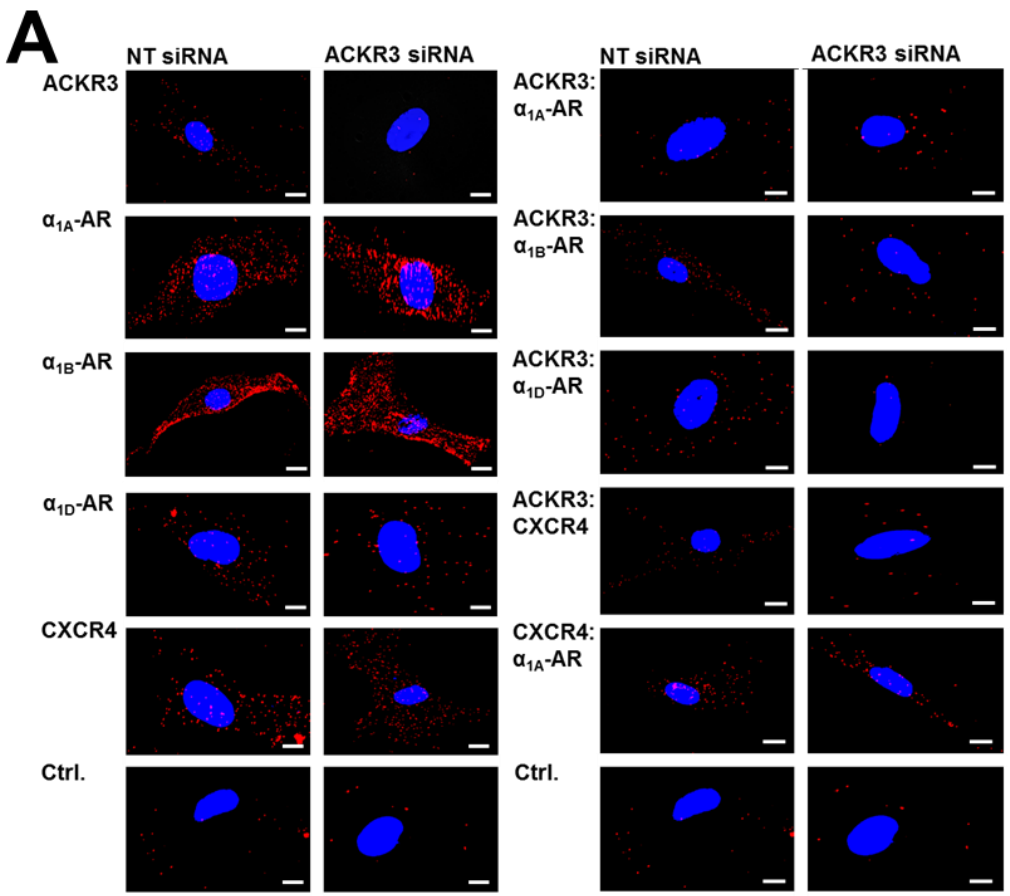
A
NT siRNA
ACKR3 siRNA
ACKR3
α1A-AR
α1B-AR
α1D-AR
CXCR4
Ctrl.
ACKR3: α1A-AR
ACKR3: α1B-AR
ACKR3: α1D-AR
ACKR3: CXCR4
CXCR4: α1A-AR
Ctrl.

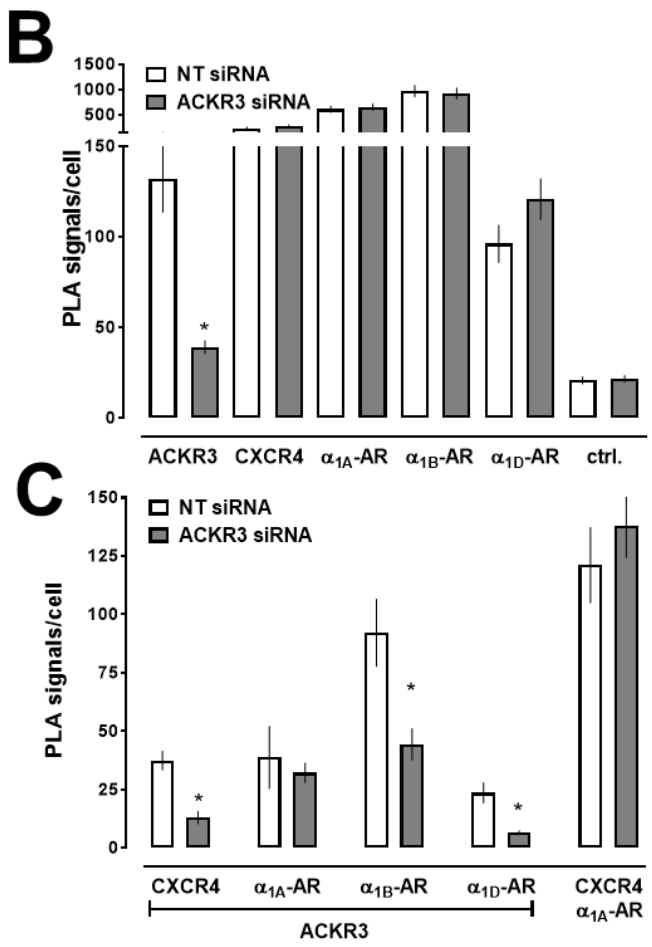
B
NT siRNA
ACKR3 siRNA
PLA signals/cell
1500
1000
500
150
100
50
0
*
ACKR3
CXCR4
α1A-AR
α1B-AR
α1D-AR
ctrl.
C
NT siRNA
ACKR3 siRNA
PLA signals/cell
150
125
100
75
50
25
0
*
CXCR4
α1A-AR
α1B-AR
α1D-AR
CXCR4 α1A-AR
ACKR3

Figure 15. ACKR3 gene silencing reduces ACKR3:$\alpha_{1B/D}$-AR and ACKR3:CXCR4 heteromerization. A. Representative PLA images for the detection of individual receptors (left) and receptor-receptor interactions (right) in hVSMC incubated with non-targeting (NT) or ACKR3 siRNA. Images show merged PLA/4′,6-diamidino-2-phenylindole dihydrochloride (DAPI) signals. Ctrl: Omission of one primary antibody. Scale bars = 10 μm. **B.** Quantification of PLA signals per cell for the detection of individual receptors, as in A. n = 4 with n = 10 images per condition and experiment. *: $p < 0.05$ vs. cells incubated with NT siRNA. **C.** Quantification of PLA signals per cell for receptor- receptor interactions, as in A. n = 4 with n = 10 images per condition and experiment. Data presented as mean ± SEM, Student's t-test with post hoc, *: $p < 0.05$ vs. cells incubated with NT siRNA.

Following incubation of hVSMC with ACKR3 siRNA or NT siRNA, IP_3 production was measured to identify how α_1-AR signaling is affected by heteromerization with ACKR3. PE stimulation induced a 4.8-*fold* increase in hVSMC treated with NT siRNA yet failed to elicit measurable changes in IP_3 after treatment with ACKR3 siRNA (Fig. 16).

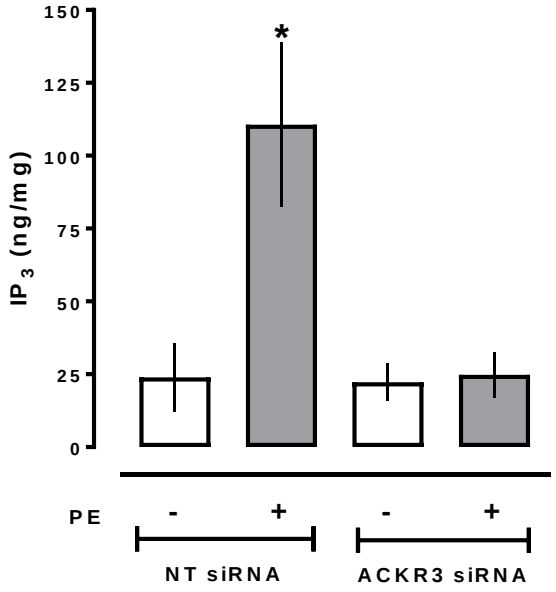

Figure 16. ACKR3 gene silencing inhibits α_1-AR signaling in hVSMC. IP_3 production of hVSMC incubated with non-targeting (NT) or ACKR3 siRNA upon stimulation with vehicle or 1 μM PE. n = 4 independent experiments. Data presented as mean ± SEM, Student's t-test with post hoc, *, $p<0.05$ vs. vehicle.

As no discernable changes were detected in ACKR3:α_{1A}-AR heteromers when hVSMC were treated with ACKR3 siRNA vs NT siRNA, we sought to identify which α_1-AR subtypes were responsible for IP_3 production in hVSMC. Stimulating hVSMC with 1μM PE led to significant increases in IP_3 production (Fig. 17). Pre-treating hVSMC with subtype selective α_1-AR antagonists (phentolamine-pan α-AR antagonist, 5'-methylurapidil – α_{1A}-AR antagonist, cyclazosin – α_{1B}-AR antagonist, BMY7378 – α_{1D}-AR antagonist) ablated the PE-induced increases with the exception of 5'-methylurapidil (Fig. 17). These data are consistent with the literature in that α_{1B}-AR and α_{1D}-AR are chiefly responsible for constriction of the vascular smooth muscle in the aorta and other larger conduit vessels [131,140,172,173]. α_{1A}-AR are primarily responsible for vasoconstriction in the smaller conduit and resistance vessels [130,132,139]. Treatment of hVSMC with 5'-methylurapidil suggest that the contribution of α_{1A}-AR is limited in our experimental approach; thus, we are unable to draw conclusions on the functional roles of α_{1A}-AR complexes.

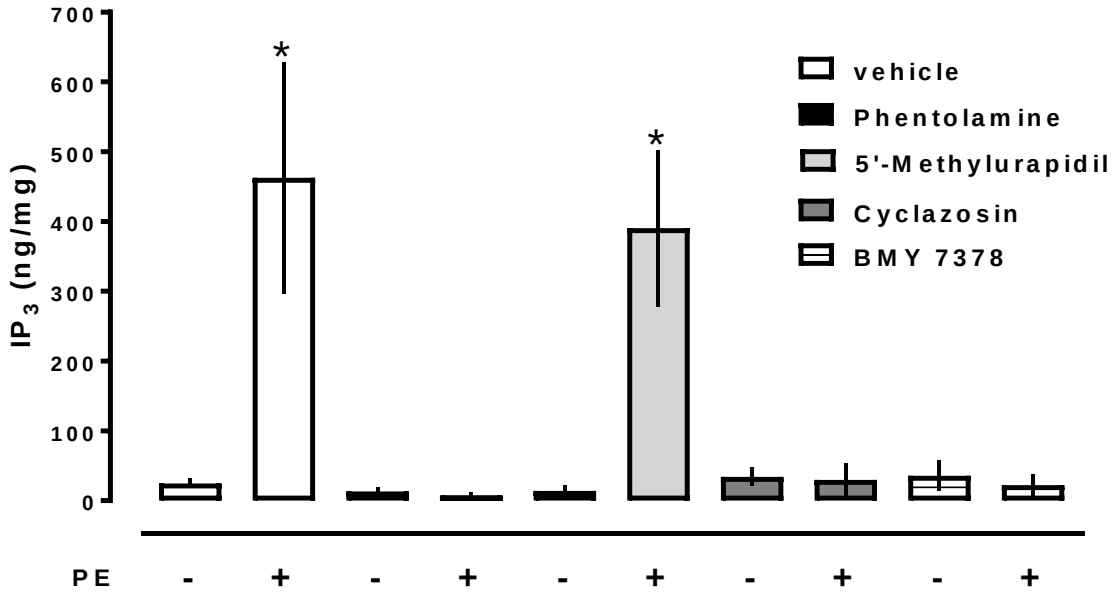

Figure 17. IP_3 production occurs via activation of $\alpha_{1B/D}$-AR in hVSMC. IP_3 production of hVSMC upon stimulation with vehicle or 1 μM PE for 5 min. Cells were pretreated (30 min, 37°C) with 10 μM of vehicle or α_1-AR antagonists. n = 3 independent experiments. Data presented as mean ± SEM, Student's t-test with post hoc, *, $p<0.05$ vs. vehicle.

Previously, CXCR4 gene silencing diminished heteromerization with $\alpha_{1A/B}$-AR and with ACKR3 [83,84]. CXCR4 depletion and subsequent loss of CXCR4:$\alpha_{1A/B}$-AR heteromers led to a loss α_1-AR signaling [83,84]. As ACKR3 knock-down did not affect CXCR4:α_{1A}-AR heteromers (Fig. 15), and α_{1A}-AR was determined to have a limited role in this experimental setup (Fig. 17), we tested whether depletion of ACKR3 impacted CXCR4:$\alpha_{1B/D}$-AR heteromers and vice versa.

PLA signals in hVSMC were significantly reduced with ACKR3 siRNA incubation for CXCR4:α_{1B}-AR (23 $\pm$ 4% of NT, $p < 0.05$ vs NT) and CXCR4:α_{1D}-AR (38 $\pm$ 6% of NT, $p < 0.05$ vs NT), again no discernable difference in CXCR4:α_{1A}-AR was observed with ACKR3 knockdown (Fig. 18A/C). When CXCR4 was depleted from hVSMC (20 $\pm$ 3% of NT), PLA signals for ACKR3:α_{1B}-AR and ACKR3:α_{1D}-AR were significantly reduced (30 $\pm$ 3% and 36 $\pm$ 5% of NT respectively, $p < 0.05$ vs NT), while no effect occurred with ACKR3:α_{1A}-AR heteromers (Fig. 18B/D). Consistent with previous findings [83,84], CXCR4, as well as ACKR3, knockdown abolished PE-induced Gα_q-protein mediated signaling (Fig. 19). These data could indicate that knockdown of ACKR3 in vascular smooth muscle would impair the ability of α_1-AR to elicit vasoconstriction in response to PE.

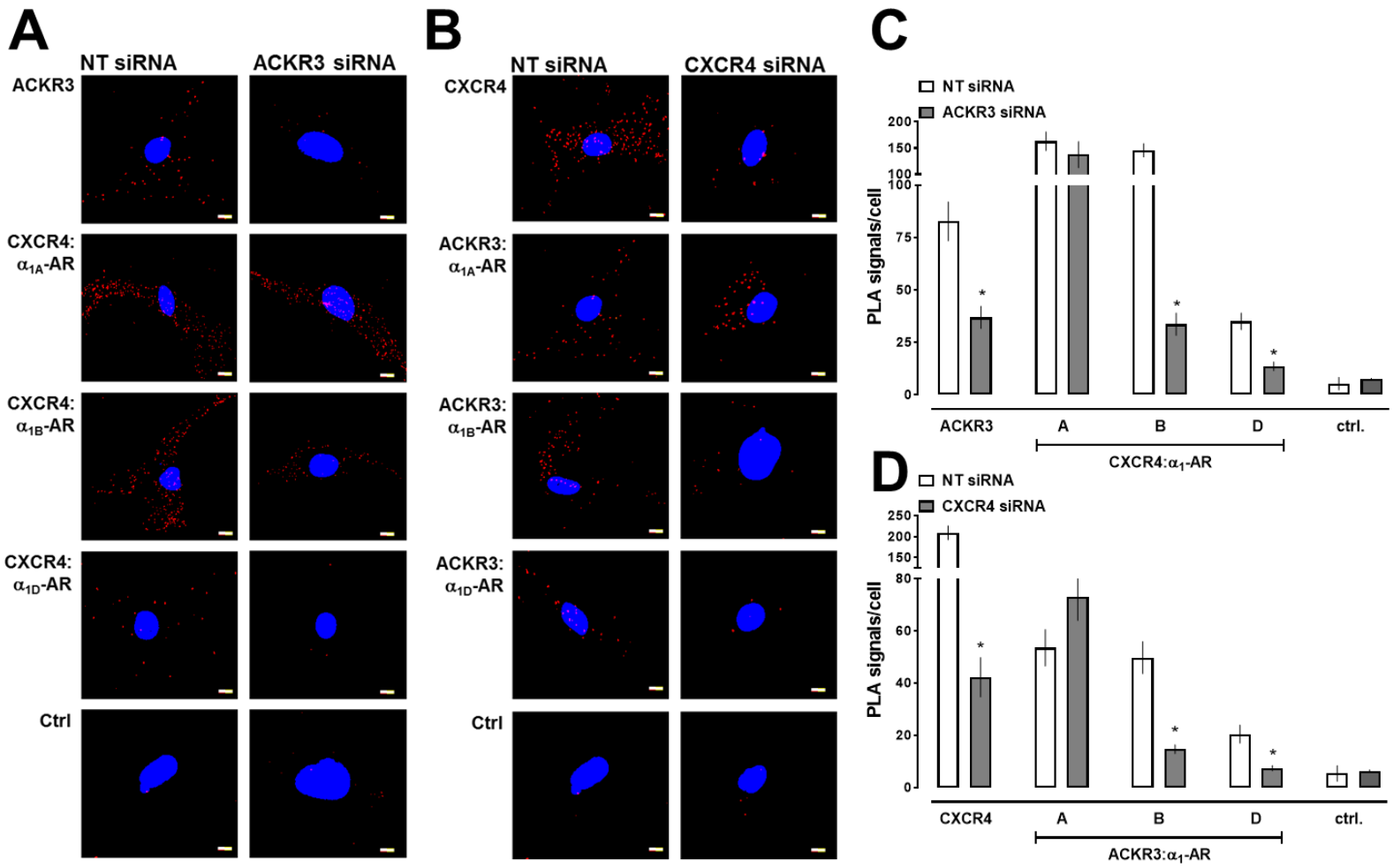
A
NT siRNA
ACKR3 siRNA
ACKR3
CXCR4: α1A-AR
CXCR4: α1B-AR
CXCR4: α1D-AR
Ctrl
B
NT siRNA
CXCR4 siRNA
CXCR4
ACKR3: α1A-AR
ACKR3: α1B-AR
ACKR3: α1D-AR
Ctrl
C
NT siRNA
ACKR3 siRNA
PLA signals/cell
200
150
100
100
75
50
25
0
ACKR3
A
B
D
ctrl.
CXCR4:α1-AR
D
NT siRNA
CXCR4 siRNA
PLA signals/cell
250
200
150
80
60
40
20
0
CXCR4
A
B
D
ctrl.
ACKR3:α1-AR

43

Figure 18. $\alpha_{1B/D}$-AR form hetero-oligomeric complexes with the ACKR3:CXCR4 heteromer in hVSMC. A. Typical PLA images for the detection of ACKR3 and CXCR4:$\alpha_{1A/B/D}$-AR heteromers in hVSMC incubated with non-targeting (NT) or ACKR3 siRNA. Images show merged PLA/4′,6-diamidino-2-phenylindole dihydrochloride (DAPI) signals. Ctrl: Omission of one primary antibody. Scale bars = 10 μm. **B.** Typical PLA images for the detection of CXCR4 and ACKR3:$\alpha_{1A/B/D}$-AR heteromers in hVSMC incubated with non-targeting (NT) or CXCR4 siRNA. Images show merged PLA/4′,6-diamidino-2-phenylindole dihydrochloride (DAPI) signals. Ctrl: Omission of one primary antibody. Scale bars = 10 μm. **C.** Quantification of PLA signals per cell for the detection of ACKR3 and CXCR4:$\alpha_{1A/B/D}$-AR heteromers, as in A. N = 3 with n = 10 images per condition and experiment. *: $p < 0.05$ vs. cells incubated with NT siRNA. **D.** Quantification of PLA signals per cell for the detection of CXCR4 and ACKR3:$\alpha_{1A/B/D}$-AR heteromers, as in B. N = 3 with n = 10 images per condition and experiment. Data presented as mean ± SEM, Student's t-test with post hoc, *: $p < 0.05$ vs. cells incubated with NT siRNA.

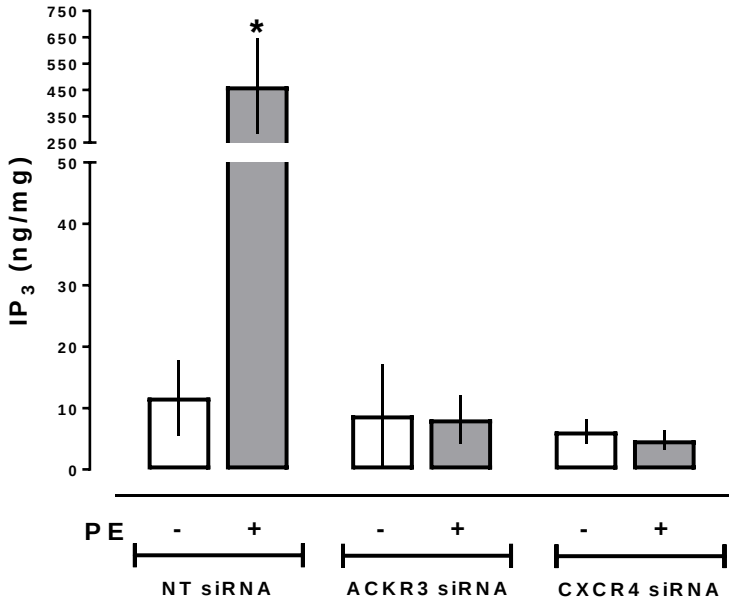

Figure 19. ACKR3 or CXCR4 gene silencing inhibits $\alpha_{1B/D}$-AR $G\alpha_q$-protein mediated signaling in hVSMC. IP_3 production of hVSMC incubated with non-targeting (NT), CXCR4, or ACKR3 siRNA upon stimulation with vehicle or 1 μM PE. n = 3. Data presented as mean ± SEM, Student's t-test with post hoc, *: $p < 0.05$ vs. cells incubated with vehicle.

3.4 ACKR3 Transmembrane Domain (TM) Derived Peptide Analogues Interfere with Heteromerization.

Use of TM derived peptide analogues to disrupt GPCR heteromeric complexes has been well established [83,84,174-176]. We tested whether peptide analogues from the second, fourth, and seventh TM domain (TM 2/4/7) of ACKR3 could interfere with the ACKR3:$\alpha_{1A/B/D}$-AR heteromers in hVSMC. TM 2/4/7 were chosen as these peptide analogues would cover most transmembrane domain interaction surfaces.

Representative PLA images for the visualization of individual receptors and receptor-receptor interactions of hVSMC treated with 10 μM of the TM peptide analogues prior to fixation are shown in Fig. 20A/B. Incubating the hVSMC with the ACKR3 TM peptide analogues did not affect the individual expression of ACKR3, $\alpha_{1A/B/D}$-AR, or CXCR4. Differential effects were observed for the visualization of receptor-receptor interactions. The TM2 peptide analogue significantly decreased ACKR3:$\alpha_{1B/D}$-AR complexes (mean $\pm$ SEM α_{1B}: TM2- 21 $\pm$ 3, vehicle- 78 $\pm$ 10; α_{1D}: TM2- 3 $\pm$ 0.6, vehicle- 33 $\pm$ 7 PLA signals/cell, $p < 0.05$ vs vehicle) yet did not alter ACKR3:α_{1A}-AR complexes (mean $\pm$ SEM α_{1A}: TM2- 18 $\pm$ 3, vehicle- 25 $\pm$ 4 PLA signals/cell, $p > 0.05$ vs vehicle) (Fig. 20D). The TM4 peptide analogue reduced ACKR3:α_{1B}-AR complexes only (mean $\pm$ SEM α_{1B}: TM4- 24 $\pm$ 5 PLA signals/cell, $p < 0.05$ vs vehicle) (Fig. 20D). In contrast, ACKR3:α_{1A}-AR complexes increased when hVSMC were treated with the TM7 peptide analogue while not impacting the ACKR3:$\alpha_{1B/D}$-AR complexes (mean $\pm$ SEM α_{1A}: TM7- 87 $\pm$ 20; α_{1B}: TM7- 94 $\pm$ 21; α_{1D}: TM7- 33 $\pm$ 4 PLA signals/cell, $p < 0.05$ vs vehicle) (Fig. 20D).

ACKR3:CXCR4 heteromers were reduced with all three TM peptides (TM2 > TM4 > TM7) (mean ± SEM TM2- 6 ± 1, TM4- 15 ± 3, TM7- 20 ± 3, vehicle- 38 ± 5 PLA signals/cell, $p < 0.05$ vs vehicle), however, CXCR4:α_{1A}-AR complexes were increased with all three TM peptide analogues (mean ± SEM TM2- 78 ± 13, TM4- 68 ± 9, TM7- 69 ± 9, vehicle- 40 ± 3 PLA signals/cell, $p < 0.05$ vs vehicle) (Fig. 20D). CXCR4:α_{1B}-AR complexes were increased with both TM2 and TM4 peptide analogues, but not with TM7 (mean ± SEM TM2- 112 ± 18, TM4- 97 ± 11, TM7- 70 ± 9, vehicle- 61 ± 6 PLA signals/cell, $p < 0.05$ vs vehicle) (Fig. 20D). The CXCR4:α_{1D}-AR complexes were unaffected by any of the TM peptides (Fig. 20D).

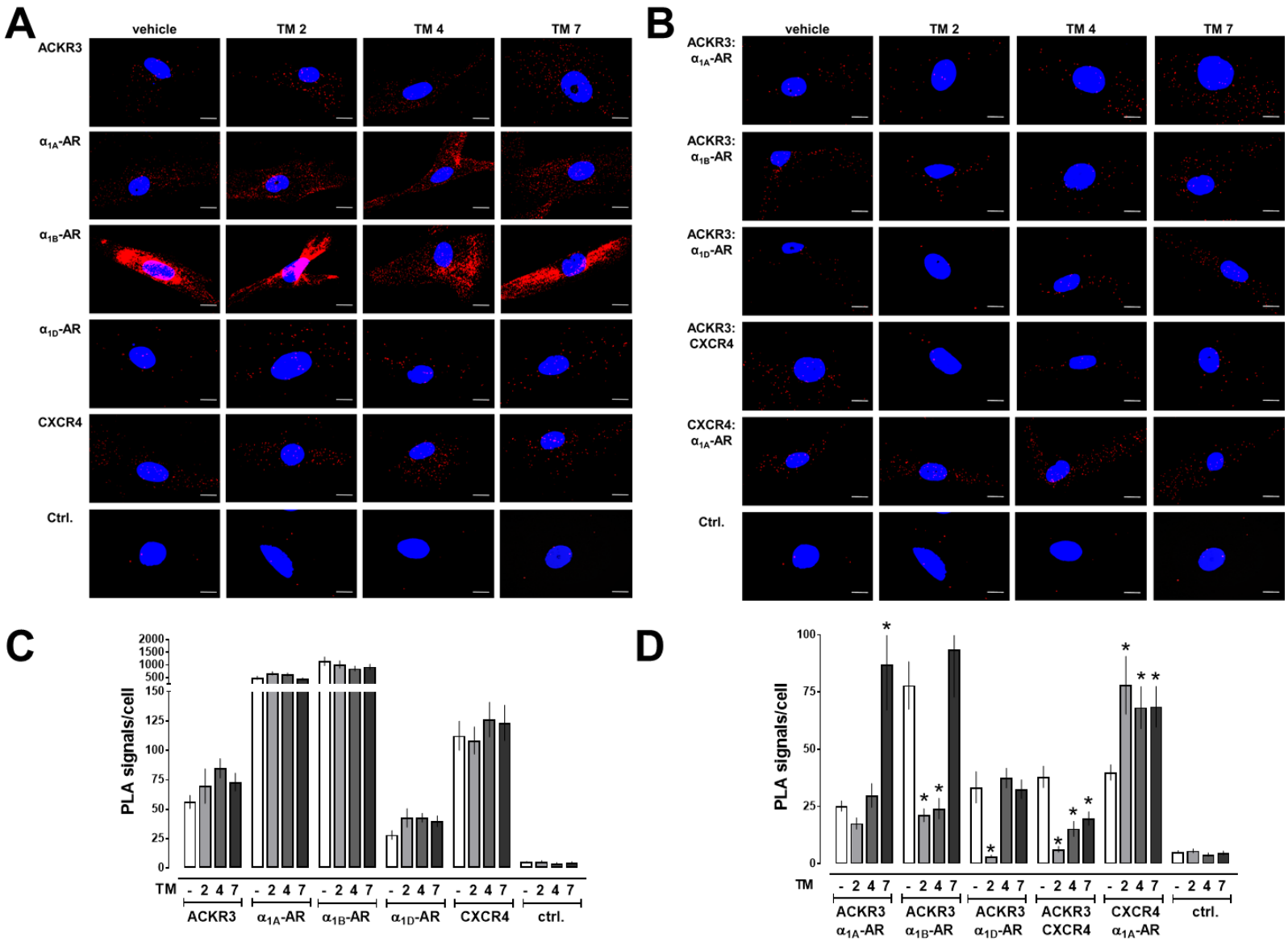
A
vehicle
TM 2
TM 4
TM 7
ACKR3
α1A-AR
α1B-AR
α1D-AR
CXCR4
Ctrl.
B
ACKR3: α1A-AR
ACKR3: α1B-AR
ACKR3: α1D-AR
ACKR3: CXCR4
CXCR4: α1A-AR
Ctrl.
C
PLA signals/cell
TM
- 2 4 7
ACKR3
α1A-AR
α1B-AR
α1D-AR
CXCR4
ctrl.
D
PLA signals/cell
ACKR3 α1A-AR
ACKR3 α1B-AR
ACKR3 α1D-AR
ACKR3 CXCR4
CXCR4 α1A-AR
ctrl.

Figure 20. Peptides derived from transmembrane domains of ACKR3 alter receptor heteromerization in hVSMC. hVSMC were treated with vehicle or TM2/4/7 peptide analogues (10 μM, 30 min at 37°C), washed and used for PLA. **A.** Typical PLA images for the detection of individual receptors. Images show merged PLA/4′,6-diamidino-2-phenylindole dihydrochloride (DAPI) signals. Ctrl: Omission of primary antibody. Scale bars = 10 μm. **B.** Typical PLA images for the detection of receptor-receptor interactions. Images show merged PLA/4′,6-diamidino-2-phenylindole dihydrochloride (DAPI) signals. Ctrl: Omission of one primary antibody. Scale bars = 10 μm. **C.** Quantification of PLA signals per cell for the detection of individual receptors, as in A. n = 3 with n = 10 images per condition and experiment. **D.** Quantification of PLA signals per cell for the detection of receptor-receptor interactions, as in B. n = 3 with n = 10 images per condition and experiment. Data presented as mean ± SEM, One-way ANOVA with Dunnett's multiple comparison post hoc, *: $p < 0.05$ vs. cells incubated with vehicle.

3.5 TM Domain-Derived Peptide Analogues of ACKR3 Interfere with Receptor Function.

To assess how disruption of ACKR3 heteromers, without the loss of individual receptors, affects signaling, we first studied whether the TM peptide analogues alter recombinant ACKR3 activity. Using the PRESTO-Tango assay, ACKR3 was expressed in HTLA cells [171], then treated with the TM peptide analogues (Fig. 21). None of the TM peptides activated ACKR3 (Fig. 21A). When evaluating the role of the TM peptide analogues on CXCL12-mediated β-arrestin 2 recruitment, only the TM2 significantly inhibited β-arrestin 2 recruitment to ACKR3 (EC_{50}: CXCL12 – 2.1 ± 0.45 nM; CXCL12 – TM2 – 37.7 ± 14.1 nM, $p < 0.05$; CXCL12 – TM4 – 14.3 ± 5.4 nM, $p > 0.05$; CXCL12 – TM7 – 3.9 ± 2.0 nM, $p > 0.05$ vs. CXCL12) (Fig. 21B). None of the TM peptide analogues affected PE-induced β-arrestin 2 recruitment to α_{1b}-AR (Fig. 21C).

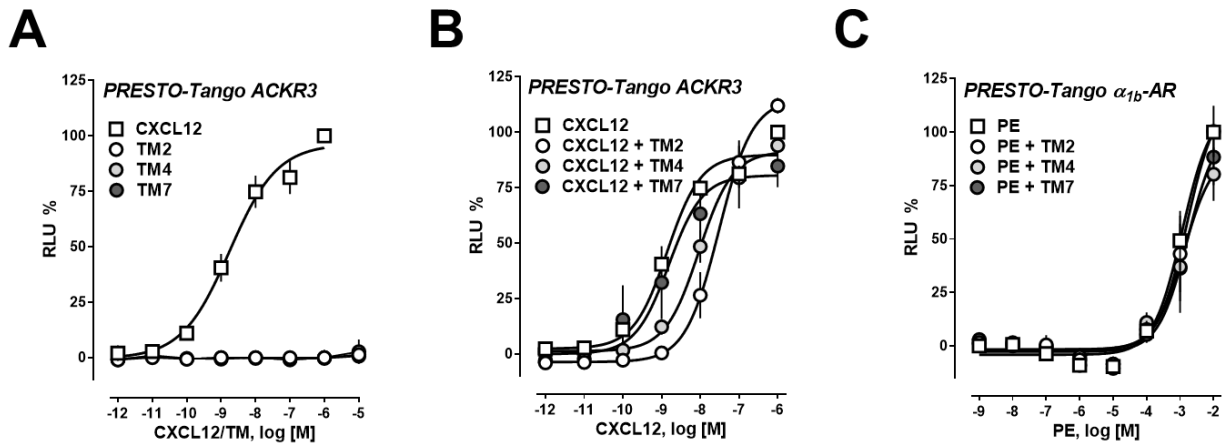

Figure 21. Peptides derived from transmembrane domains of ACKR3 modulate receptor function. A. β-arrestin 2 recruitment assay (PRESTO-Tango) for ACKR3. Cells were treated CXCL12 or TM2/4/7 peptide analogues. RLU (%): relative luminescence units in % of the RLU after treatment with 1 μM CXCL12 (=100%). **B.** β-arrestin 2 recruitment assay (PRESTO-Tango) for ACKR3. Cells were treated CXCL12 or CXCL12 plus 10 μM of the TM2/4/7 peptide analogues. RLU (%): relative luminescence units in % of the RLU after treatment with 1 μM CXCL12 (=100%). **C.** β-arrestin 2 recruitment assay (PRESTO-Tango) for α_{1b}-AR. Cells were treated phenylephrine (PE) or PE plus 10 μM of the TM2/4/7 peptide analogues. RLU (%): relative luminescence units in % of the RLU after treatment with 10 mM PE (=100%). N=3 independent experiments, non-linear regression analysis.

To further evaluate the role of receptor heteromerization, IP_3 production in hVSMC was measured after stimulation with 1μM of PE. hVSMC were pre-treated with 10μM of the TM peptide analogues. The TM2 and TM4 peptide analogues abolished the PE-induced increase in IP_3 production (Fig. 22A). No effect was observed for the hVSMC pre-treated with the TM7 peptide analogue (Fig. 22A). CXCL12 inhibited PE-induced IP_3 responses (Fig. 11, 22B), yet it is unknown whether the TM peptide analogues would alter this response. As observed in Fig. 22B, PE-induced IP_3 production was diminished when hVSMC were pre-treated with 1μM CXCL12 alone and in the presence of 10μM of the TM peptide analogues. The TM2 peptide analogue caused an increase in the

CXCR4:α_{1B}-AR heteromer, and when hVSMC were treated with CXCL12, an agonist for both ACKR3 and CXCR4 [96,97,102,103,123], no increase in IP_3 was observed upon PE stimulation (Fig. 22B).

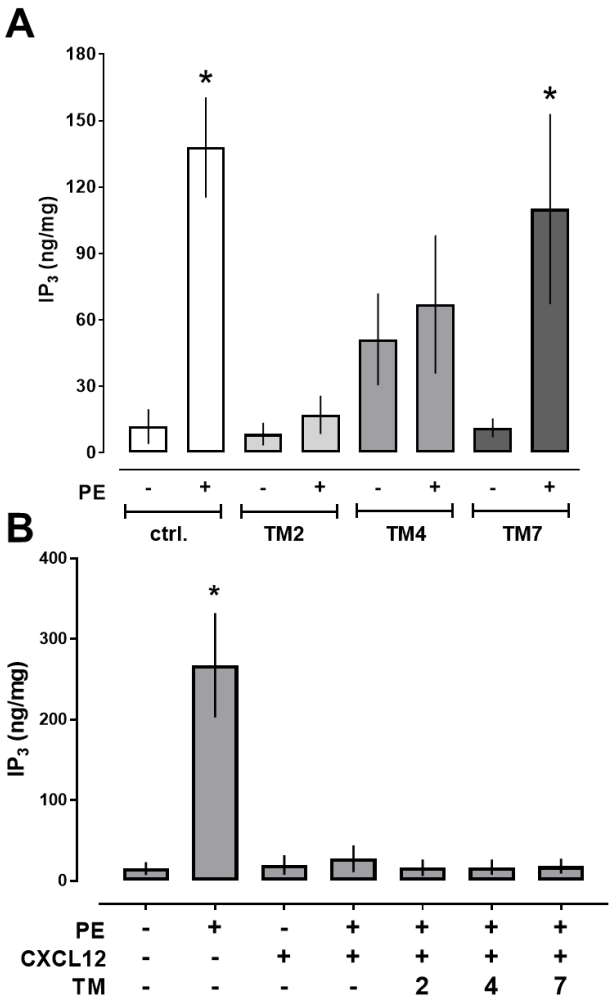

Figure 22: Peptides derived from transmembrane domains 2/4 of ACKR3 inhibit receptor function. A. Inositol trisphosphate (IP_3) production was measured in hVSMC pretreated with vehicle or the TM2/4/7 peptide analogues (10 µM, 30 min at 37°C) and then stimulated with vehicle or 1 µM PE for 5 min. * $p < 0.05$ vs vehicle/no PE; #: $p<0.05$ vs. vehicle plus PE, n = 4 independent experiments. **B.** IP_3 production was measured in hVSMC pretreated with vehicle or the TM2/4/7 peptide analogues (10 µM, 30 min at 37°C) plus vehicle or CXCL12 (1 µM, 15 min at 37°C) and then stimulated with vehicle or 1 µM PE for 5 min. n=4 independent experiments. Data presented as mean ± SEM, Student's t-test with post hoc, *: $p < 0.05$ vs. cells incubated with vehicle.

To evaluate if the IP_3 data in hVSMC correspond to effects on intrinsic vascular function, we tested the effects of the ACKR3 TM peptide analogues in isolated rat mesenteric arteries. Third to fourth order mesenteric arteries were isolated and pressurized to 80mmHg in pressure myography. Vessels were pre-treated with 10 μM or 100 μM TM peptide analogues followed by a dose response to PE. None of the ACKR3 TM peptide analogues elicited an effect on PE-induced at 10 μM, however at 100 μM the TM2 peptide analogue significantly decreased the potency of PE to induce vasoconstriction (EC_{50} for PE: vehicle 1.8 $\pm$ 0.5 μM; TM2 6.3 $\pm$ 0.3 μM, $p < 0.05$ vs. vehicle; TM4 3.0 $\pm$ 0.7 μM, $p > 0.05$ vs. vehicle; TM7 4.2 $\pm$ 1.7 μM, $p > 0.05$ vs vehicle) (Fig. 23).

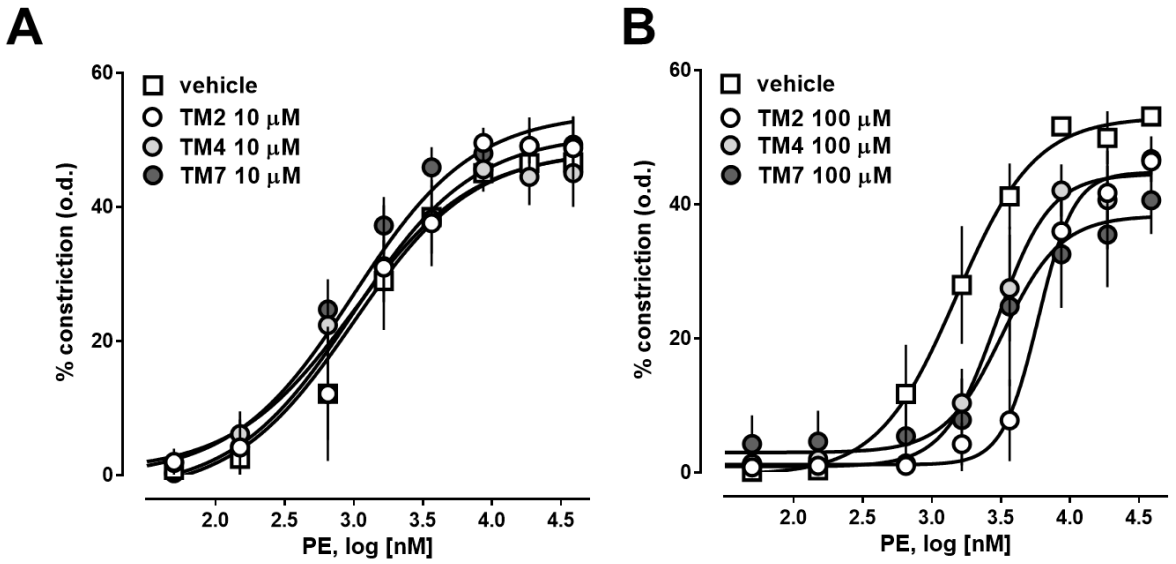

Figure 23: ACKR3 TM2 peptide antagonizes PE-induced vasoconstriction. A/B. Pressure myography with rat mesenteric arteries. Arteries were pressurized to 80 mmHg and pre-treated with vehicle, 10 μM (**A**) or 100 μM (**B**) of the TM2/4/7 peptide analogues. Increasing concentrations of PE were then added to the vessel bath and dose-response curves generated. % o.d.: Outer artery diameter (o.d.) in % of the o.d. in the absence of PE. N=3 independent experiments, data analyzed via non-linear regression analysis.

Discussion

In this chapter, it was demonstrated that heteromeric complexes between $\alpha_{1AB/D}$-AR and ACKR3 are constitutively expressed in hVSMC. The data imply that hetero-oligomerization between $\alpha_{1A/B/D}$-AR and ACKR3:CXCR4 is necessary for $\alpha_{1B/D}$-AR function (Fig. 24). Additionally, the findings show that the formation of GPCR complexes within the plasma membrane is a dynamic process that depends on the relative abundance and affinity between available receptor partners (Fig. 24).

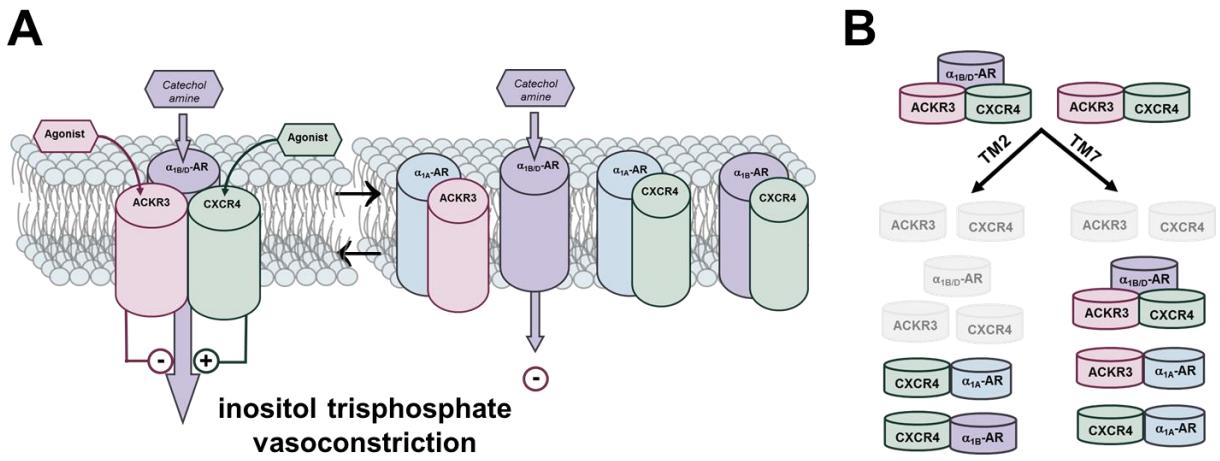

Figure 24. Working model of ACKR3:CXCR4:α_1-AR hetero-oligomeric complex. **A.** Hetero-oligomeric complexes between $\alpha_{1B/D}$-AR and the ACKR3:CXCR4 heteromer are responsible for $\alpha_{1B/D}$-AR signaling in hVSMC. Activation of ACKR3 inhibits, whereas CXCR4 activation sensitizes this response via allosteric modulation within the hetero-oligomeric complex. Disruption of this complex ablates $\alpha_{1B/D}$-AR signaling and shifts the pattern of receptor heteromerization within the network towards a new equilibrium, which allows for heteromerization between α_{1A}-AR with the ACKR3 protomer or the CXCR4 homodimer. **B.** Disruption of the hetero-oligomeric complex with TM peptides leads to assembly of newly formed heteromers.

The observation that ACKR3 agonists ablate α_1-AR mediated IP_3 production is consistent with our laboratory's previous findings [114] on the effects of ACKR3 agonists on PE-induced constriction of isolated resistance arteries, thus confirming functional cross-talk between ACKR3 and α_1-AR in hVSMC. Therefore, these data suggest that ACKR3 activation inhibits α_1-AR mediated signaling.

CXCL12 activates both ACKR3 or CXCR4 [97], however, consistent with our previous findings [114], CXCL12 preferentially acts as an ACKR3 agonist in hVSMC. This behavior could be due to higher binding affinity to ACKR3 than CXCR4 [97] or it may be due to increased density of ACKR3 than CXCR4 present on the surface of hVSMC [51]. CXCL12 enhanced the potency of PE to raise blood pressure in normal animals via activation of CXCR4, which could indicate that the function of CXCL12 depends on the relative contribution of CXCR4 and ACKR3 to the specific experimental or pathophysiological environment [84].

ACKR3 and α_1-AR are located within a proximity to allow for direct physical interactions to occur as evidenced by PLA and co-immunoprecipitation studies. The results of the present study that siRNA knockdown of either ACKR3 or CXCR4 reduces heteromeric complexes between ACKR3:$\alpha_{1B/D}$-AR and between CXCR4:$\alpha_{1B/D}$-AR indicates that hetero-oligomeric complexes between ACKR3:CXCR4:$\alpha_{1B/D}$-AR are necessary for $\alpha_{1B/D}$-AR function. This conclusion was reinforced by the findings with the ACKR3 TM2 peptide analogue. TM2 disrupted ACKR3:$\alpha_{1B/D}$-AR and ACKR3:CXCR4 complexes in hVSMC, eliminated PE-induced IP_3 production, abolished PE-mediated vasoconstriction

in isolated rat mesenteric arteries, and increased the number of CXCR4:$\alpha_{1A/B}$-AR heteromers (Fig. 24).

Interference of ACKR3 heteromerization through either ACKR3 knockdown or TM peptide analogues selectively disrupted some heteromers while increasing the proportion of other ACKR3 or CXCR4 heteromeric complexes. The data indicate that $\alpha_{1B/D}$-AR form complexes with the ACKR3:CXCR4 heteromer, yet α_{1A}-AR forms heteromeric complexes with the ACKR3 protomer and/or CXCR4 homodimer. Complete ablation of either ACKR3 or CXCR4 in hVSMC was not achieved via gene silencing approaches. Interactions with α_{1A}-AR may be favored over heteromerization with $\alpha_{1B/D}$-AR and it is only when reduction of ACKR3 or CXCR4 falls below a specific threshold that changes in α_{1A}-AR heteromerization can be observed. Additionally, it is also plausible that α_{1A}-AR are not physically connected to ACKR3 or CXCR4 and are instead stabilized by other proteins within the same microdomain. Therefore, GPCR heteromerization is a dynamic process, wherein interference with heteromers shifts the pattern of complex formation within the entire receptor network towards a new equilibrium. Assuming that heteromerization modulates the pharmacological properties of each receptor partner, such regulation implies that receptor function is rapidly adapted to the specific environment.

In conclusion, we provide evidence that ACKR3 and α_1-AR engage in receptor cross-talk, demonstrate recombinant and native receptors form heteromeric complexes, and provide initial functional characterization through disruption of heteromerization via

ACKR3 knockdown and TM peptide analogues. The biochemical fingerprint of α_1-AR is ablated when the ACKR3-CXCR4 hetero-oligomeric complex is perturbed, thus these findings fulfill the recently proposed criteria to validate novel heteromeric complexes in native tissues [62].

These studies provide novel insight into the molecular mechanisms governing α_1-AR function and stress the importance of heteromerization on GPCR function. Moreover, it was demonstrated that hetero-oligomerization of endogenous GPCRs is a dynamic process, which may be responsible for biologic variability of medications targeting GPCRs. The results from these studies could allow for the development of new therapeutic strategies targeting the hetero-oligomeric ACKR3:CXCR4:α_1-AR complexes, which would be beneficial for treating vascular dysfunction.

CHAPTER 4

IDENTIFICATION AND FUNCTIONAL CHARACTERIZATION OF ACKR3:AVPR1A HETEROMERS IN VASCULAR SMOOTH MUSCLE

Introduction

Multiple lines of evidence have suggested that the GPCRs CXCR4 and ACKR3 are crucial for the regulation of vascular function in both healthy and pathological states [81,83,84,94,104,114,169,170]. Recently, our laboratory reported that CXCR4 sensitizes α_1-AR mediated vasoreactivity, whereas ACKR3 antagonizes this effect [83,114]. We then demonstrated that the hetero-oligomeric ACKR3:CXCR4:α_1-AR complex is essential for α_1-AR function [82]. Furthermore, our laboratory determined that simultaneous activation of ACKR3 and inhibition of CXCR4 via the synthetic ligand TC14012 results in vasodilatory shock and cardiovascular collapse in normal animals [114]. These effects are unlikely to be solely attributed to ACKR3 inhibition of α_1-AR in vascular smooth muscle, therefore suggesting additional interactions between ACKR3 and the vasoactive neurohormonal system.

Numerous studies indicate interactions between CXCL12 and aVP in the central nervous system [65,68,80,99,159,160]. However, to date, no information exists about the role of AVPR1A and chemokine receptors on cardiovascular function. Thus, we tested whether AVPR1A cross-talks with ACKR3 and/or CXCR4 in vascular smooth muscle.

Here we provide evidence that endogenous ACKR3 forms heteromeric complexes on hVSMC with AVPR1A. We demonstrate that these heteromers facilitate AVPR1A-mediated $G\alpha_q$-mediated IP_3 release and modulate aVP-induced β-arrestin 2 recruitment to AVPR1A. Additionally, it was determined that activation of ACKR3 antagonizes aVP-mediated IP_3 production and vasoconstriction in isolated rat mesenteric arteries. Finally, it was observed that activation of either ACKR3 or AVPR1A leads to co-internalization of both receptors in native cells. Together, these data suggest that ACKR3 negatively regulates AVPR1A-mediated signaling in hVSMC.

Results

4.1 Activation of ACKR3 Antagonizes aVP-Mediated $G\alpha_q$-Signaling and Function in Vascular Smooth Muscle.

Pressure myography was utilized to evaluate if ACKR3 and/or CXCR4 activation influences aVP-mediated constriction of rat isolated mesenteric resistance vessels. A functional interaction between ACKR3, CXCR4, and α_1-AR was previously demonstrated (Chapter 3) [82,84,114]. Thus, PE-induced vasoconstriction served as a positive control. CXCL12, CXCL11, and ubiquitin have previously been characterized in pressure myography experiments; these agonists do not induce vasoconstriction alone [114]. Vessels were pre-constricted to 50% with either PE or aVP, then agonists for ACKR3 (CXCL11/12) or CXCR4 (ubiquitin) were added to the vessel bath, and the changes in outer diameter were recorded. CXCL11 antagonized α_1-AR-mediated vasoconstriction, whereas activation of CXCR4 via ubiquitin [95,96] enhanced the PE-induced

vasoconstriction (mean ± SEM, CXCL11 68.9 ± 9.5; ubiquitin -36.6 ± 6.7 % change $p < 0.05$ for both vs. veh.) (Fig. 25A). Ubiquitin failed to affect aVP-mediated vasoconstriction, whereas CXCL11 treatment antagonized aVP-mediated vasoconstriction (mean ± SEM, CXCL11 94.2 ± 7.1; ubiquitin 9.4 ± 13.3 % change $p < 0.05$ for CXCL11 vs. veh.) (Fig. 25B). To further explore receptor cross-talk the effects of CXCL12 and a CXCL11 mutant were tested. CXCL12 is an agonist for both ACKR3 and CXCR4. $CXCL11_{3\text{-}73}$, an N-terminal truncated form of CXCL11 which lacks the first two amino acids, that are essential for signaling, was also tested [177,178]. The ability of these agonists to recruit β-arrestin 2 to ACKR3 in the PRESTO-tango assay [171] was established to compare the activity of these ACKR3 ligands. CXCL12 exhibited a higher potency to recruit β-arrestin 2 to ACKR3 (EC_{50} (95% CI) 1.3 (0.8-2.1) nM) than CXCL11(EC_{50} (95% CI) 2.9 (2.1-4.0) nM, $p < 0.01$). Both agonists displayed comparable efficacy. However, $CXCL11_{3\text{-}73}$ had significantly reduced efficacy and potency to recruit β -arrestin 2 to ACKR3 (EC_{50} (95% CI) 11(4-240) nM, top plateau 65 ± 7 % RLU, $p < 0.01$ for both vs. CXCL11 and CXCL12) (Fig. 26). When these agonists were used in pressure myography experiments, CXCL11 and CXCL12 significantly antagonized PE and aVP-mediated vasoconstriction (mean ± SEM, PE-CXCL11 72.7 ± 8.9; PE-CXCL12 42.6 ± 14.7; aVP-CXCL11 103.6 ± 22.6; aVP-CXCL12 64.2 ± 14.0 % change $p < 0.05$ for both vs. veh.) (Fig. 25C/D). $CXCL11_{3\text{-}73}$ had no significant effect of PE or aVP-mediated vasoconstriction (mean ± SEM, PE-$CXCL11_{3\text{-}73}$ 21.4 ± 11.2; aVP-$CXCL11_{3\text{-}73}$ 15.5 ± 13.6 % change $p > 0.05$ for $CXCL11_{3\text{-}73}$ vs. veh.) (Fig. 25C/D). These data

suggest that activation of ACKR3 antagonizes AVPR1A-induced vasoconstriction, yet CXCR4 activation had no significant effect on AVPR1A-induced vasoconstriction.

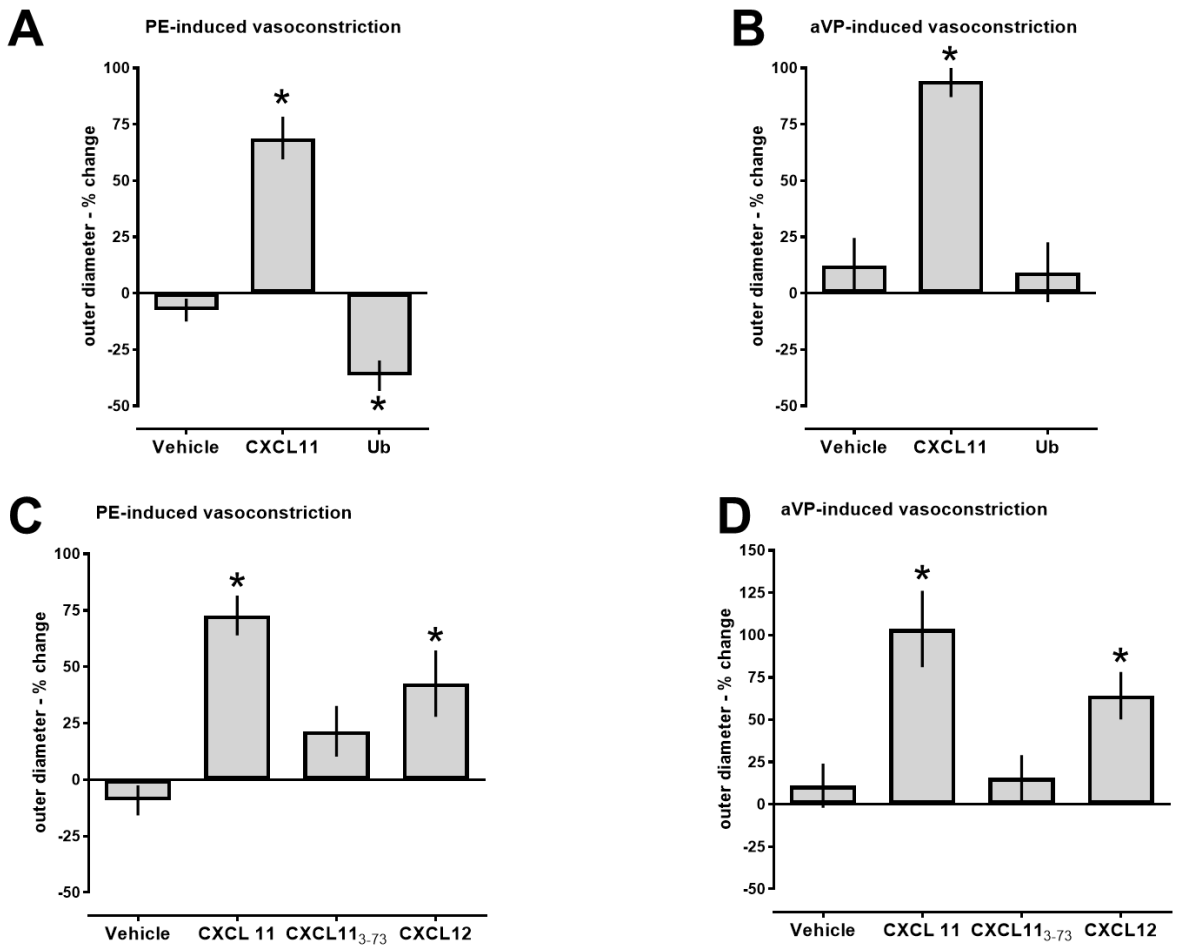

Figure 25. ACKR3 agonists antagonize aVP-mediated function in vascular smooth muscle. Pressure myography with rat mesenteric arteries. Arteries were pressurized to 80 mmHg, pre-constricted with 2 μM PE (***A***) or 0.5 nM aVP (***B***), followed by the addition of vehicle (*n* = 4) or 10 μM of CXCL11 (*n* = 6) or ubiquitin (*n* = 7). Outer diameter % change: percent change in outer diameter after the addition of the CXCR4/ACKR3 ligands. **p* < 0.05 vs. vehicle. (***C***) Pressure myography experiments as in (***A***); PE-induced vasoconstriction. All ACKR3 ligands were tested at a concentration of 10 μM. Vehicle (*n* = 5), CXCL11 (*n* = 7), CXCL11 (3–73) (*n* = 9) and CXCL12 (*n* = 14). **p* < 0.05 vs. vehicle. (***D***) Pressure myography experiments as in (***B***); aVP-induced vasoconstriction. All ACKR3 ligands were tested at a concentration of 10 μM. Vehicle (*n* = 4), CXCL11 (*n* = 3), CXCL11 (3–73) (*n* = 3) and CXCL12 (*n* = 3). **p* < 0.05 vs. vehicle. Data presented as mean ± SEM, One-way ANOVA with Dunnett's multiple comparison post hoc, *: p < 0.05 vs. vehicle.

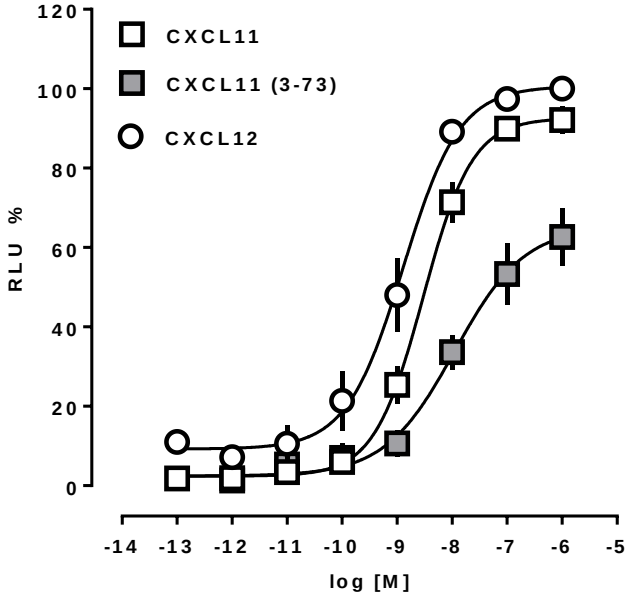

Figure 26. ACKR3 agonists recruit β-arrestin 2 to ACKR3 in HTLA cells. B-arrestin 2 recruitment assay (PRESTO-Tango) for ACKR3. HTLA cells were treated with CXCL12, CXCL11, or CXCL11 (3-73). RLU (%): relative luminescence units in % RLU after treatment with 1 μM CXCL12 (=100%). n=3 independent experiments. Data analyzed via non-linear regression analysis.

To ascertain whether this receptor cross-talk occurred at the level of $G\alpha_q$ signaling, IP_3 production in hVSMC was measured. aVP stimulation of hVSMC increased cellular IP_3 concentrations 8.3-*fold* (Fig. 27). Pretreatment of cells with 10μM CXCL12, CXCL11, and TC14012 abolished this response, indicating that ACKR3 activation inhibits AVPR1A mediated signaling. The same pattern of inhibition of $G\alpha_q$-mediated signaling by ACKR3 was observed in hVSMC with α_1-AR mediated IP_3 production (Chapter 3, Fig. 11). Taken together, the pressure myography studies and hVSMC $G\alpha_q$ signaling data indicate that activation of ACKR3 ablates AVPR1A-mediated effects.

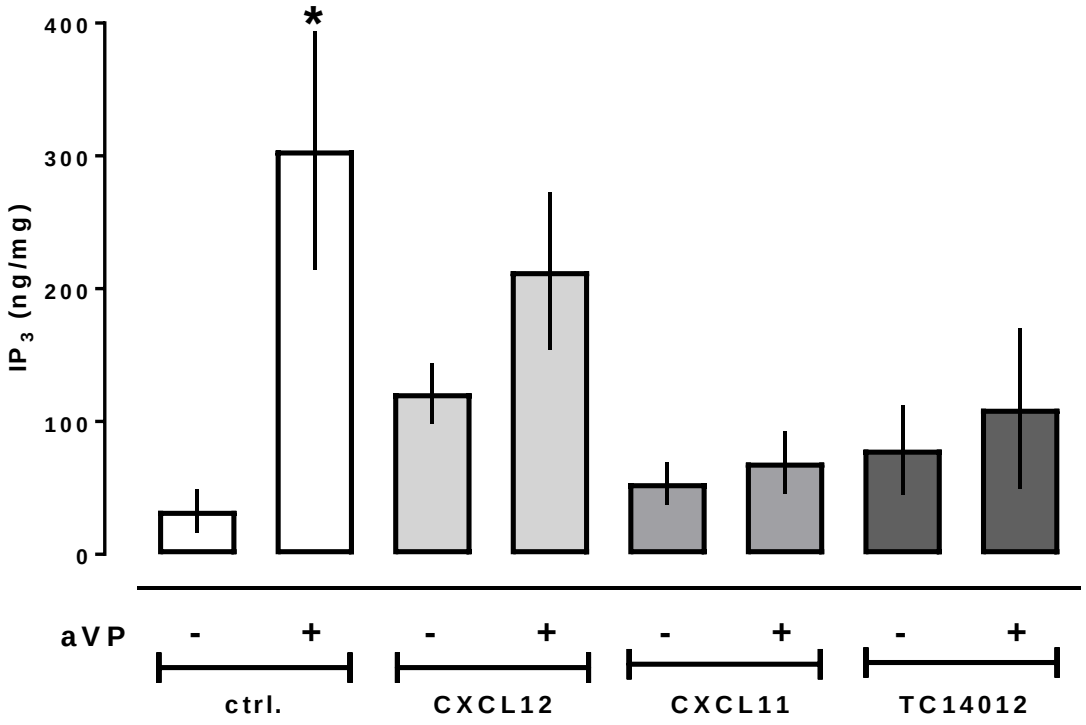

Figure 27. ACKR3 agonists attenuate aVP-mediated G-protein signaling in hVSMC. hVSMC were pre-treated with either vehicle (ctrl.) or ACKR3 ligands (1 μM, 15 min) and then stimulated with 1 μM aVP for 5 min. Inositol trisphosphate (IP_3) production was measured by ELISA. n=4. Data presented as mean ± SEM, Student's t-test with post hoc, *: $p < 0.05$ vs. cells incubated with vehicle.

4.2 ACKR3 Forms Heteromeric Complexes with AVPR1A.

Previously, we established that α_1-AR exist in hetero-oligomeric receptor complexes with ACKR3 and CXCR4 [82]. Therefore, we tested whether ACKR3 and CXCR4 can form heteromeric complexes with AVPR1A. Recombinant N-terminal FLAG-tagged ACKR3 or CXCR4 was co-expressed with HA-tagged AVPR1A in HEK 293T cells and PLA was used to visualize and quantify receptor-receptor interactions as well as individual receptors at single molecule resolution. FLAG-ACKR3 formed interactions with HA-AVPR1A (mean ± SEM 34 ± 4 PLA signals $p < 0.05$ vs. ctrl) (Fig. 28). However, when

FLAG-CXCR4 was co-expressed with HA-AVPR1A, statistically significant signals were not observed compared to our negative control (mean + SEM 11 ± 2 PLA signals, $p > 0.05$ vs ctrl (6 ± 1)). We could, however, detect significant signals for HA-AVPR1A and FLAG-CXCR4 individual receptors in these cells (Fig. 28). To confirm PLA findings, HA-AVPR1A was immunoprecipitated with anti-HA antibodies, then immunoblotted for FLAG-ACKR3 using anti-FLAG antibodies (Fig. 29A). As shown in Fig. 29A, when the cell lysate was probed with anti-HA, a band below 50kDa was detected along with higher molecular mass aggregates. A similar pattern was observed when immunoblotting with anti-FLAG antibodies (Fig. 29A right). BRET experiments have been the gold-standard for the detection of recombinant GPCR heteromers [18,36,53,179]. Thus, we utilized AVPR1A-hRluc (Renilla reniformis), enhanced yellow fluorescent protein (EYFP), and ACKR3-EYFP for intermolecular BRET assays (Fig. 29B/C). When EYFP and AVPR1A-hRuc were co-expressed, the BRET signal was low and increased linearly with increasing acceptor:donor ratios, which is consistent with non-interacting proteins (Fig. 29B). When AVPR1A-hRlu was co-expressed with ACKR3-EYFP, a hyperbolic progression of the BRET signal with increasing acceptor:donor ratios (Fig. 29B) was detectable. The BRET signal was independent of the concentrations of BRET partners when tested at a fixed acceptor:donor ration (Fig. 29C), indicating constitutive heteromerization [53]. These observations suggest that recombinant ACKR3 interacts with recombinant AVPR1A when co-expressed.

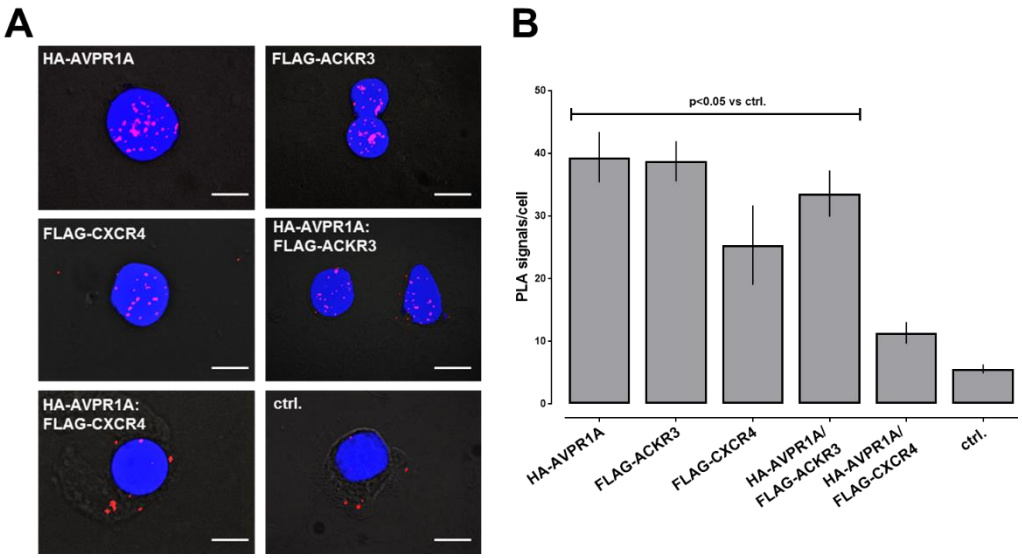

Figure 28. ACKR3 forms heteromeric complexes with AVPR1A in HEK 293T cells. **A.** Typical PLA images for the detection of individual receptors and receptor-receptor interactions in HEK293T cells transfected with DNA encoding HA- or FLAG-tagged receptors. Ctrl: Cells transfected with pcDNA3. Images show merged PLA/4′,6-diamidino-2-phenylindole dihydrochloride (DAPI) signals. Scale bars = 10 µm. **B.** Quantification of PLA signals per cell as in A. n=3 independent experiments with n=10 images per condition and experiment. Data presented as mean ± SEM, One-way ANOVA with Dunnett's multiple comparison post hoc, *: $p < 0.05$ vs. ctrl.

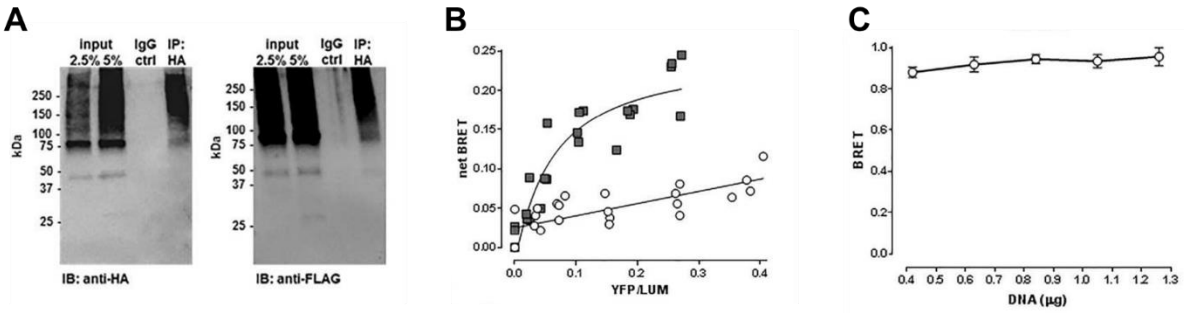

Figure 29. Recombinant ACKR3 and AVPR1A interact. (**A**) HEK293T cells expressing HA-AVPR1A and FLAG-ACKR3 were lysed (input), the lysate was immunoprecipitated (IP) with anti-HA, followed by immunoblotting (IB) to detect HA-AVPR1A (left) and FLAG-ACKR3 (right) in the IP samples. IP control: precipitate after incubation of cell lysates with IgG-coupled resin. (**B,C**) Intermolecular BRET assays. Cells were co-transfected with AVPR1A-hRluc plus EYFP (open circles) or ACKR3-EYFP (grey squares) at various acceptor:donor ratios (**B**) and with increasing amounts of AVPR1A-hRluc and ACKR3-EYFP at a constant ratio of 1:10 (**C**). n=3 independent experiments.

To assess whether endogenous ACKR3 can form heteromeric complexes with AVPR1A, PLA was utilized to visualize individual receptors and receptor-receptor interactions using a combination of anti-ACKR3, anti-CXCR4, and anti-AVPR1A antibodies. Consistent with the findings in the expression system, ACKR3 and AVPR1A are located within close proximity to form interactions (mean $\pm$ SEM 61 $\pm$ 7 PLA signals $p < 0.05$ vs. ctrl), whereas CXCR4 and AVPR1A do not form significant interactions in hVSMC when compared to control (mean $\pm$ SEM 18 $\pm$ 2 PLA signals, $p > 0.05$ vs ctrl (3 $\pm$ 1)) (Fig. 30). Omission of one primary antibody served as a negative control (Fig. 30). To ensure that the PLA signals corresponded to extracellular receptors or receptor-receptor interactions, we stained for phosphorylated (Ser-19) myosin light chain (pMLC) 2, an intracellular protein (Fig. 30). When hVSMC were permeabilized, positive signals for pMLC2 were detected, yet were absent in non-permeabilized cells (Fig. 30). This provides an additional layer of evidence that the PLA signals detected for GPCRs are located on the extracellular leaflet of the plasma membrane. This assumption is supported by a 3D reconstruction of the PLA signals from deconvolved z-stack images for the ACKR3:AVPR1A interaction (Fig. 30). All of the signals were localized within a single plane.

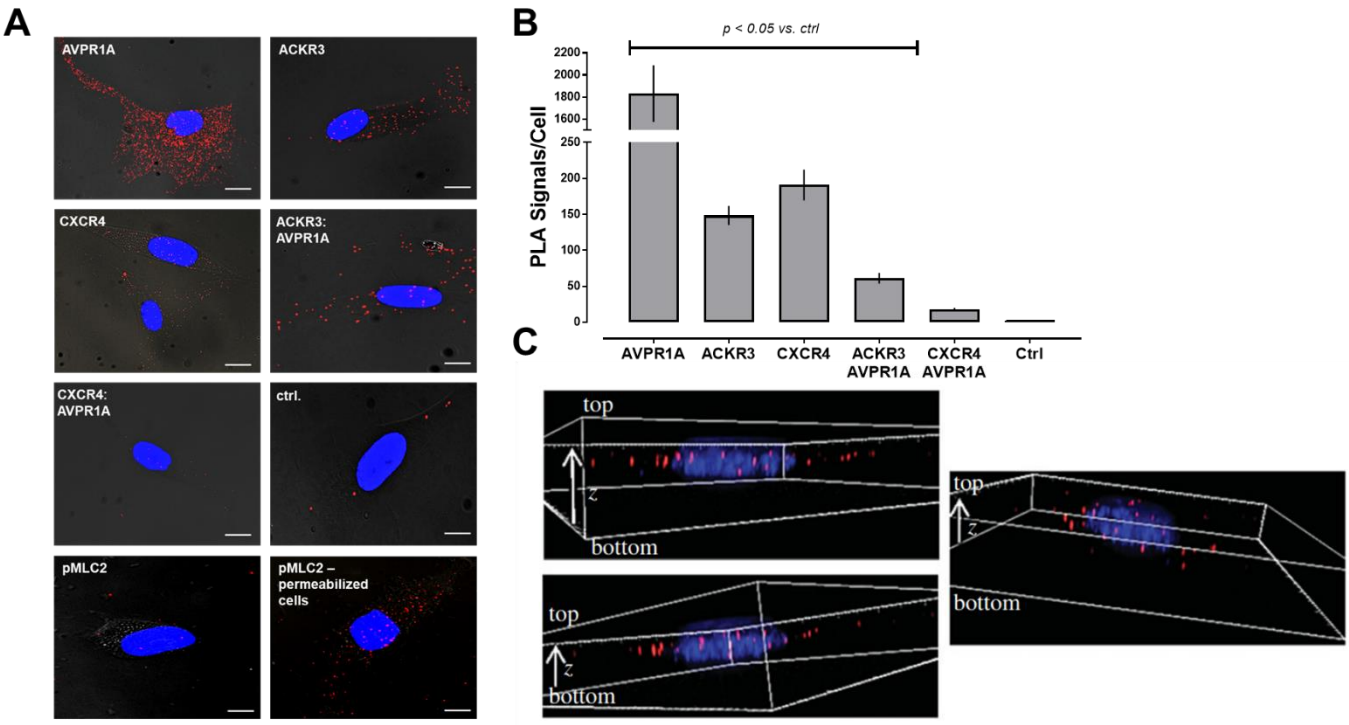

Figure 30. ACKR3 forms heteromeric receptor complexes with AVPR1A in hVSMC. **A.** Representative PLA images for the detection of individual receptors and receptor-receptor complexes in hVSMC. Ctrl: Omission of one primary antibody. Images show merged PLA/4′,6-diamidino-2-phenylindole dihydrochloride (DAPI) signals. Scale bars = 10 µm. **B.** Quantification of PLA signals per cell as in A. n=4 independent experiments with n=10 images per condition and experiment. **C.** Three-dimensional representations of ACKR3:AVPR1A interactions in hVSMC. Deconvolved images were generated from z-stack images (n = 20; thickness: 0.5 µm, bottom to top). Images show merged PLA/DAPI signals. Data presented as mean ± SEM, One-way ANOVA with Dunnett's multiple comparison post hoc, *: $p < 0.05$ vs. ctrl.

Confirmation of PLA findings was then achieved via immunoprecipitation of AVPR1A, followed by subsequent immunoblotting for ACKR3, CXCR4, and β_2-AR. AVPR1A could be immunoprecipitated with anti-AVPR1A from hVSMC lysate (Fig. 31). Both ACKR3 and CXCR4 could also be immunoprecipitated with anti-AVPR1A (Fig. 31). β_2-AR was utilized as a negative control. This receptor is abundantly expressed in hVSMC but it is a GPCR that can not be immunoprecipitated with AVPR1A.

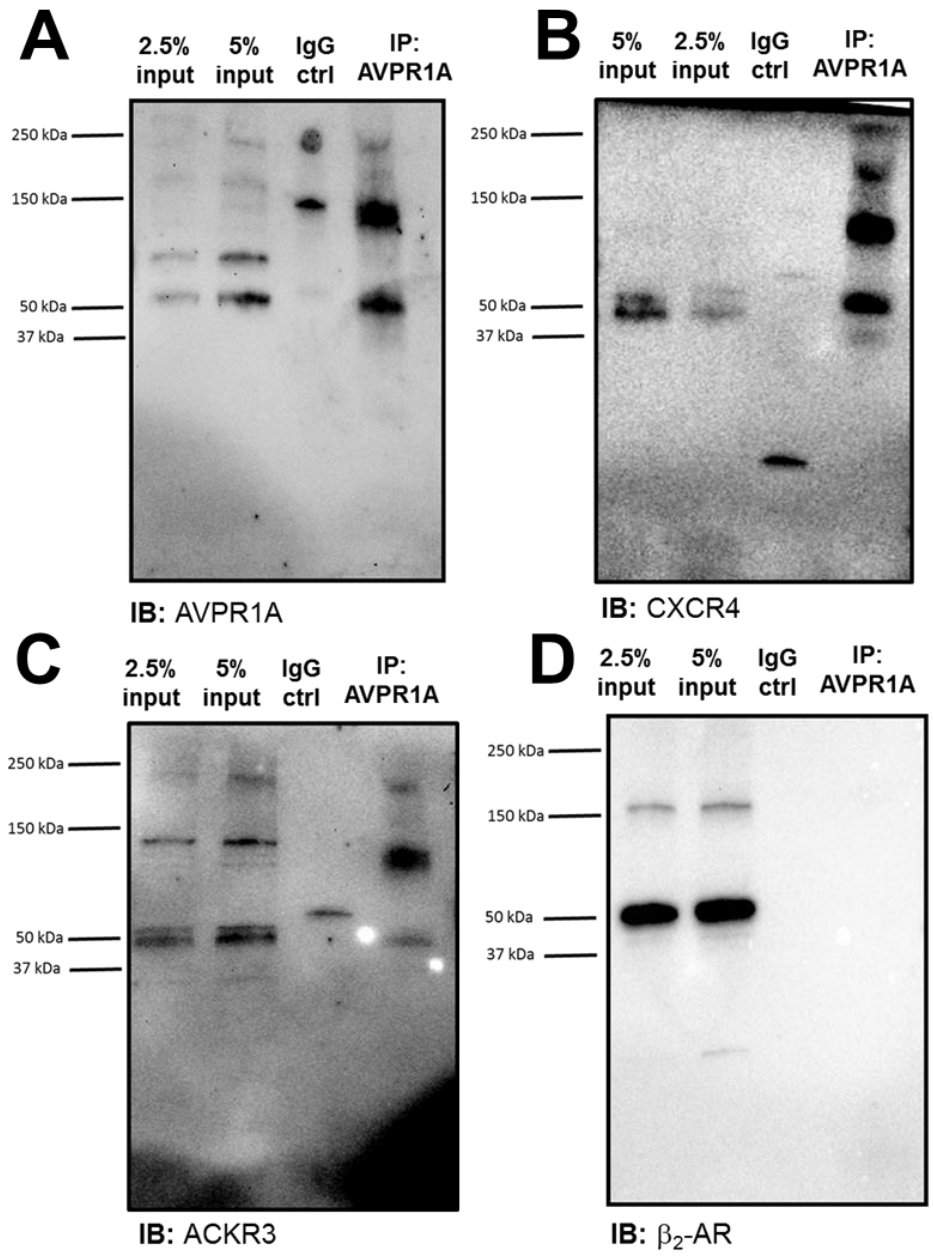

Figure 31. ACKR3 can be immunoprecipitated with AVPR1A in hVSMC. A-D. hVSMC were lysed (=input) and AVPR1A was immunoprecipitated (IP) followed by immunoblotting (IB) to detect AVPR1A (**A**), CXCR4 (**B**), ACKR3 (**C**), and β_2-AR (**D**) in the IP samples. IP control: precipitate after incubation of cell lysates with IgG-coupled resin. Images are representative of n=4 independent experiments.

4.3 Depletion of ACKR3:AVPR1A Heteromers by ACKR3 Gene Silencing Increases AVPR1A:CXCR4 Interactions and Inhibits aVP-Induced $G\alpha_q$-Signaling.

To assess the functional role of the ACKR3:AVPR1A heteromeric complex, ACKR3 gene silencing was utilized to disrupt ACKR3:AVPR1A heteromers in hVSMC. Representative PLA images and the quantification for the detection of individual receptors and receptor-receptor interactions on hVSMC after incubation with either NT or ACKR3 siRNA are shown in Fig.32. ACKR3 siRNA reduced the number of PLA signals corresponding to ACKR3 by over 60%, as compared with cells incubated with NT siRNA. Incubation of hVSMC with ACKR3 siRNA did not alter the expression of AVPR1A or CXCR4 compared to NT siRNA (Fig. 32). Reducing ACKR3 from the cell surface significantly decreased the expression of ACKR3:AVPR1A heteromers by 80% (mean $\pm$ SEM ACKR3 siRNA 21 $\pm$ 4, NT siRNA 155 $\pm$ 43 PLA signals/cell, $p < 0.05$ vs. NT siRNA) (Fig. 32). As a positive control the ACKR3:CXCR4 heteromeric complex changes were visualized and a 50% decrease in ACKR3:CXCR4 heteromers was observed in the ACKR3 siRNA treated cells compared to NT siRNA (mean $\pm$ SEM ACKR3 siRNA 27 $\pm$ 3, NT siRNA 46 $\pm$ 3 PLA signals/cell, $p < 0.05$ vs. NT) (Fig. 32). Remarkably, hVSMC treated with ACKR3 siRNA had PLA signals corresponding to CXCR4:AVPR1A interactions rise to 510% of PLA signals corresponding to hVSMC incubated with NT siRNA (mean $\pm$ SEM ACKR3 siRNA 146 $\pm$ 20, NT siRNA 28 $\pm$ 3 PLA signals/cell, $p < 0.05$ vs. NT) (Fig. 32).

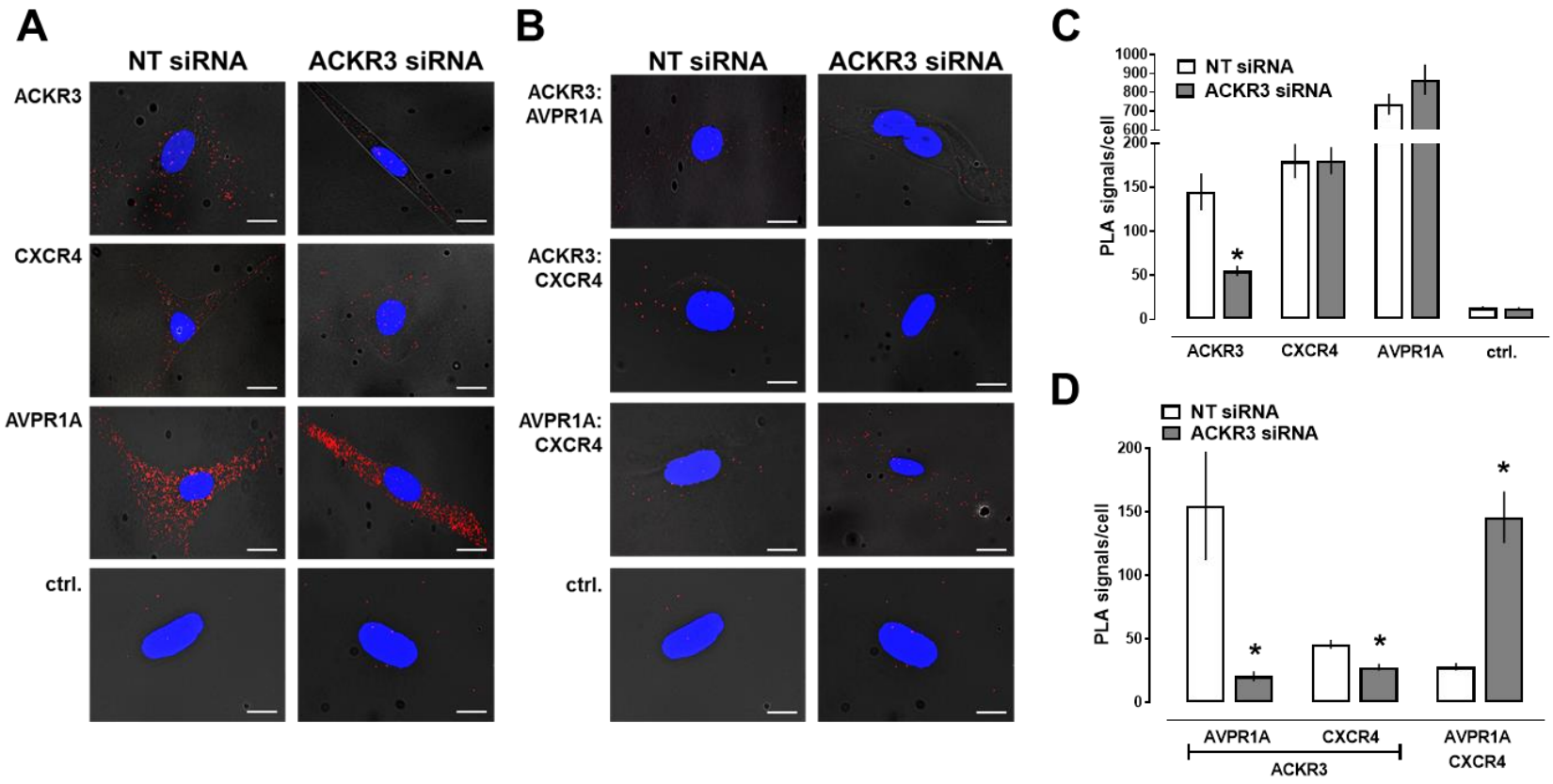

Figure 32. ACKR3 gene silencing reduces ACKR3:AVPR1A and ACKR3:CXCR4 heteromers and increases AVPR1A:CXCR4 interactions. A/B. Representative PLA images for the detection of individual receptors (**A**) and receptor-receptor interactions (**B**) in hVSMC after incubation with non-targeting (NT) or ACKR3 siRNA. Ctrl: Omission of one primary antibody. Images show merged PLA/4′,6-diamidino-2-phenylindole dihydrochloride (DAPI) signals. **C/D**. Quantification of PLA signals per cell for the detection of individual receptors (**C**) and receptor-receptor interactions (**D**) as in A/B. n=4 independent experiments with n=10 images per condition and experiment. Data presented as mean ± SEM, Student's t-test with post hoc, *: $p < 0.05$ vs. NT siRNA

To confirm these observations, the ACKR3 silencing experiments were repeated using the rat VSMC line A7r5. Fig. 33 shows representative images for the detection of individual receptors and receptor-receptor interactions. While the rat and human ACKR3 have 93% sequence identity, rat and human AVPR1A only share 79% sequence identity. The positive signals for ACKR3:AVPR1A heteromers in A7r5 indicate that these differences in sequence identity are not crucial for heteromerization. As with the hVSMC, ACKR3 siRNA led to a 276% increase in AVPR1A:CXCR4 interactions and significant decreases in both ACKR3:AVPR1A and ACKR3:CXCR4 heteromers (Fig. 33).

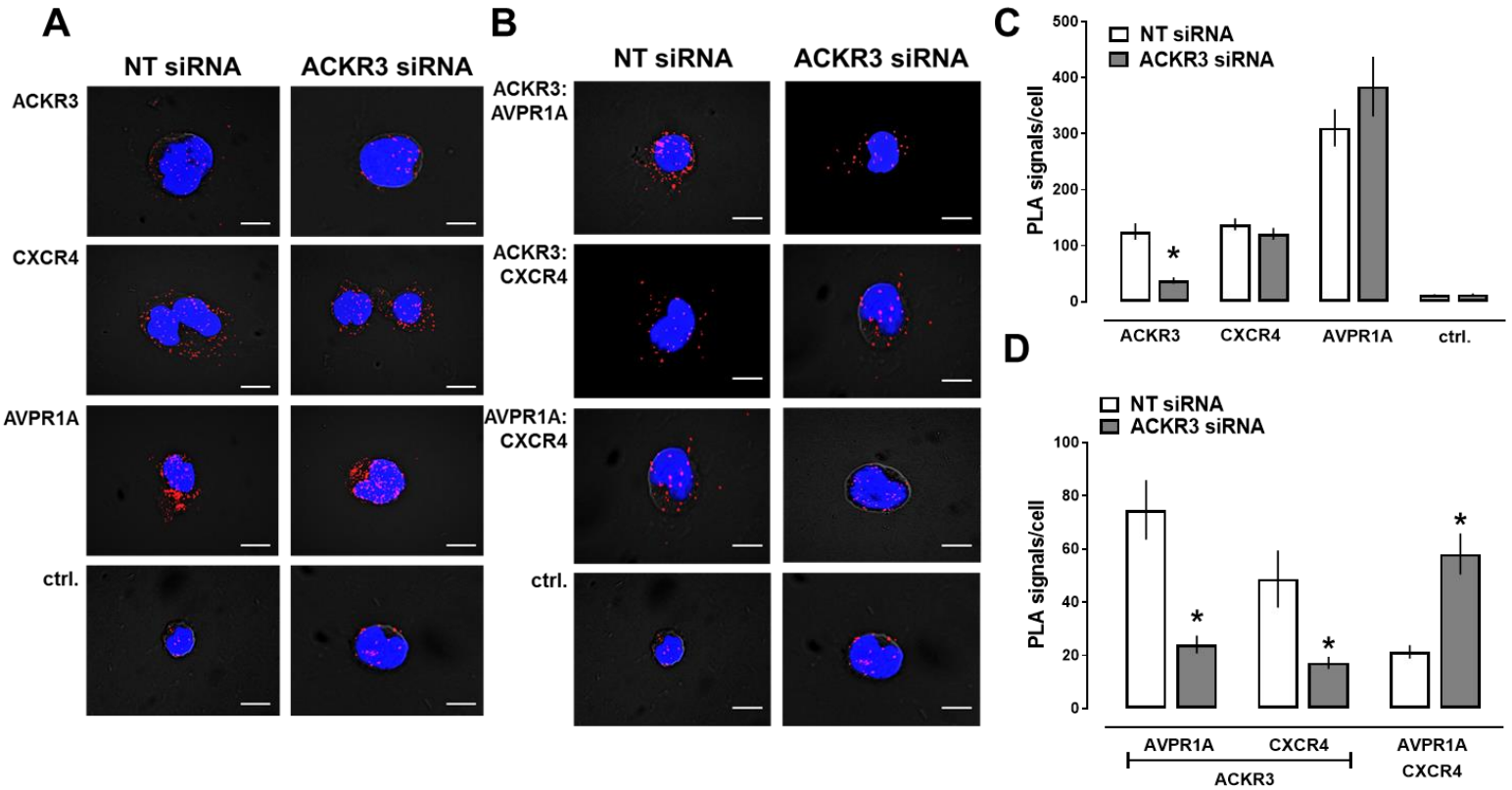

Figure 33. ACKR3 gene silencing reduces ACKR3: AVPR1A and ACKR3 : CXCR4 heteromers and increases AVPR1A : CXCR4 interactions in A7r5 cells. (A/B) Representative PLA images for the detection of individual receptors (**A**) and receptor–receptor interactions (**B**) in A7r5 cells after incubation with NT or ACKR3 siRNA. Ctrl: omission of one primary antibody. Images show merged PLA/4′,6-diamidino-2-phenylindole dihydrochloride (DAPI) signals acquired from *z*-stack images (*n* = 10; thickness 1 µm, bottom to top). (**C/D**) Quantification of PLA signals per cell for the detection of individual receptors (**C**) and receptor–receptor interactions (**D**) as in (**A/B**). n = 6 independent experiments with n = 10 images per condition and experiment. Data presented as mean ± SEM, Student's t-test with post hoc, **p* < 0.05 vs. cells incubated with NT-siRNA.

To determine if CXCR4 silencing affects ACKR3:AVPR1A heteromerization, CXCR4 siRNA was used to deplete CXCR4 from hVSMC. Representative images and the quantification from PLA experiments with hVSMC incubated with either CXCR4 siRNA or NT siRNA are shown in Fig. 34. CXCR4 siRNA led to a 70% decrease in CXCR4 expression when compared to NT siRNA. Reduction of CXCR4 did not alter the number of ACKR3:AVPR1A heteromers (mean ± SEM ACKR3 siRNA 31 ± 4, NT siRNA 289 ± 3 PLA signals/cell, $p > 0.05$ vs. NT) (Fig. 34). A significant decrease in CXCR4:AVPR1A interactions was also observed.

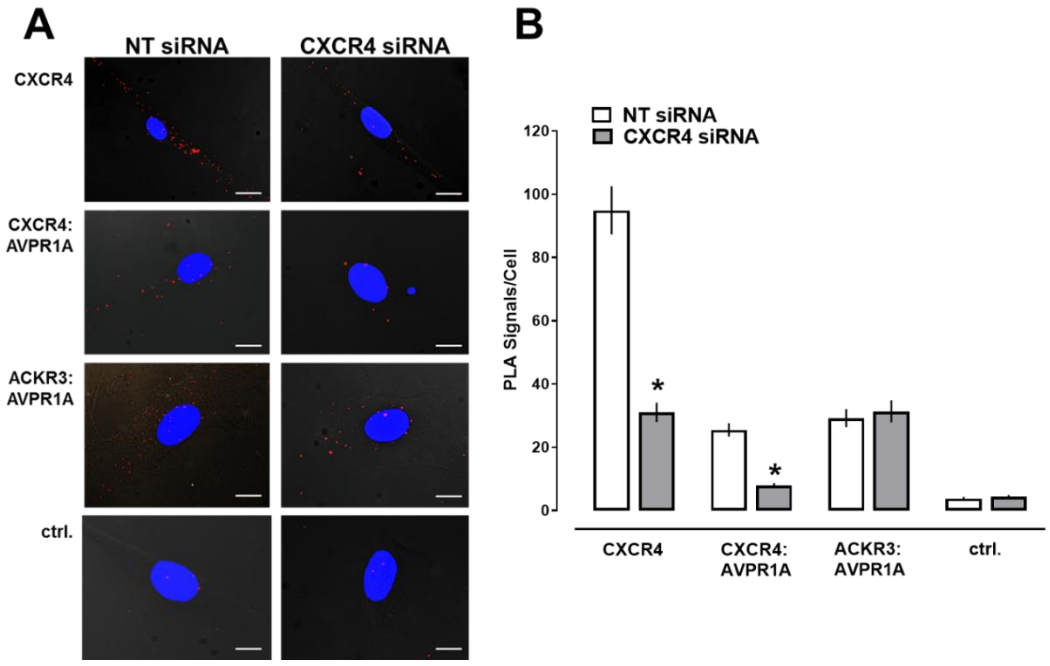

Figure 34. CXCR4 knock down does not affect ACKR3:AVPR1A heteromerization. A. Representative PLA images for the detection of CXCR4 and receptor-receptor interactions in hVSMC after incubation with non-targeting (NT) or CXCR4 siRNA. Ctrl: Omission of one primary antibody. Images show merged PLA/4′,6-diamidino-2 phenylindole dihydrochloride (DAPI) signals. Scale bars = 10 µm. **B.** Quantification of PLA signals per cell as in A. n=4 independent experiments with n=10 images per condition and experiment. Data presented as mean ± SEM, Student's t-test with post hoc,*: $p < 0.05$ vs. cells incubated with NT siRNA.

Cellular IP_3 production was then used to assess the role of the ACKR3:AVPR1A heteromeric receptor complex on AVPR1A signaling. When hVSMC incubated with NT siRNA were treated with 1μM aVP, a significant increase in IP_3 was observed, however incubating cells with ACKR3 siRNA ablated this response (mean ± SEM, NT siRNA * – 11.1 ± 2.3 untreated vs. 893.2 ± 313.1 aVP; ACKR3 siRNA – 4.7± 3.2 untreated vs. 1.9 ± 1.5 aVP, IP_3 ng/mg, * $p < 0.05$ vs. untreated) (Fig. 35). When cells incubated with CXCR4 siRNA were treated with aVP no significant change in IP_3 was detected, as compared to cells incubated with NT siRNA (mean ± SEM, CXCR4 siRNA * – 6.8 ± 5.9 untreated vs. 402.8 ± 37.5 aVP, IP_3 ng/mg, * $p < 0.05$ vs. untreated) (Fig. 35).

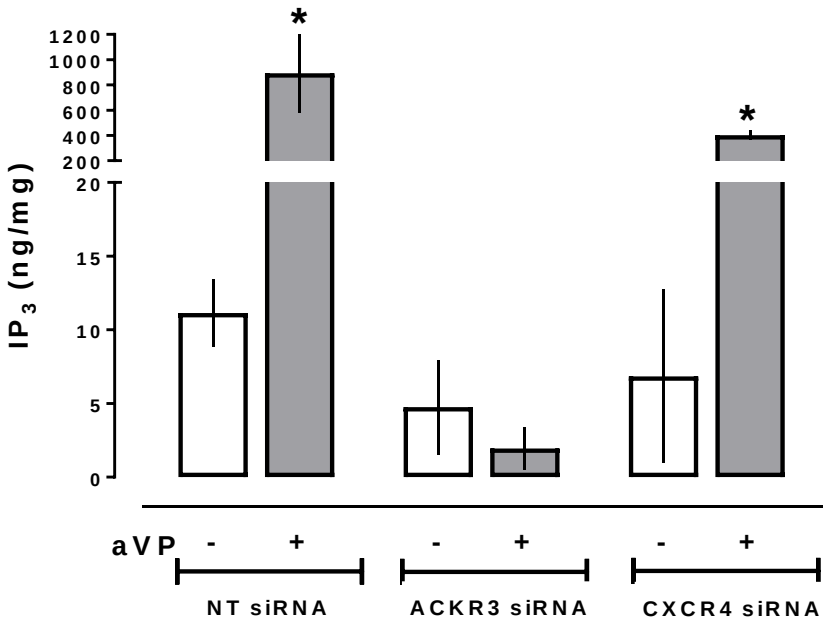

Figure 35. ACKR3 gene silencing inhibits aVP-mediated $G\alpha_q$ signaling, whereas CXCR4 gene silencing does not affect aVP-mediated $G\alpha_q$ signaling. IP_3 production of hVSMC incubated with NT, ACKR3, or CXCR4 siRNA upon stimulation with vehicle (-) or 1 μM aVP (+) for 5 min. n=4 independent experiments. Data presented as mean ± SEM, Student's t-test with post hoc, *: $p < 0.05$ vs. untreated.

4.4 TM-Domain Derived Peptide Analogues of ACKR3 Interfere with ACKR3:AVPR1A Heteromerization and aVP-Induced IP_3 Production.

We tested whether peptide analogues of ACKR3 (TM2, TM4, and TM7) would interfere with ACKR3:AVPR1A heteromeric complexes by utilizing PLA. Representative PLA images and the quantification of the individual receptors are shown in Fig. 36. The TM peptides did not affect the expression of ACKR3, CXCR4, or AVPR1A (Fig. 36). When hVSMC were pre-incubated with the ACKR3 TM peptides, profound changes in heteromerization were observed via PLA. TM2 and TM4 peptide analogues, but not the TM7 peptide analogue led to diminished expression of ACKR3:AVPR1A heteromers

(mean ± SEM, veh. – 164 ± 43; TM2- 22 ± 4; TM4- 37 ± 12; TM7- 121 ± 33 PLA signals/cell, $p < 0.05$ TM2 and TM4 vs veh.) (Fig. 36), similar to the pattern observed with ACKR3: α_{1B}-AR heteromers (Fig. 20) [82]. As a positive control changes in heteromerization between ACKR3 and CXCR4 were visualized. All ACKR3 TM peptide analogues disrupted ACKR3:CXCR4 heteromeric receptor complexes (mean ± SEM, vehicle – 157 ± 29, TM2 * – 40 ± 7, TM4 *- 47 ± 9, TM7 *- 42 ± 9 PLA signals/cell, * $p < 0.05$ vs. vehicle) (Fig. 36). Interestingly, none of the ACKR3 TM peptides altered the expression of AVPR1A:CXCR4 complexes (mean ± SEM, vehicle – 27 ± 4, TM2 – 27 ± 3, TM4 - 18 ± 2, TM7 - 29 ± 4 PLA signals/cell, $p > 0.05$ vs. vehicle) (Fig. 36) as was observed with ACKR3 gene silencing (Fig. 32).

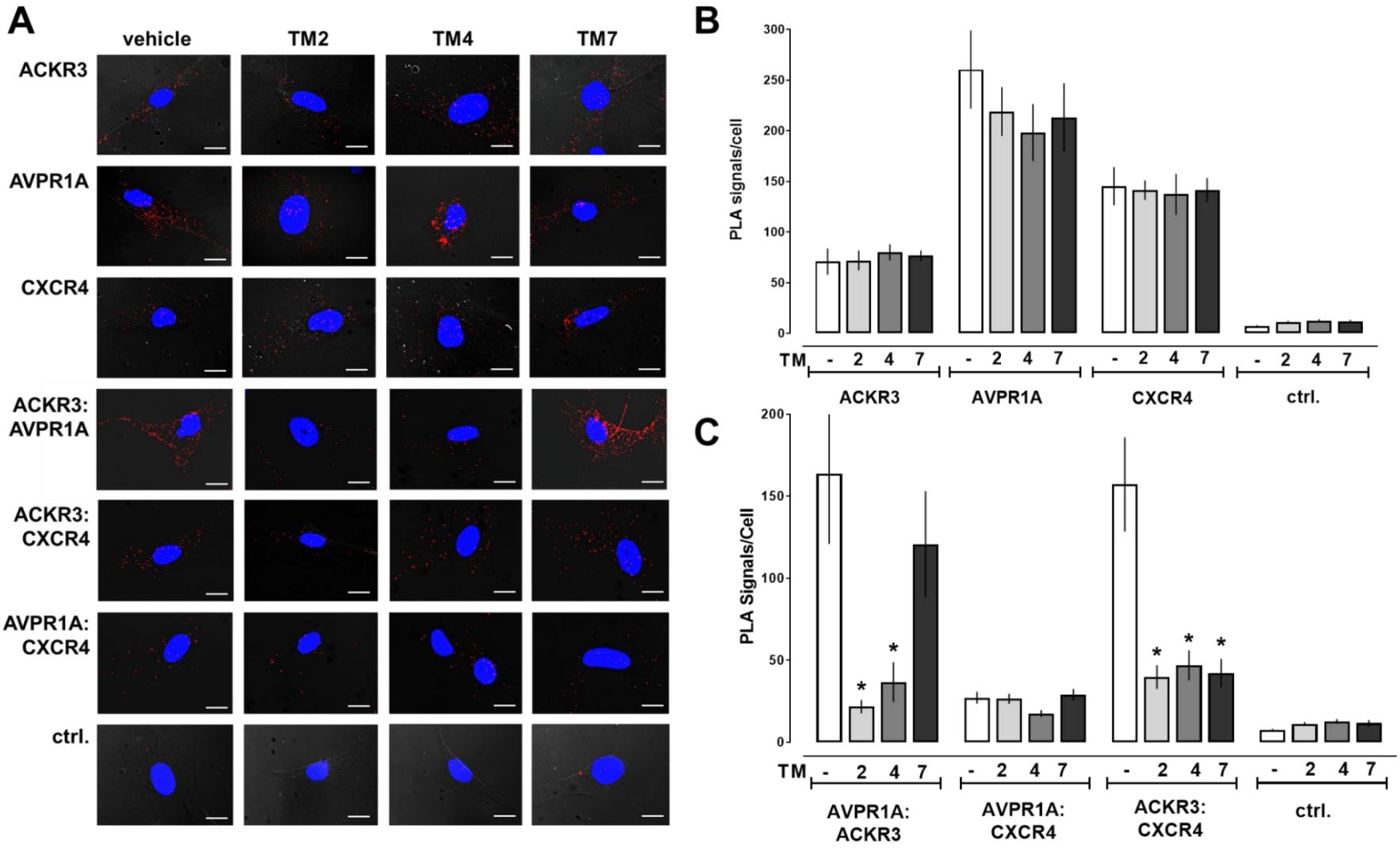
A
vehicle
TM2
TM4
TM7
ACKR3
AVPR1A
CXCR4
ACKR3:
AVPR1A
ACKR3:
CXCR4
AVPR1A:
CXCR4
ctrl.
B
PLA signals/cell
300
250
200
150
100
50
0
TM - 2 4 7 - 2 4 7 - 2 4 7 - 2 4 7
ACKR3
AVPR1A
CXCR4
ctrl.
C
PLA Signals/Cell
200
150
100
50
0
TM - 2 4 7 - 2 4 7 - 2 4 7 - 2 4 7
AVPR1A:
ACKR3
AVPR1A:
CXCR4
ACKR3:
CXCR4
ctrl.

Figure 36. ACKR3 derived transmembrane domain (TM) peptide analogues disrupt ACKR3:AVPR1A and ACKR3:CXCR4 heteromeric complexes. hVSMC were incubated with vehicle, TM2, TM4, or TM7 (10 μM, 30 min at 37^{o}C), washed, and fixed for PLA. **A.** Typical PLA images for the detection of individual receptors or receptor-receptor complexes are shown. Ctrl: Omission of one primary antibody. Images show merged PLA/4′,6-diamidino-2-phenylindole dihydrochloride (DAPI) signals. Scale bars = 10 μm. **B-C.** Quantification of PLA signals per cell for individual receptors (**B**) and receptor-receptor interactions (**C**). n=4 independent experiments with n=10 images per condition and experiment. Data presented as mean ± SEM, One-way ANOVA with Dunnett's multiple comparison post hoc, *: $p < 0.05$ vs. cells incubated with vehicle.

When hVSMC were pre-treated with ACKR3 TM peptide analogues, analogous effects were observed between α_1-AR and AVPR1A-mediated IP_3 release (Figs. 22, 37) [82]. Consistent with their disruptive effects on ACKR3:AVPR1A heteromerization, incubation with the TM2 and TM4 peptide analogues led to diminished IP_3 responses when hVSMC were stimulated with aVP (Fig. 37A). The TM7 peptide analogue, however, was unsuccessful at impairing IP_3 production in hVSMC. To identify if the ACKR3 peptides affected recombinant AVPR1A signaling, we utilized the PRESTO-Tango assay. None of the ACKR3 TM peptide analogues affected aVP-mediated β-arrestin 2 recruitment to AVPR1A (Fig. 37B).

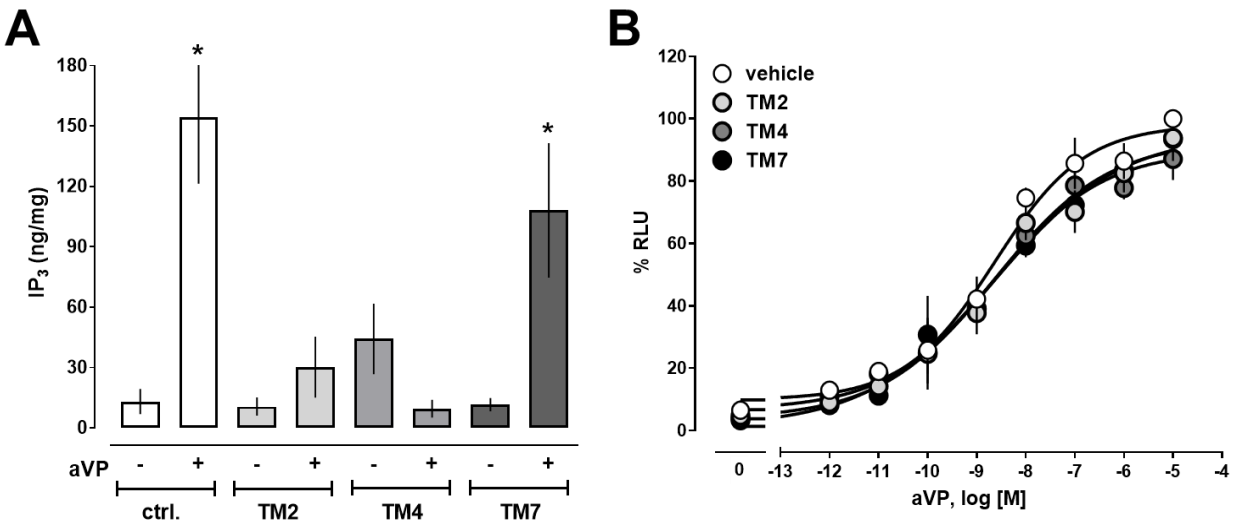

Figure 37. ACKR3 derived transmembrane domain (TM) peptide analogues inhibit aVP-induced Gα_q signaling in hVSMC. (**A**) IP_3 production was measured in hVSMC pre-treated with vehicle or TM2/4/7/ peptide analogues (10 µM, 30 min at 37°C) and then stimulated with either vehicle (-) or aVP (1 µM, 5 min) (+). n=4 independent experiments. *: $p < 0.05$ vs. vehicle-treated cells. β-arrestin 2 recruitment assay (PRESTO-Tango) for AVPR1A. (**B**) HTLA cells expressing FLAG-AVPR1A-Tango were incubated with either vehicle or ACKR3 TM2/4/7 (10 µM, 30 min at 37°C) and then stimulated with aVP overnight. RLU (%): relative luminescence units in % RLU after treatment with 10 µM aVP (=100%). n=3 independent experiments. Data presented as mean ± SEM, Student's t-test with post hoc, *: $p < 0.05$ vs. untreated.

4.5 The ACKR3:AVPR1A Heteromeric Complex Modulates β-arrestin Recruitment to Each Receptor Partner and Displays Asymmetric β-arrestin Cross-Recruitment Upon Agonist Stimulation.

The PRESTO-Tango assay [171] was utilized to evaluate whether ACKR3:AVPR1A heteromerization affects β-arrestin 2 recruitment. FLAG-AVPR1A-Tango was co-expressed with HA-ACKR3 or empty vector (pcDNA3). Comparable FLAG-AVPR1A-Tango expression was confirmed via flow cytometry and the dose-response for β-

arrestin 2 recruitment with aVP stimulation was determined (Fig. 38B). Co-expressing FLAG-AVPR1A-Tango with HA-ACKR3 led to a significant decrease in efficacy (top plateau 32 $\pm$ 4 % RLU, $p < 0.001$ vs. AVPR1A-Tango/pcDNA3) when compared with cells expressing AVPR1A-Tango and pcDNA3 (top plateau 97 $\pm$ 7 % RLU). Cells that were co-expressed with AVPR1A-Tango and either pcDNA3 or ACKR3 both recruited β-arrestin 2 with a similar potency (EC_{50} (95% CI) of 2.5 (0.8-8.8) nM, EC_{50} (95% CI) of 6.1 (0.7-58) nM, $p > 0.05$, respectively) (Fig. 38). CXCL11 and CXCL12 did not induce β-arrestin 2 recruitment to AVPR1A-Tango in the presence or absence of ACKR3 (Fig. 38). These data suggest that ACKR3 and AVPR1A exist in complex, and this complex not only influences G-protein mediated signaling, but also β-arrestin signaling.

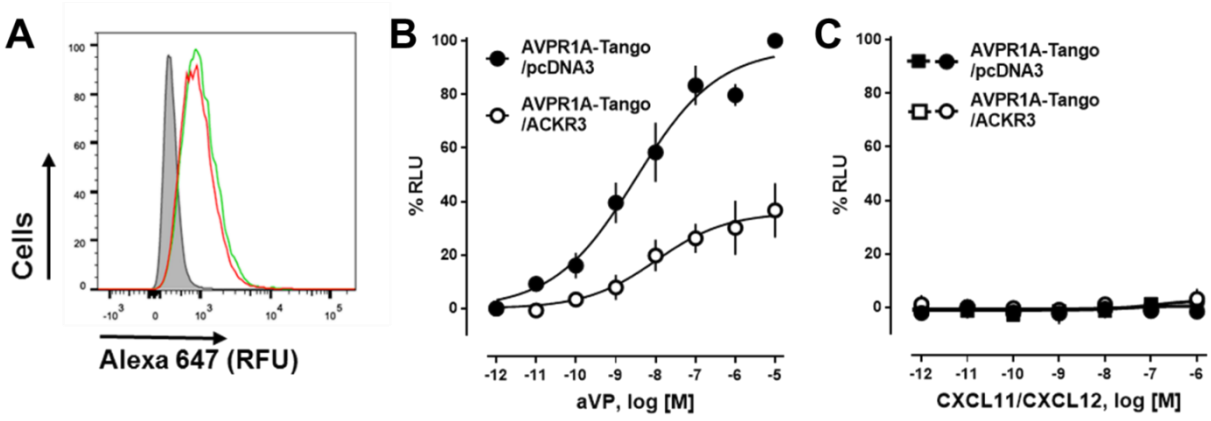

Figure 38. β-arrestin 2 recruitment to AVPR1A-Tango. A-C: HTLA cells were co-transfected with 0.75 µg DNA for FLAG-AVPR1A-TANGO plus 0.75 µg pcDNA3 or HA-ACKR3. **A.** Measurement of FLAG-AVPR1A-Tango expression by flow cytometry. Cells were labeled with Alexa Fluor 647 anti-FLAG. Grey area: unstained cells. Red line: cells transfected with FLAG-AVPR1A-TANGO/ pcDNA3. Green line: cells transfected with FLAG-AVPR1A-TANGO/ HA-ACKR3. RFU: relative fluorescence units. Data are representative of n=3 independent experiments. **B/C.** β- arrestin 2 recruitment assay (PRESTO-Tango) for AVPR1A. Cells were stimulated with aVP (**B**), CXCL11 and CXCL12 (**C**). Black symbols: cells transfected with FLAG-AVPR1A-TANGO/ pcDNA3; white symbols: cells transfected with FLAG AVPR1A-TANGO/ HA-ACKR3. n=3 independent experiments.

In cells expressing similar levels of ACKR3-Tango plus pcDNA3 or HA-AVPR1A, HA-AVPR1A co-expression significantly reduced the efficacy of CXCL11 and CXCL12 to recruit β-arrestin 2, while the potency was unchanged (top plateau CXCL11 37 $\pm$ 5 % RLU; CXCL12 50 $\pm$ 7 %RLU $p < 0.05$ vs. ACKR3-Tango/pcDNA3) compared to cells expressing ACKR3-Tango with pcDNA3 (top plateau CXCL11 104 $\pm$ 6 % RLU; CXCL12 97 $\pm$ 5 %RLU) (Fig. 39). Surprisingly, co-expressing AVPR1A led to aVP-induced cross-recruitment of β-arrestin 2 to ACKR3-Tango (top plateau 90 $\pm$ 7 % RLU) (Fig. 39). ACKR3-Tango with pcDNA3 did not respond to aVP stimulation (top plateau 7 $\pm$ 3 %RLU).

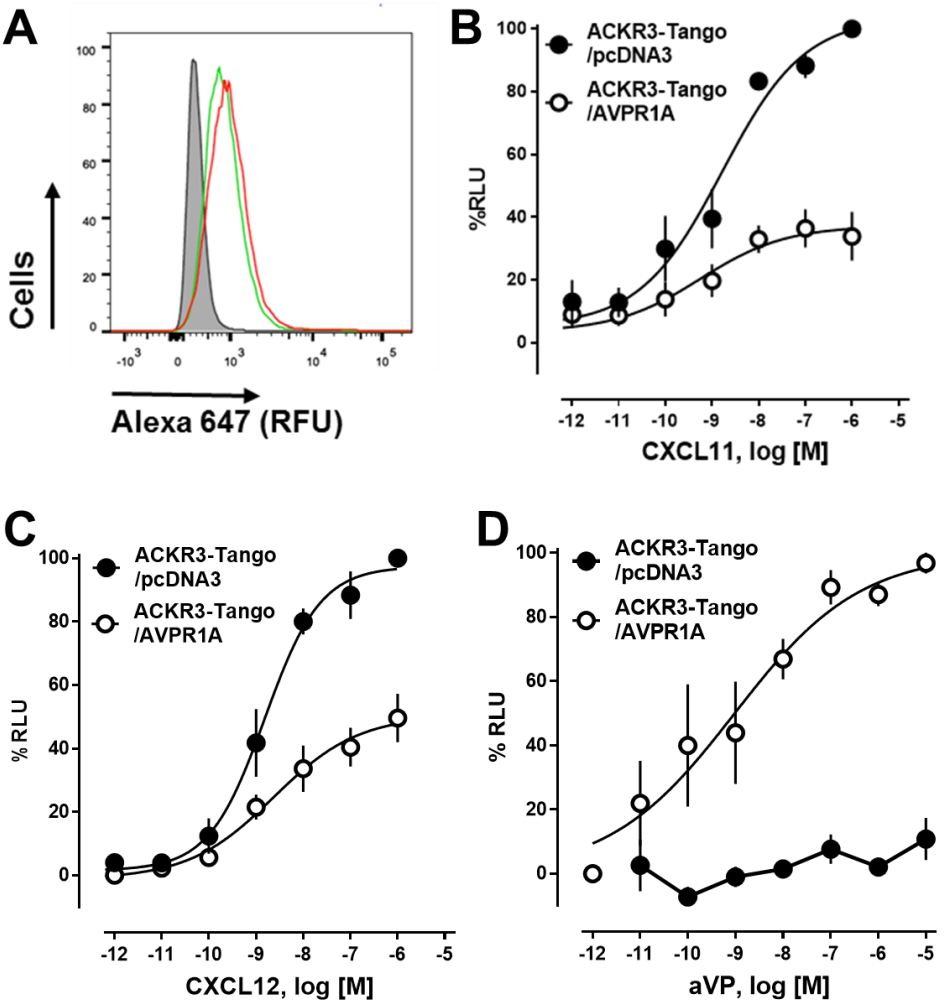

Figure 39. β**-arrestin 2 recruitment to ACKR3-Tango. A-D.** HTLA cells were co-transfected with 0.75 µg DNA for FLAG-ACKR3-TANGO plus 0.75 µg pcDNA3 or HA-AVPR1A. **A**. Measurement of FLAG-ACKR3-Tango expression by flow cytometry. Cells were labeled with Alexa Fluor 647 anti-FLAG. Grey area: unstained cells. Red line: cells transfected with FLAG-ACKR3-TANGO/ pcDNA3. Green line: cells transfected with FLAG-ACKR3-TANGO /HA-AVPR1A. RFU: relative fluorescence units. Data are representative of n=3 experiments. **B-D**. β-arrestin 2 recruitment assay (PRESTO-Tango) for ACKR3. Cells were stimulated with CXCL11 (**B**), CXCL12 (**C**) and aVP (**D**). Black circles: cells transfected with FLAG-ACKR3-TANGO/pcDNA3; white circles: cells transfected with FLAG-ACKR3-TANGO/ HA-AVPR1A. n=3 independent experiments.

The effects of the ACKR3 TM peptide analogues on β-arrestin 2 recruitment are consistent with their ability to interfere with ACKR3:AVPR1A heteromerization. When ACKR3-Tango was co-expressed with AVPR1A, TM2 and TM4 peptide analogues significantly inhibited the efficacy of aVP to induce β-arrestin 2 to ACKR3-Tango compared to vehicle treated cells (top plateau vehicle – 105 $\pm$ 5; TM2# - 42 $\pm$ 21; TM4* – 65 $\pm$ 40; TM7 – 87 $\pm$ 11 %RLU # $p < 0.0001$, * $p < 0.005$) (Fig. 40). The ACKR3 TM7 peptide analogue did not exhibit significant changes to the efficacy or potency of aVP to recruit β-arrestin 2 to ACKR3-Tango/AVPR1A expressing cells. Recently, the TM2 peptide analogue was reported to demonstrate the pharmacological behavior of a competitive antagonist for β-arrestin 2 recruitment to ACKR3-Tango upon agonist stimulation, whereas the TM7 peptide analogue was inactive; the TM4 peptide exhibited a behavior similar to the TM2 peptide, but this effect did not reach statistical significance (Fig. 21B) [82]. In the present study, the TM2 and TM4 peptides acted as non-competitive antagonists, which prohibited aVP-induced β-arrestin 2 recruitment to ACKR3-Tango with similar efficacy.

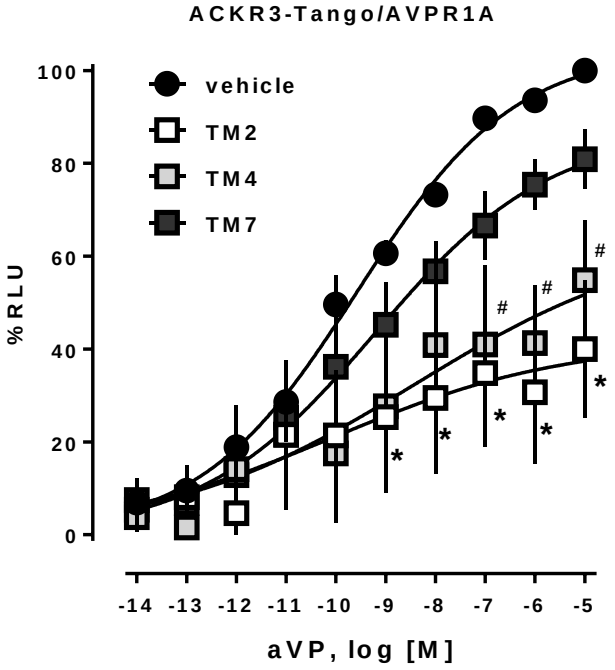

Figure 40. β-arrestin 2 recruitment to ACKR3:AVPR1A heteromeric complex. β-arrestin 2 recruitment assay (PRESTO-Tango) with HTLA cells co-expressing FLAG-AVPR1A- Tango/ HA-ACKR3. Cells were treated with vehicle or TM2/4/7 peptides (10 μM, 30 min at 37°C) and then stimulated with aVP. n=3 independent experiments. Black circle: vehicle. Open squares: TM2. Light grey squares: TM4. Dark grey squares: TM7. n=4 independent experiments.

4.6 ACKR3 and AVPR1A Co-Internalize Upon Agonist Stimulation in hVSMC.

Receptor expression on the plasma membrane is often reduced upon agonist-induced β-arrestin recruitment. This can occur either via receptor-mediated endocytosis or through inhibition of receptor recycling [49,51,69,89]. As activation of recombinant AVPR1A induced cross-recruitment of β-arrestin 2 to ACKR3-Tango (Figs. 39D, 40), we tested whether endogenous ACKR3 and AVPR1A in hVSMC co-internalize upon agonist stimulation. hVSMC were stimulated with 1μM CXCL11 or 1μM aVP and ACKR3 and

AVPR1A cell surface expression was quantified after double-immunofluorescence staining by flow cytometry. Fig. 41 depicts representative 2-dimensional scatter plots for the detection of both receptors throughout a 60 min time period after stimulation of hVSMC with CXCL11 and aVP. A time-dependent reduction of both ACKR3 and AVPR1A upon CXCL11 or aVP stimulation of hVSMC was observed. The time course and the degree of receptor depletion from the cell surface was comparable for both agonists, indicating symmetrical agonist-induced co-internalization of ACKR3 and AVPR1A. Co-internalization of ACKR3 and AVPR1A upon aVP stimulation matches well with the observed aVP-induced β-arrestin 2 cross-recruitment to ACKR3 within the ACKR3:AVPR1A complex (Fig. 39).

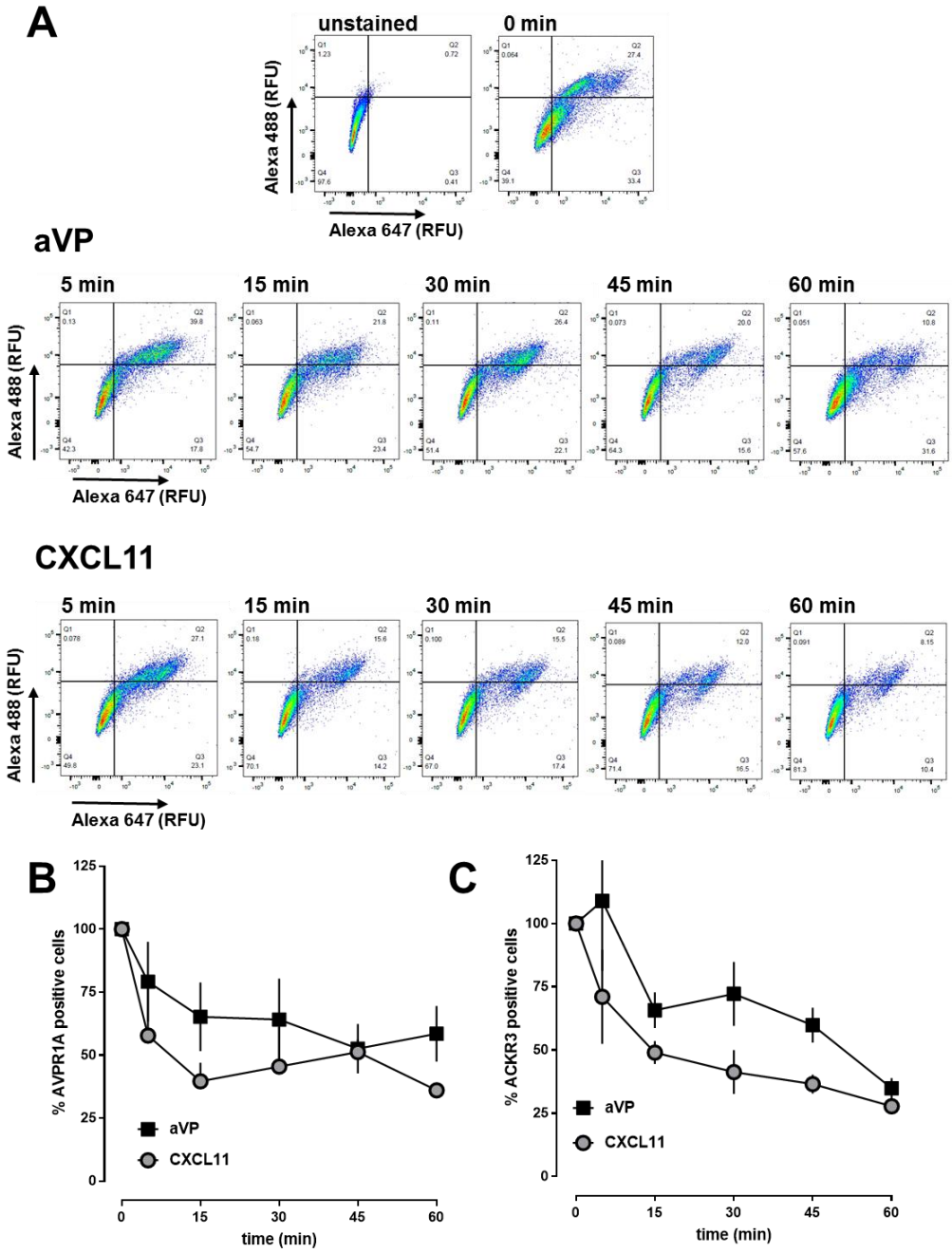

Figure 41. AVPR1A and ACKR3 co-internalize upon agonist stimulation in hVSMC. A. hVSMC were treated with 1 μM aVP or CXCL11 for up to 60 minutes, stained at 4°C with rabbit anti-AVPR1A/donkey anti-rabbit-Alexa Fluor 647 and mouse anti- ACKR3/goat anti-mouse-Alexa Fluor 488 and analyzed for receptor expression via flow cytometry. RFU: relative fluorescence units. The horizontal and vertical lines show the gating thresholds for ACKR3 (Alexa 488) and AVPR1A (Alexa 647). **B.** Quantification of AVPR1A positive cells after incubation with aVP and CXCL11, as in A. n=3 independent experiments. **C.** Quantification of ACKR3 positive cells after incubation with aVP and CXCL11, as in A. n=3 independent experiments.

Discussion

The results of the present study indicate that endogenous ACKR3 and AVPR1A form heteromers in hVSMC, endogenous ACKR3:AVPR1A complexes can be disrupted with selective ACKR3-derived TM peptide analogues or via ACKR3 siRNA without altering expression levels of the individual receptors, and interference with ACKR3:AVPR1A heteromerization in hVSMC alters receptor function. These findings fulfill recently proposed criteria for GPCR heteromers in native tissues [62]. This notion is supported by data in expression system studies, which provided additional mechanistic insight into molecular events at the ACKR3:AVPR1A heteromer level and demonstrated that heteromerization affects the biochemical fingerprint of each receptor partner [61].

Activation of CXCR4 had no effect on aVP-mediated vasoconstriction (Fig. 25B) and recombinant and endogenous CXCR4 and AVPR1A did not form significant interactions (Figs. 28, 30). Although CXCR4 could be immunoprecipitated with anti-AVPR1A in hVSMC, CXCR4 has been shown to form interactions with ACKR3 in hVSMC (Chapter 3) and thus could be indirectly interacting with AVPR1A in co-immunoprecipitation experiments (Fig. 31). These receptors likely exist within the same microdomain on the plasma membrane yett are not in a proximity to facilitate direct physical interactions. These findings provide additional evidence for the selectivity of the α_1-AR:CXCR4 interaction and could explain why CXCR4 fails to influence aVP-mediated signaling events. When ACKR3 was depleted from the cell surface, profound increases of CXCR4:AVPR1A heteromers were detected (Figs. 32-33). However, when the

ACKR3:AVPR1A heteromers were disrupted with TM2 and TM4, no increases were detected in the CXCR4:AVPR1A heteromers (Fig. 36). These observations suggest that ACKR3 hinders the CXCR4:AVPR1A interaction and only when ACKR3 is depleted from the cell surface can interactions form between CXCR4:AVPR1A. Such a behavior is in agreement with previous findings (Chapter 3) implying that hetero-oligomeric complexes exist in a dynamic environment. When the equilibrium of receptors is shifted, a new pattern of receptor interactions develops. Furthermore, AVPR1A appears to follow the same pattern of heteromerization as α_{1A}-AR with the ACKR3 protomer or CXCR4 homodimer. Whereas the pattern of AVPR1A heteromerization with ACKR3 is in direct contrast to $\alpha_{1B/D}$-AR interactions which preferentially form hetero-oligomeric complexes with the ACKR3:CXCR4 heteromer.

Although the pattern of AVPR1A heteromerization is in contrast to $\alpha_{1B/D}$-AR, consonant signaling events were observed (Fig. 19). ACKR3 gene silencing ablated aVP-induced IP_3 production (Fig. 34), whereas α_{1A}-AR was not shown to be essential for IP_3 production in hVSMC (Fig. 17). Furthermore, the effects of the TM peptides on signaling events in hVSMC were consistent between AVPR1A and $\alpha_{1B/D}$-AR (Figs. 22, 37).

Disruption of the ACKR3:AVPR1A alters both $G\alpha_q$-protein and β-arrestin mediated signaling events. The loss of aVP- responsiveness in terms of IP_3 production with the TM peptide analogues (Fig. 37) was in fact due to disruption of ACKR3:AVPR1A heteromeric complexes as β-arrestin 2 recruitment to AVPR1A-Tango was not affected

(Fig. 37). When ACKR3-Tango was co-expressed with AVPR1A, aVP-induced β-arrestin 2 recruitment to ACKR3-Tango (Figs. 39-40). This effect can be blocked with the TM2 and TM4 peptide analogues. ACKR3 expression led to a reduction in aVP-induced β-arrestin 2 recruitment to AVPR1A-Tango. Furthermore, the presence of AVPR1A enabled β-arrestin 2 recruitment to ACKR3-Tango upon aVP stimulation which indicates that AVPR1A activation within the heteromeric ACKR3:AVPR1A complex leads to β-arrestin 2 recruitment to both receptor partners. However, CXCL11 and CXCL12 failed to cross-recruit β-arrestin 2 to AVPR1A-Tango in the presence of ACKR3 (Fig. 38). These findings imply that ACKR3, within the ACKR3:AVPR1A heteromeric receptor complex, attenuates β-arrestin 2 recruitment to AVPR1A through allosteric interactions. In combination with the observed effects of ACKR3:AVPR1A heteromerization on aVP-induced $G\alpha_q$-mediated signaling events, these data suggest that ACKR3 within the ACKR3:AVPR1A heteromer regulates the balance between AVPR1A-mediated $G\alpha_q$ and β-arrestin signaling. These data demonstrate asymmetrical agonist-induced cross-regulation of ACKR3 by AVPR1A within the heteromeric receptor complex. Such a pharmacological behavior of the ACKR3:AVPR1A heteromeric complex is similar to the signaling behavior of other GPCR heteromers, for which ligand-induced symmetrical and asymmetrical cross-activation and cross-inhibition of various signaling read-outs have previously been described [34,63,180,181].

Currently, no conclusions can be drawn regarding the physiological consequences of ACKR3:AVPR1A heteromerization on ACKR3-mediated effects on cell function due to the lack of appropriate read-outs that are characteristic for ACKR3 and independent of

CXCR4. To assess this point, future studies could include complete knock-out of CXCR4 via CRISPR to identify ACKR3 signaling.

Additionally, the possible roles of CXCR4:AVPR1A heteromers, which occur after ACKR3 depletion, remain elusive. These findings indicate that ACKR3:AVPR1A complexes are essential for AVPR1A function in vascular smooth muscle and suggest that ACKR3 activation within the heteromeric complex attenuates aVP mediated vasoconstriction.

These data provide a molecular mechanism for the previously described effects of synthetic ACKR3 ligands on blood pressure regulation in animals [114,170] and for interactions between the innate immune and vasoactive neurohormonal systems [65,68,80,99,159,160]. This function of ACKR3 offers a mechanistic basis for the clinical observation that systemic levels of CXCL12, which preferentially acts as an ACKR3 agonist in VSMC [114], are significantly elevated in patients with sepsis and septic shock; the latter typically present with hypotension due to vasodilatory shock and vasopressor refractoriness [109,111-113,182]. Significantly increased systemic CXCL11 concentrations have recently been described in patients with hypertension [183], that may reflect an adaptive response to reduce vascular resistance. These findings provide another example for the functional relevance of GPCR heteromers and insights into the regulation and biological functions of ACKR3 and AVPR1A, which could facilitate the development of improved pharmacological strategies to modulate vascular function.

CHAPTER 5

CONCLUSIONS AND FUTURE DIRECTIONS

Introduction

GPCR heteromerization is a rapidly evolving field. Increasing evidence reports that heteromerization may be responsible for the pharmacological heterogeneity of GPCRs [61-63,184-187]. The role of heteromeric complexes has been attributed to receptor maturation and trafficking, signal transduction of both G-protein mediated pathways and β-arrestin signaling cascades, allosteric and orthosteric modulation, cooperativity, and receptor internalization [28,46,56,61,62]. With the ever-evolving landscape of pharmacological therapeutics, understanding the mechanisms regulating GPCR function is essential.

Evidence for Receptor Cross-Talk

Cross-talk between GPCRs is a key mechanism cells utilize to integrate and amplify multiple signaling cascades [39,188,189]. Cross-talk can occur downstream of the receptors, somewhere along the signaling pathway, or at the receptor level itself. More recently, cross-talk between GPCRs has been linked to receptor heteromerization [6,46,56,61-63,77,78,115,185,186,188-191].

In chapters 3 and 4 we determined that ACKR3 antagonizes α_1-AR and AVPR1A-mediated $G\alpha_q$-protein signaling [82,114]. It was determined that the cross-talk between CXCR4 and α_1-AR [84,114], was specific for CXCR4:α_1-AR interactions as CXCR4

activation does not impact AVPR1A-mediated function in pressure myography experiments and CXCR4 gene silencing does not affect aVP-induced IP_3 production.

Investigation into the functional role of ACKR3 in cells has been hampered by lack of selective agonists and pharmacological inhibitors. CXCL12 activates both CXCR4 and ACKR3, although preferentially activates ACKR3 [82,119,123]. The apparent opposing effects of these receptors on α_1-AR mediated function is challenging to dissect with CXCL12 alone. Ubiquitin, a non-chemokine, non-cognate agonist for CXCR4, aids in understanding mechanisms of receptor cross-talk [94,95,104]. Ubiquitin enhanced PE-induced vasoconstriction although it had no effect on aVP-induced vascular reactivity (Fig. 25). CXCL11 activates both ACKR3 and CXCR3; however, previous studies have shown that CXCR3 is not expressed in vascular smooth muscle cells [51]. In the pressure myography studies, CXCL12 attenuated both α_1-AR and AVPR1A-mediated vasoconstriction, however not to the level of CXCL11 administration (Fig. 25). CXCL12 treatment resulted in greater vasorelaxation for aVP than PE; further supporting the findings that AVPR1A forms heteromeric complexes with ACKR3 and does not form significant interactions with CXCR4 (Fig. 29). TC14012, a specific ACKR3 agonist and CXCR4 antagonist, inhibited both α_1-AR and AVPR1A-mediated IP_3 release (Figs. 11, 27).

Future studies would benefit from an ACKR3 antagonist. CCX733 has been utilized as an ACKR3 antagonist [51], however, it has also been demonstrated to activate the receptor at higher concentrations [192]. Therefore, it is not an ideal candidate to fill the void of an ACKR3 antagonist. By antagonizing the receptor, a better understanding could be determined as to how heteromerization with ACKR3 modulates the function of

α_1-AR and/or AVPR1A. Treating hVSMC with CXCL11 led to co-internalization of both ACKR3 and AVPR1A (Fig. 41), which could explain why decreased IP_3 production with the addition of ACKR3 agonists was observed (Figs. 11, 27). Therefore, a selective antagonist is needed to fully grasp how these receptors are engaging in cross-talk.

The findings that ACKR3 activation antagonizes α_1-AR and AVPR1A-mediated effects are similar to other receptor heteromeric complexes. The adenonsine$_1$ (A_1R) and dopamine$_1$ (D_1R) heteromer exhibits differential effects depending upon the ligand used for stimulation [22,26,28,77,193]. A_1R agonists decrease the binding affinity of D_1R as well as inhibit D_1R signaling [22,77,194,195]. The α_{2A}-AR:μ-opioid receptor (MOR) heteromer exhibits consonant effects to that of the CXCR4:α_1-AR heteromer, wherein treatment with either α_{2A}-AR or MOR agonists, sensitizes the effects of the alternate receptor [66,196-198]. These studies along with the present study demonstrate that receptor cross-talk is dependent upon the receptor partners available for heteromerization and the cellular environment in which interactions could occur. A limitation of these studies could be that we did not allow for the influence of additional untested receptors in our interpretations of receptor cross-talk. Perhaps activation of CXCR4 may induce a conformational change within the micro-domain of receptors, and it is this indirect interaction that influences PE-mediated effects.

Identification of ACKR3 Heteromeric Complexes

Identification of heteromeric receptor complexes has primarily been achieved through the utilization of expression systems. Use of fusion proteins in BRET and FRET provide excellent evidence supporting recombinant receptor interactions [61-63,91,119]. However, the stoichiometry may be altered when co-expressing two or more receptors; thus, it is

necessary to confirm interactions in native cells. Currently, only four heteromers fulfill the criteria set forth to validate heteromers in native tissues [62].

Visualization of ACKR3 heteromers was achieved in chapters 3 and 4. We first identified that ACKR3 interacts with recombinant $\alpha_{1a/b/d}$-AR and AVPR1A in HEK 293T cells (Figs. 12, 28). Interactions with CXCR4 served as a positive control. Consistent with the expression system data, interactions of endogenous receptors were confirmed in hVSMC utilizing both PLA and co-immunoprecipitation experiments (Figs. 13-14, 29-30).

Ligand stimulation can enhance or diminish the presence of heteromers [28,46,47,56,115,188]. When A_1R:D_1R is pre-treated with A_1R agonists, increased concentrations of the heteromer is detected, but the reverse occurs with pre-treatment of D_1R [22,193-195]. α_{2A}-AR:MOR heteromer is enhanced with treatment of either agonist, yet these receptors have also been shown to co-internalize [21,66,88,196]. One future direction for the current studies would be to evaluate how agonist and antagonist stimulation affects expression of heteromeric complexes. We have demonstrated that ACKR3 interacts with both α_1-AR and AVPR1A. It appears likely that these receptors exist within a microdomain on the plasma membrane. Therefore, altering the conformation state of one receptor (i.e. activated state vs. unbound state) could have considerable effects on the heteromerization of other receptors. This line of thought is supported by the data with the ACKR3 TM peptide analogues and gene silencing. Disrupting the interaction between two receptors led to increases in heteromerization at other sites (Figs. 20, 31-32, 35).

We did not account for changes in heteromerization that could be occurring with ligand stimulation to reflect the receptor cross-talk observed. ACKR3 activation appears to induce internalization of AVPR1A, yet we did not test whether ACKR3 activation affects α_1-AR expression in hVSMC. Nor did we test whether CXCR4 activation alters the individual expression of AVPR1A, ACKR3, or α_1-ARs.

Interference of ACKR3 Heteromerization

To identify if the receptor interactions are functional heteromers, we disrupted the ACKR3 complexes then determined the biochemical fingerprint of the heteromers [16,17,62,199]. We employed two differing strategies to interfere with ACKR3 heteromerization, gene silencing and TM peptide analogues. Perturbing ACKR3 heteromeric complexes allowed for differentiation of the signaling cascades between the proto/homomer and heteromer (Figs. 16, 19, 22, 34, 36, 40).

ACKR3 gene silencing and subsequent loss of heteromeric complexes led to ablation of α_1-AR and AVPR1A signaling events (Figs. 19, 34). Other studies found that perturbing GPCR heteromerization led to ineffective receptor function. Transgenic mice deficient in D_4R had decreased expression of D_2R:D_4R heteromers. When D_4R was knocked-in, neurotransmitter release was restored, thus implying that the D_2R:D_4R heteromeric complex is necessary for proper function [200]. Furthermore, mice expressing a mutated melatonin$_2$ receptor (MT) were unable to form functional heteromers with MT_1. Lack of MT_1:MT_2 heteromers led to decreased photosensitivity of their rod photoreceptors, again indicating the necessity of GPCRs to exist in multimeric complexes *in vivo* [93]. When ACKR3 was depleted from hVSMC or A7r5 cells, increases in CXCR4:AVPR1A

interactions were observed (Figs. 31, 32), which we attributed to a shift in the equilibrium of available sites for interaction within the multimeric complex.

To assess if the loss of function occurring from ACKR3 depletion was due to interference of heteromerization and not from ACKR3 loss, TM peptide analogues were utilized to disrupt ACKR3 heteromers. Consistent with studies observing the δOR:μOR heteromer in native tissue [31], the findings in this dissertation indicate that it is not only the presence of ACKR3 on the cell surface required for α_1-AR and AVPR1A function, but that ACKR3 must exist in complex with these receptors for vasoreactivity. Interfering with the δOR:μOR heteromer via TM peptides derived from domain 1 of μOR led to decreased expression of receptor interactions and affected morphine sensitivity [31]. TM peptide analogues have also been employed to break apart homodimerization. TM6 of the β_2-AR ablates β_2-AR function and presence of homodimers [175,201]. TM peptides were thought to potentially be utilized to map specific interaction sites of heteromers [202,203]. When endogenously expressed heteromers are exposed to TM peptides, heteromerization at one site may be disrupted, yet this disruption can shift the configuration of receptors within a microdomain on the plasma membrane making it appear that new interactions are formed.

Oligomerization of GPCRs may also serve to affect receptor stability. Rhodopsin homodimers were disrupted via Rhodopsin derived TM1,2,4, and 5 peptides [202]. Although the disruption of Rhodopsin oligomers did not affect the rate of G protein activation, receptor stability significantly declined with incubation of the TM peptides, suggesting that GPCR supramolecular organization may also be critical for receptor stability [202]. Orphan receptors may indeed have a role in heteromerization, not to bind

ligand, but instead to provide a scaffold to stabilize other GPCRs or intracellular signaling molecules [46,57]. Future studies examining the coupling of G proteins and/or β-arrestin may provide clues to the molecular basis of how hetero/homomerization of GPCRs affects signaling cascades, receptor stability, and receptor function. Additionally, future studies which utilized complete ablation of ACKR3 would indicate the functional role of ACKR3. Gene silencing did not induce complete knockdown of the receptors, thus it is a limitation of these studies.

Co-Internalization of ACKR3 and AVPR1A

With the discovery of GPCR heteromeric complexes, receptor co-internalization appeared to one significant consequence of heteromerization [19,39,41,43,44,48,87,141,203,204]. Receptor internalization can occur through recruitment of β-arrestin to the cell surface [39-41,43,44,47-51]. Utilizing the PRESTO-Tango assay [171], cross-recruitment of β-arrestin2 to ACKR3-Tango when co-expressed with non-tango AVPR1A was observed when the cells were stimulated with aVP (Fig. 39). To address the possible functional role of β-arrestin2 recruitment, we observed that the expression of both endogenous ACKR3 and AVPR1A declined in a time dependent manner when hVSMC were exposed to either agonist, CXCL11 or aVP (Fig. 41). Similar findings were observed with α_{1a}-AR:α_{1b}-AR heteromers. Agonist stimulation of the monomeric form of α_{1a}-AR does not typically lead to receptor internalization yet α_{1b}-AR is rapidly internalized upon agonist stimulation [87]. When these two receptors are co-expressed, stimulation with PE or norepinephrine induces co-internalization of both receptors [87,129,205]. When α_{1a}-AR was co-expressed with CXCR2, the CXCR2 inverse agonist inhibited β-arrestin2 recruitment to α_{1a}-AR-Tango. Furthermore, in that same system, a heteromer-specific biased ligand was

detected. Labetalol, a non-selective β-AR antagonist, resulted in full recruitment of β-arrestin2 recruitment to CXCR2-Tango when co-expressed with α_{1a}-AR, yet only induced minor IP_3 fluxes [144]. Co-expression of D_1R and D_2R results in the co-internalization of both receptors upon agonist stimulation [29]. β_2-AR internalizes when co-expressed with δOR in the presence of etorphine, a selective δOR agonist, whereas β_2-AR does not internalize when stimulated with etorphine when solely expressed and vice versa with δOR and isoprenanline, a selective β_2-AR agonist [206]. The aforementioned studies are aligned with the findings presented in chapter 4; however, these studies were performed in a heterologous cell system. The current studies differed in that co-internalization of endogenously expressed receptors was observed in native cells.

Conclusions

Activation of ACKR3 attenuates PE and aVP-induced vasoconstriction (Fig. 25) and signaling events (Figs. 11, 27). Additionally, ACKR3 agonists induce co-internalization of AVPR1A, thus it is likely this phenomenon also occurs with α_1-AR and could be how ACKR3 exhibits inhibitory effects. When TC14012 is administered to healthy mammals, it leads to cardiovascular collapse [114], yet the mechanism remains elusive. We demonstrated that these receptors exist as hetero-oligomeric complexes in hVSMC, thus TC14012 could lead to internalization of both AVPR1A and α_1-AR, thereby providing a mechanism for the observed cardiovascular collapse. Alternately, heteromerization with ACKR3 may alter the conformational state of AVPR1A and α_1-AR. When ACKR3 is bound to an agonist, this activated state of the receptor may affect the ligand binding region of AVPR1A or α_1-AR, decreasing the affinity of aVP or catecholamine. Studies to examine the binding kinetics of aVP or catecholamine to

AVPR1A and α_1-AR in the presence or absence of ACKR3 agonists could aid in the understanding of ACKR3 heteromerization. Several articles comment on the necessity of determining the binding kinetics of endogenously expressed agonists in the setting of GPCR heteromerization [17,46,56,182,183,193]. Instead, if the focus is shifted to identifying novel sites for receptor activation within the context of heteromerization, clinically relevant drug targets may emerge.

Development of biased ligands to preferentially activate one signaling cascade over another within a monomer is challenging, hetero-oligomerization compounds the complexity. The study by Mustafa *et al.*[144] indicates that heteromer-specific biased-ligands can exist, although the detection of CXCR2:α_{1A}-AR heteromers in native tissue has not been achieved. Many have questioned whether it is possible to selectively target endogenous hetero-oligomers. One strategy would be to utilize a combination of drugs to target two or more receptors within a complex. For example, if ACKR3 could be activated without antagonizing CXCR4 as occurs with TC14012, then perhaps this is a way to combat hypertension. Additionally, antagonizing ACKR3 may aid in regulating hypotension if a specific antagonist were available. A second strategy would be to develop and utilize small molecule ligands to bind to highly selective regions within hetero-oligomers, thus reducing off-target effects. Regardless of the methodology utilized, GPCR oligomers represent a vast, untapped resource for the pharmacologic treatment of disease.

GPCR heteromerization has not yet been studied in disease states. Furthermore, information regarding the role of endogenous receptors remains incomplete. Translationally, the roles of GPCR heteromerization would be far reaching. In diseases

such as diabetes insipidus, where the vasopressin receptors are over-expressed due to lack of endogenous aVP, alterations in AVPR heteromerization would occur. These changes may not only affect renal AVPR heteromers but could also impact vascular and neural GPCR oligomers. Any disease process which overexpresses or depletes receptors would have far-reaching effects. ACKR3 may simply be acting as a scaffold protein within the described hetero-oligomeric complex. When ACKR3 is bound to it's ligand, a conformational change in ACKR3 is initiated, and with this change, it may shift other proteins within the complex, thereby inhibiting IP_3 production.

This dissertation has provided an overview of GPCR hetero-oligomerization and delineated the role of ACKR3 acting as a master regulator of hVSMC function. Starting with the evidence that ACKR3 activation attenuates aVP and PE-mediated signaling, we then identified that ACKR3 heteromerizes with AVPR1A, CXCR4, and α_1-AR in various combinations in hVSMC. By interfering with ACKR3 heteromerization, $G\alpha_q$-protein mediated signaling by AVPR1A and α_1-AR was ablated. Furthermore, we ascertained that GPCR heteromerization is a dynamic process. Binding of receptors is dependent upon the affinity for and the available interaction sites of receptor partners. Differential receptor expression is observed in disease states [207-210], therefore receptor heteromerization would also be affected. Stabilization of receptor heteromers presents a potential therapeutic target in addition to preferentially activating the signaling cascade from one receptor within a heteromeric complex. These data suggest that ACKR3 acts as a regulator of vascular smooth muscle function and represents therapeutic potential for the treatment and management of diseases associated with impaired vascular reactivity.

CHAPTER 6

MATERIALS AND METHODS

Proteins, Peptides, and Reagents

Phenylephrine, Arginine Vasopressin, Phentolamine, 5'-Methylurapidil, Cyclazosin and BMY 7378 were purchased from Sigma Aldrich, CXCL11 and CXCL12 were from Protein Foundry, Ubiquitin was from R&D systems, and TC14012 was from Tocris Biosciences.

$CXCL11_{3-73}$ was purified as N-terminal His 6SUMO fusion proteins in E. coli as previously described [114,211,212] by our collaborator at Medical College of Wisconsin. Cells were grown in Terrific Broth and induced with 1 mM isopropyl β-D-1-thiogalactopyranoside (IPTG) before being harvested and stored at -80 ˚C. Cell pellets were lysed, and lysates clarified by centrifugation (12,000 x g for 20 minutes). The supernatant and solubilized inclusion body pellets were loaded onto Ni-NTA resin and after 1 hour proteins were eluted with 6 M guanidinium chloride, 50 mM Na2PO4 (pH 7.4), 300 mM NaCl, 500 mM imidazole, 0.2 % sodium azide, and 0.1 % β-mercaptoethanol. The eluate was pooled and refolded via dilution overnight before cleavage of the His6SUMO fusion tag by Ulp1 protease for 4 hours. The His6SUMO fusion tag and chemokine were separated using cation-exchange chromatography (SP Sepharose Fast Flow resin GE Healthcare UK Ltd.) and the eluate subjected to reverse phase high-performance liquid chromatography as a final purification. Proteins were

frozen, lyophilized and stored at -20 ˚C. Purification, folding, and homogeneity of recombinant proteins were verified by SDS-PAGE, MALDI-TOF spectroscopy and 1H-15N HSQC NMR spectroscopy.

The peptide analogs of transmembrane helix 2 (TM2; YILNLAIADLWVVLTIPVWVV DDD), helix 4 (TM4; VVCILWLLAFCVSLPDTYYLDD), and helix 7 (TM7; DDDLHVTQCLSLVHCCVNPVLYSFIN) of ACKR3 were generated using the Fmoc protected amino acids in a solid-phase synthesis on a 433A Applied Biosciences Peptide Synthesizer and Liberty Blue Microwave peptide synthesizer (CEM Corporation, Charlotte, NC, USA) using Fmoc chemistry by our collaborators at University of Illinois Chicago. The peptides were cleaved from the resin and deprotected with a mixture of 90.0% (v/v) trifluoroacetic acid (TFA) with 2.5% water, 2.5% triisopropyl-silane, 2.5% 2,2′-(ethylenedioxy) diethanethiol and 5% thioanisol. Peptides were purified on a preparative (25 mm × 250 mm) Atlantis C3 reverse phase column (Agilent Technologies, Santa Clara, CA, USA) in a 90 min gradient of 0.1% (v/v) trifluoroacetic acid in water and 0.1% trifluoroacetic acid in acetonitrile, with a 10 mL/min flow rate. The fractions containing peptides were analyzed on Agilent 6100 LC/MS spectrometer (Agilent Technologies, Santa Clara, CA, USA) with the use of a Zorbax 300SB-C3 PoroShell column and a gradient of 5% acetic acid in water and acetonitrile. Fractions that were more than 95% pure were combined and freeze dried. The TM peptide analogues were resuspended in 5% DMSO/PBS and then added to hVSMC in media for treatments as appropriate.

Cells

Human vascular smooth muscle cells (hVSMC; primary aortic smooth muscle cells, ATCC-PCS-100-012), HEK 293T cells (ATCC-CRL-11268) were purchased from American Type Culture Collection. hVSMC were cultured in vascular basal media (ATCC PCS-100-030) supplemented with the vascular smooth muscle growth kit (ATCC PCS-100-042), 100 U/mL penicillin, 100 µg/mL streptomycin. hVSMCs were used between passages 2-5. HEK 293T cells were cultured in high-glucose Dulbecco's Modified's Eagle Medium containing, 10 mg/mL sodium pyruvate, 2 mM L-glutamine, 10% (vol/vol) FBS, 100 U/mL penicillin, and 100 µg/mL streptomycin. The HTLA cell line, a HEK293 cell line stably expressing a tTA-dependent luciferase reporter and a β-arrestin2-TEV fusion gene [171], was generously provided by the laboratory of Dr. Brian Roth and maintained in high glucose Dulbecco's Modified Eagle Medium supplemented with 10% heat-inactivated FBS, 1x non-essential amino acids, 100 U/mL penicillin, 100 µg/mL streptomycin100 µg/mL, 100 µg/mL hygromycin B, and 2 µg/mL puromycin. All cells were cultured in a humidified environment at 37ºC, 5% CO_2.

Proximity Ligation Assays

Proximity ligation assays (PLA) were utilized to detect individual receptors and receptor-receptor interactions in both hVSMC and HEK cells. This technique allows for visualization of native receptors at single molecule resolution [91]. PLA was extensively employed throughout this dissertation to monitor changes in receptor expressed when heteromerization was perturbed.

Cells were grown in appropriate media on 16-well chamber slides (Nunc) until they reached 70% confluency. The media was aspirated, the cells were washed two times with Dulbecco's modified phosphate buffered saline (DPBS), then fixed with 4% paraformaldehyde for 15 min at room temperature. The fixative agent was washed three times with DPBS; the cells were blocked with 3% bovine serum albumin (BSA) in PBS overnight at 4^{o}C. Previously validated primary antibodies (see Chapter 2) were diluted in 3% BSA/PBS to a final concentration of 1:500 and added to the cells in the chamber slides for 105 min at 37^{o}C in a humidified environment. After washing the cells thrice with DPBS to remove the primary antibodies, the cells were incubated with species specific secondary antibodies, probes, conjugated to a short oligonucleotide sequence diluted 1:5 for 60 minutes at 37^{o}C in a humidified environment. PLUS and MINUS strands of the probes (Duolink, Sigma) were added to the cells, dependent upon the primary antibodies. For example, to assess the interaction between ACKR3 and CXCR4, I added mouse anti-ACKR3 (R&D systems, MAB42273) and goat anti-CXCR4 (Abcam, Ab1670) for the primary antibodies, then I added donkey anti-mouse PLUS strand and donkey anti-goat MINUS strand probes.

Following incubation with the probes, the cells were washed three times with PLA wash buffer A (Duolink, Sigma). To form a circular DNA template, the ends of the PLUS and MINUS strands were ligated by diluting the ligation stock (Duolink, Sigma) 1:5 in ultrapure water and adding ligase (Duolink, Sigma) diluted 1:40 to each chamber for 30 min at 37^{o}C in a humidified environment.

Hybridization of fluorescent probes was achieved by performing rolling circle amplification utilizing the circular DNA templated created via the ligation step. The cells

were washed thrice prior to amplification with PLA wash buffer A. Rolling circle amplification and hybridization of fluorescent probes occurred simultaneously by diluting the detection reagent (Duolink, Sigma) 1:5 in ultrapure water with the polymerase diluted 1:80. The amplification mixture was added to the cells for 100 min at 37ºC in a dark, humidified environment. Detection reagents were washed off by two washes with PLA wash buffer B and one wash with PLA wash buffer 0.01X B (Duolink, Sigma). The chambers were removed, and the slides were allowed to fully dry in the dark before staining the nucleus.

Nuclear material staining was achieved by adding a small amount of PLA mounting medium (Duolink, Sigma), containing 4′,6-diamidino-2- phenylindole (DAPI) overnight, and PLA signals (Duolink In Situ Detection Reagents Green (λexcitation/emission 495/527 nm) or Red (λexcitation/emission 598/634 nm)) were identified as fluorescent spots under a fluorescence microscope (Carl Zeiss Axiovert 200M with EC Plan-Neofluor objective lenses (40×/1.30 oil) equipped with Axio CamMRc5 (Carl Zeiss) and AxioVision Rel. 4.9.1 (Carl Zeiss) acquisition software) at room temperature. PLA signals were quantified using the Duolink Image Tool software (Sigma). Images were imported in merged.tiff formats containing DIC, signal, and nuclei channels. Merged images were visually verified for analytical quality. Comparisons and statistical analyses were performed only when PLA assays were performed on the same day in parallel experiments and fluorescence microscopy was performed with the identical settings. For each vision field 10 z-stack images in 1 µm sections were acquired and compressed. 10 randomly selected non-overlapping vision fields were analyzed. DIC

images were utilized to outline the cells in the Duolink Image Tool software, thus only the PLA signals within the cellular boundaries were analyzed.

Deconvolution Three-Dimensional Imaging

Deconvolution three-dimensional imaging was performed as described previously [84]. In brief, z-stack images were collected (from bottom to top, 20 sections of 0.5 mm) using identical acquisition parameters with a DeltaVision widefield fluorescent microscope (Applied Precision, GE) equipped with a digital camera (CoolSNAP HQ; Photometrics), using a 1.4-numerical aperture 100 objective lens. Excitation light was generated using the Insight SSI solid-state illumination module (Applied Precision, GE), and images were deconvolved with the SOFTWORX deconvolution software (Applied Precision, GE). Following deconvolution, images were quantified by IMARIS (Bitplane) software using the Surfaces feature function, generating surfaces around red puncta. Three-dimensional views of images were generated using the Surpass mode of IMARIS software.

Co-Immunoprecipitation

Co-immunoprecipitation experiments with hVSMC and HEK293T cells were performed using the Thermo Scientific Pierce co-immunoprecipitation kit (cat no. 26149), as described [82,84]. 50 µg of anti-ACKR3 (R&D systems, MAB42273), anti-AVPR1A (Bioss, BS11598R), anti-HA (Bioss bsm-50131M), or anti-mouse IgG1 (Abcam Ab81032) were incubated with 50 µL Amino Link Plus coupling resin for 150 minutes at room temperature. 500 µg of cell lysate was precleared with 50 µL of the control agarose resin slurry (60 min at 4°C). Immobilized anti-ACKR3 resin, anti-AVPR1A resin, anti-HA

resin, and anti-IgG1 resin were incubated with precleared lysate for 48 hours at 4 °C. After incubation, the resins were washed three times with 200 µL IP lysis/wash buffer, once with conditioning buffer, and protein was eluted using 50 µL of elution buffer. Samples were analyzed by Western blotting.

Intramolecular Bioluminescence Resonance Energy Transfer Assays

HEK293T cells were seeded in 12-well plates and transfected with AVPR1A-hRluc alone or together with plasmids encoding EYFP or ACKR3-EYFP using the Lipofectamine 3000 transfection reagent (ThermoScientific). For BRET titration assays, AVPR1A-hRluc at the fixed amount of 50 ng was co-transfected with increasing amounts of EYFP or ACKR3-EYFP. For BRET assays at a constant acceptor:donor ratio, increasing amounts of AVPR1A-hRluc and ACKR3-EYFP were co-transfected at a ratio of 1 : 10. In all assays, empty vector pcDNA3 was added to maintain the total cDNA amount for each transfection reaction constant. After an overnight incubation, cells were seeded in poly-L-lysine coated 96-well white plates and incubated again overnight. Cells were then washed with PBS and fluorescence was measured in a Biotek Synergy II plate reader (λexcitation 485 nm, λemission 528 nm). For BRET measurements, coelenterazine H (Nanolight Technology) at 5 mM in PBS was added to the cells. After 10 min incubation at room temperature, luminescence was measured at 460$\pm$40 and 528$\pm$20 nm. The BRET signal is calculated as the ratio of RLU measured at 528+20 nm over RLU at 460$\pm$40 nm. The net BRET is calculated by subtracting the BRET signal detected when the AVPR1A-hRLuc was transfected alone. For titration experiments, net BRET ratios are expressed as a function of EYFP/total luminescence

Western Blotting

Western blotting with rabbit anti-AVPR1A (Bioss BS-11598R), rabbit anti-ACKR3 (AbCam Ab38089), goat anti-CXCR4 (Abcam Ab1670), rabbit anti-β2-AR (Abcam Ab36956), rabbit anti-α_{1A}-AR (Abcam Ab137123), rabbit anti-α_{1B}-AR (Abcam Ab169523), goat anti-α_{1D}-AR (Santa Cruz SC27099), mouse anti-α_{2C}-AR (Abcam Ab167433), mouse anti-HA (Bioss bsm-50131M) or mouse anti-FLAG (SigmaAldrich F1804) in combination with anti-rabbit, anti-mouse (GE Healthcare) or anti-goat (Sigma-Aldrich) IgG horseradish peroxidase-linked whole antibody was performed as described previously [82-84].

Inositol 1,4,5- trisphosphate (IP_3) Assays

To evaluate changes in G protein-mediated signaling, production of IP_3 was measured. IP_3 enzyme-linked immunosorbent assays were purchased from LS Bio and performed according to the manufacturer's protocol (LS BIO F10644). In brief, hVMSCs were grown to confluency in 6-well dishes (Nunc) and then treated as described in the results section. Cells were then washed once with cold PBS, 225 µL of cold PBS was added to each well and cells were lysed by ultrasonication. The cell lysate was centrifuged for 10 minutes at 4ºC at 1500g to remove cellular debris. The total protein concentration in the supernatant was determined with the Bio-Rad DC Protein Assay according to manufacturer's protocol (Bio-Rad 500-0116). Equivalent amounts of total protein were added to the ELISA strips diluted in the provided sample diluent (1:5 and 1:10). The assay was then completed as per manufacturer's protocol. Optical densities were read on a Biotek Synergy II microplate reader (absorbance at 450 nm) and IP3 concentrations were extrapolated from the standard curve.

Gene Silencing via RNA Interference

ACKR3, CXCR4, and AVPR1A gene silencing was performed as described previously [82]. In brief, hVSMC cells were grown in 2 mL Accell siRNA delivery media per well (Dharmacon) in 6-well plates (Nunc). Commercially available Accell ACKR3, CXCR4, and AVPR1A siRNA were reconstituted with 1× siRNA buffer to a stock concentration of 100 μM. Cells were then transfected with 1μM ACKR3/CXCR4 siRNA and incubated for 72 h at 37 °C, 5% CO2. Accell NT siRNA pool was used as negative control. After 72 h, cells were assayed for receptor cell-surface expression and used for signaling experiments or to validate antibody selectivity.

GPCR Gene Transfections

HEK293T cells were transiently transfected with 1.5 μg of DNA encoding either HA-AVPR1A, FLAG-ACKR3, FLAG-CXCR4, HA-ACKR3, FLAG-ACKR3, HA-CXCR4, FLAG-α_{1a}-AR, FLAG-α_{1b}-AR, or FLAG-α_{1d}-AR with a combination of two GPCR encoding DNAs, as indicated, (all plasmids from Addgene) using Lipofectamine 3000 (Thermo Scientific) as per manufacturer's protocol. Empty vector, pcDNA, was used as a control. Twenty-four hours later, cells were fixed on chamber slides for PLA.

PRESTO-Tango β-arrestin Recruitment Assays

The PRESTO-Tango (parallel receptorome expression and screening via transcriptional output, with transcriptional activation following arrestin translocation) assay was performed as recently described [171]. The ACKR3 -Tango plasmid was a gift from Dr. Bryan Roth (Addgene plasmids #66265). HTLA cells (2.5x105/well) were seeded in a 6-well plate and transfected with 1.5 μg of the Tango plasmids using Lipofectamine 3000

(Thermo Scientific). The following day, transfected HTLA cells ($1x10^5$ cells/well) were plated onto Poly-L-Lysine pre-coated 96-well microplates and allowed to attach to the plate surface for at least 4 hours prior to treatment. Proteins used for treatment were prepared in twice the final concentration in culture media, added at a 1:1 vol/vol ratio and incubated overnight at 37°C, 5% CO_2 in a humidified environment. The following morning, media was removed from cell culture plates and replaced with a 100 µL 1:5 mixture of Bright-Glo (Promega) and 1x HBSS, 20 mM HEPES solution. Plates were then incubated at room temperature before measuring luminescence on a Biotek Synergy II plate reader.

Receptor Internalization Assays

Assessment of receptor internalization upon agonist stimulation was achieved via flow cytometry. hVSMCs were treated with 1µM of aVP or CXCL11 for various time points. The cells were washed once with ice cold DPBS, blocked, and stained with rabbit anti-AVPR1A (Bioss BS-11598R) and mouse anti- ACKR3 (R&D MAB42273) antibodies at 1:200 dilution for 1h on ice. Cells were then washed twice with FACS wash buffer (1X PBS, 2% FBS, 0.01% NaN_3) and secondary antibodies were added at a 1:500 dilution and incubated for 30 min on ice (donkey anti-rabbit Alexa Fluor 647, Invitrogen A-31573 and donkey anti-mouse Alexa Fluor 488, Invitrogen A-21202). Cells were washed twice with FACS wash buffer and then fixed with 4% paraformaldehyde at room temperature for 15 min. After two additional washes, the cells were counted on a BD FACS Canto II (BD Biosciences) flow cytometer. The fluorescence intensities of at least 3×10^4 cells were recorded and analyzed using the FlowJo software (Tree Star).

Flow Cytometry

Flow cytometry was utilized to assess equivalent recombinant Tango receptor expression. HTLA cells were labeled with rabbit anti-FLAG-Alexa Fluor 647 (R&D Systems IC8529R) on ice for 45 min following a blocking step. Cells were then washed twice with FACS wash buffer (1X PBS, 2% FBS, 0.01% NaN_3). Cells were then fixed with 4% paraformaldehyde at room temperature for 15 min. After two additional washes, the cells were counted on a BD FACS Canto II (BD Biosciences) flow cytometer. The fluorescence intensities of at least 3 x 10^4 cells were recorded and analyzed using the FlowJo software (Tree Star).

Pressure Myography

All procedures involving animals were conducted in accordance with the Guide for the Care and Use of Laboratory Animals, 8th Edition and were approved by the Institutional Animal Care and Use Committee of Loyola University Chicago. Pressure myography was performed as described in detail previously with slight modifications [83,114]. Male Sprague-Dawley rats (Harlan) were anesthetized with 3.5% isoflurane. The mesentery was immediately removed and placed in 130 mM NaCl, 4.7 mM KCl, 1.18 mM KH2PO4, 1.17 mM MgSO4, 14.9 mM, NaHCO3, 5.5 mM D-Glucose, 0.026 mM EDTA, 1.16 mM CaCl2 aerated with 95% O2, 5% CO2 at 37^{o}C. The animal was then euthanized by cardiectomy and bilateral decompression of the lungs. Third or 4th order mesenteric arteries were dissected free from the mesentery, mounted onto two glass cannulae with United States Pharmacopeia (USP) scale 11-0 sutures and pressurized to 80 mmHg in a DMT 110P pressure myograph system (DMT-USA). The intraluminal solution and the vessel bath solution were the same as described before. The vessel bath solution was continuously aerated with 95% O2, 5% CO_2 throughout the experiment. The outer

diameter (o.d.) of the pressurized vessel was then continuously measured and recorded via digital video-edge detection upon addition of increasing doses of phenylephrine (PE) or arginine vasopressin (aVP) to the vessel bath.

Technical Assistance

Pressure myography experiments were performed by Heather M. LaPorte. Jonathon M. Eby performed the PRESTO-Tango experiments in Figs. 10, 21, 26. Xianlong Gao made all plasmids and performed BRET experiments in Fig. 29B/C. Abhishek Tripathi performed PLA and co-immunoprecipitation experiments with the exception of the ACKR3:α_{1D}-AR in Figs. 13-14. Adarsh Dharan assisted with the three-dimensional deconvolution microscopy in Fig. 30C.

Data Analyses

Data are expressed as mean ± standard error of the mean (SEM) from n independent experiments that were performed on different days. Data were analyzed using the GraphPad-Prism 7 software. Unpaired Student's t test or one-way analyses of variance (ANOVA) with Dunnett's multiple comparison post-hoc test for multiple comparisons were used, as appropriate. Dose response curves were generated using non-linear regression analyses. A two-tailed $p < 0.05$ was considered significant.

LIST OF REFERENCES

1. Mozaffarian D, Benjamin EJ, Go AS, et al. Heart disease and stroke statistics-2015 update : A report from the american heart association. *Circulation*. 2015;131(4):e29-e39.

2. Benjamin EJ, Blaha MJ, Chiuve SE, et al. Heart disease and stroke statistics'2017 update: A report from the american heart association. *Circulation*. 2017;135(10):e146-e603.

3. Yapps B, Shin S, Bighamian R, et al. Hypotension in ICU patients receiving vasopressor therapy. *Sci Rep*. 2017;7(1).

4. Imming P, Sinning C, Meyer A. Drugs, their targets and the nature and number of drug targets. *Nat Rev Drug Discov*. 2006;5(10):821-834.

5. Salazar NC, Chen J, Rockman HA. Cardiac GPCRs: GPCR signaling in healthy and failing hearts. *Biochim Biophys Acta Biomembr*. 2007;1768(4):1006-1018.

6. Filmore D. *It's a GPCR world.* Vol 7. ; 2004:24-28.

7. Rockman HA, Koch WJ, Lefkowitz RJ. Seven-transmembrane-spanning receptors and heart function. *Nature*. 2002;415(6868):206-212.

8. Hopkins AL, Groom CR. The druggable genome. *Nat Rev Drug Discov*. 2002;1(9):727-730.

9. Dewire SM, Violin JD. Biased ligands for better cardiovascular drugs: Dissecting g-protein-coupled receptor pharmacology. *Circ Res*. 2011;109(2):205-216.

10. Lefkowitz RJ. The superfamily of heptahelical receptors. *Nature Cell Biol*. 2000;2(7):E133-E136.

11. Pierce KL, Premont RT, Lefkowitz RJ. Seven-transmembrane receptors. *Nat Rev Mol Cell Biol*. 2002;3(9):639-650.

12. Gether U, Kobilka BK. G protein-coupled receptors. *J Biol Chem*. 1998;273(29):17979-17982.

13. Kobilka BK. G protein coupled receptor structure and activation. *Biochim Biophys Acta Biomembr*. 2007;1768(4):794-807.

14. Venkatakrishnan AJ, Deupi X, Lebon G, Tate CG, Schertler GF, Madan Babu M. Molecular signatures of G-protein-coupled receptors. *Nature*. 2013;494(7436):185-194.

15. Fredriksson R, Lagerström MC, Lundin L-, Schiöth HB. The G-protein-coupled receptors in the human genome form five main families. phylogenetic analysis, paralogon groups, and fingerprints. *Mol Pharmacol*. 2003;63(6):1256-1272.

16. Attwood TK, Findlay JBC. Fingerprinting g-protein-coupled receptors. *Protein Eng Des Sel*. 1994;7(2):195-203.

17. Farran B. An update on the physiological and therapeutic relevance of GPCR oligomers. *Pharmacol Res*. 2017;117:303-327.

18. Milligan G. G-protein-coupled receptor heterodimers: Pharmacology, function and relevance to drug discovery. *Drug Discov Today*. 2006;11(11-12):541-549.

19. Milligan G. A day in the life of a G protein-coupled receptor: The contribution to function of G protein-coupled receptor dimerization. *Br J Pharmacol*. 2008;153(SUPPL. 1):S216-S229.

20. Larocca TJ, Schwarzkopf M, Altman P, et al. ß2-adrenergic receptor signaling in the cardiac myocyte is modulated by interactions with CXCR4. *J Cardiovasc Pharmacol*. 2010;56(5):548-559.

21. Glass MJ, Pickel VM. A2a-adrenergic receptors are present in μ-opioid receptor containing neurons in rat medial nucleus tractus solitarius. *Synapse*. 2002;43(3):208-218.

22. Ferré S, Torvinen M, Antoniou K, et al. Adenosine A1 receptor-mediated modulation of dopamine D1 receptors in stably cotransfected fibroblast cells. *J Biol Chem*. 1998;273(8):4718-4724.

23. Liu R, Ramani B, Soto D, De Arcangelis V, Xiang Y. Agonist dose-dependent phosphorylation by protein kinase A and G protein-coupled receptor kinase regulates ß2 adrenoceptor coupling to gi proteins in cardiomyocytes. *J Biol Chem*. 2009;284(47):32279-32287.

24. Sohy D, Parmentier M, Springael J-. Allosteric transinhibition by specific antagonists in CCR2/CXCR4 heterodimers. *J Biol Chem*. 2007;282(41):30062-30069.

25. Stott JB, Povstyan OV, Carr G, Barrese V, Greenwood IA. G-protein βγ subunits are positive regulators of Kv7.4 and native vascular Kv7 channel activity. *Proc Natl Acad Sci U S A*. 2015;112(20):6497-6502.

26. Cao Y, Sun W-, Jin L, Xie K-, Zhu X-. Activation of adenosine A1 receptor modulates dopamine D1 receptor activity in stably cotransfected human embryonic kidney 293 cells. *Eur J Pharmacol*. 2006;548(1-3):29-35.

27. Fuxe K, Ferré S, Canals M, et al. Adenosine A2A and dopamine D2 heteromeric receptor complexes and their function. *J Mol Neurosci*. 2005;26(2-3):209-219.

28. Canals M, Marcellino D, Fanelli F, et al. Adenosine A2A-dopamine D2 receptor-receptor heteromerization: Qualitative and quantitative assessment by fluorescence and bioluminescence energy transfer. *J Biol Chem*. 2003;278(47):46741-46749.

29. So CH, Varghese G, Curley KJ, et al. D1 and D2 dopamine receptors form heterooligomers and cointernalize after selective activation of either receptor. *Mol Pharmacol*. 2005;68(3):568-578.

30. Zheng M, Han QD, Xiao RP. Distinct beta-adrenergic receptor subtype signaling in the heart and their pathophysiological relevance. *Sheng Li Xue Bao*. 2004;56(1):1-15.

31. Fujita W, Gomes I, Devi LA. Heteromers of μ-δ opioid receptors: New pharmacology and novel therapeutic possibilities. *Br J Pharmacol*. 2015;172(2):375-387.

32. Radács M., Gálfi M., Nagyéri Gy., et al. Significance of the adrenergic system in the regulation of vasopressin secretion in rat neurohypophyseal tissue cultures. *Regul Pept*. 2008;148(1-3):1-5.

33. Guimarães S, Moura D. Vascular adrenoceptors: An update. *Pharmacol Rev*. 2001;53(2):319-356.

34. Goupil E, Fillion D, Clement S, et al. Angiotensin II type I and prostaglandin F2alpha receptors cooperatively modulate signaling in vascular smooth muscle cells. *J Biol Chem*. 2015;290(5):3137-3148.

35. Medina P, Acuña A, Martínez-León JB, et al. Arginine vasopressin enhances sympathetic constriction through the V1 vasopressin receptor in human saphenous vein. *Circulation*. 1998;97(9):865-870.

36. Jaeger WC, Armstrong SP, Hill SJ, Pfleger KDG. Biophysical detection of diversity and bias in GPCR function. *Front Endocrinol*. 2014;5(MAR).

37. Terrillon S, Barberis C, Bouvier M. Heterodimerization of V1a and V2 vasopressin receptors determines the interaction with ß-arrestin and their trafficking patterns. *Proc Natl Acad Sci U S A*. 2004;101(6):1548-1553.

38. Howl J, Wheatley M. Molecular pharmacology of V1a vasopressin receptors. *Gen Pharmacol Vasc Syst*. 1995;26(6):1143-1152.

39. Daaka Y, Luttrell LM, Ahn S, et al. Essential role for G protein-coupled receptor endocytosis in the activation of mitogen-activated protein kinase. *J Biol Chem*. 1998;273(2):685-688.

40. DeWire SM, Ahn S, Lefkowitz RJ, Shenoy SK, eds. *ß-arrestins and cell signaling.* ; 2007Annual Review of Physiology; No. 69.

41. Ferguson SSG. Evolving concepts in G protein-coupled receptor endocytosis: The role in receptor desensitization and signaling. *Pharmacol Rev*. 2001;53(1):1-24.

42. Lefkowitz RJ, Shenoy SK. Transduction of receptor signals by ß-arrestins. *Science*. 2005;308(5721):512-517.

43. Hunyady L, Catt KJ, Clark AJL, Gáborik Z. Mechanisms and functions of AT1 angiotensin receptor internalization. *Regul Pept*. 2000;91(1-3):29-44.

44. Luttrell LM, Lefkowitz RJ. The role of ß-arrestins in the termination and transduction of G-protein-coupled receptor signals. *J Cell Sci*. 2002;115(3):455-465.

45. Shenoy SK, Lefkowitz RJ. ß-arrestin-mediated receptor trafficking and signal transduction. *Trends Pharmacol Sci*. 2011;32(9):521-533.

46. Agnati LF, Ferré S, Lluis C, Franco R, Fuxe K. Molecular mechanisms and therapeutical implications of intramembrane receptor/receptor interactions among heptahelical receptors with examples from the striatopallidal GABA neurons. *Pharmacol Rev*. 2003;55(3):509-550.

47. Aramori I, Zhang J, Ferguson SSG, Bieniasz PD, Cullen BR, Caron MG. Molecular mechanism of desensitization of the chemokine receptor CCR-5: Receptor signaling and internalization are dissociable from its role as an HIV-1 co-receptor. *EMBO J*. 1997;16(15):4606-4616.

48. Ferguson SSG, Zhang J, Barak LS, Caron MG. Molecular mechanisms of G protein-coupled receptor desensitization and resensitization. *Life Sci*. 1998;62(17-18):1561-1565.

49. Luker KE, Steele JM, Mihalko LA, Ray P, Luker GD. Constitutive and chemokine-dependent internalization and recycling of CXCR7 in breast cancer cells to degrade chemokine ligands. *Oncogene*. 2010;29(32):4599-4610.

50. Hunton DL, Barnes WG, Kim J, et al. ß-arrestin 2-dependent angiotensin II type 1A receptor-mediated pathway of chemotaxis. *Mol Pharmacol*. 2005;67(4):1229-1236.

51. Rajagopal S, Kim J, Ahn S, et al. Beta-arrestin- but not G protein-mediated signaling by the "decoy" receptor CXCR7. *Proc Natl Acad Sci U S A*. 2010;107(2):628-632.

52. Wacker D, Stevens RC, Roth BL. How ligands illuminate GPCR molecular pharmacology. *Cell*. 2017;170(3):414-427. doi: https://doi-org.archer.luhs.org/10.1016/j.cell.2017.07.009.

53. Kamal M, Maurice P, Jockers R. Expanding the concept of G protein-coupled receptor (GPCR) dimer asymmetry towards GPCR-interacting proteins. *Pharmaceuticals*. 2011;4(2):273-284.

54. Devi LA. Heterodimerization of G-protein-coupled receptors: Pharmacology, signaling and trafficking. *Trends Pharmacol Sci*. 2001;22(10):532-537.

55. Mustafa S, Ayoub MA, Pfleger KDG. Uncovering GPCR heteromer-biased ligands. *Drug Discov Today Techn*. 2010;7(1):e77-e85.

56. Albizu L, Moreno JL, González-Maeso J, Sealfon SC. Heteromerization of G protein-coupled receptors: Relevance to neurological disorders and neurotherapeutics. *CNS Neurol Disord Drug Targets*. 2010;9(5):636-650.

57. Howard AD, McAllister G, Feighner SD, et al. Orphan G-protein-coupled receptors and natural ligand discovery. *Trends Pharmacol Sci*. 2001;22(3):132-140.

58. Fawzi AB, Macdonald D, Benbow LL, et al. SCH-202676: An allosteric modulator of both agonist and antagonist binding to G protein-coupled receptors. *Mol Pharmacol*. 2001;59(1):30-37.

59. Khoury E, Clément S, Laporte SA. Allosteric and biased G protein-coupled receptor signaling regulation: Potentials for new therapeutics. *Front Endocrinol*. 2014;5(MAY).

60. Shukla AK, Singh G, Ghosh E. Emerging structural insights into biased GPCR signaling. *Trends Biochem Sci*. 2014;39(12):594-602.

61. Ferré S, Baler R, Bouvier M, et al. Building a new conceptual framework for receptor heteromers. *Nat Chem Biol*. 2009;5(3):131-134.

62. Gomes I, Ayoub MA, Fujita W, Jaeger WC, Pfleger KDG, Devi LA, eds. *G protein-coupled receptor heteromers.* ; 2016Annual Review of Pharmacology and Toxicology; No. 56.

63. Ferré S, Casadó V, Devi LA, et al. G protein-coupled receptor oligomerization revisited: Functional and pharmacological perspectives. *Pharmacol Rev*. 2014;66(2):413-434.

64. Jordan BA, Devi LA. G-protein-coupled receptor heterodimerization modulates receptor function. *Nature*. 1999;399(6737):697-700.

65. Callewaere C, Fernette B, Raison D, et al. Cellular and subcellular evidence for neuronal interaction between the chemokine stromal cell-derived factor-1/CXCL 12 and vasopressin: Regulation in the hypothalamo-neurohypophysial system of the brattleboro rats. *Endocrinology*. 2008;149(1):310-319.

66. Vilardaga J-, Nikolaev VO, Lorenz K, Ferrandon S, Zhuang Z, Lohse MJ. Conformational cross-talk between a2A-adrenergic and μ-opioid receptors controls cell signaling. *Nat Chem Biol*. 2008;4(2):126-131.

67. Pepe S, Van Den Brink OWV, Lakatta EG, Xiao R-. Cross-talk of opioid peptide receptor and ß-adrenergic receptor signalling in the heart. *Cardiovasc Res*. 2004;63(3):414-422.

68. Szmydynger-Chodobska J, Gandy JR, Varone A, Shan R, Chodobski A. Synergistic interactions between cytokines and AVP at the blood-CSF barrier result in increased chemokine production and augmented influx of leukocytes after brain injury. *PLoS ONE*. 2013;8(11).

69. Terrillon S, Bouvier M. Roles of G-protein-coupled receptor dimerization. *EMBO Rep*. 2004;5(1):30-34.

70. Wilson S, Wilkinson G, Milligan G. The CXCR1 and CXCR2 receptors form constitutive homo- and heterodimers selectively and with equal apparent affinities. *J Biol Chem*. 2005;280(31):28663-28674.

71. Floyd DH, Geva A, Bruinsma SP, Overton MC, Blumer KJ, Baranski TJ. C5a receptor oligomerization: II. fluorescence resonance energy transfer studies of a human G protein-coupled receptor expressed in yeast. *J Biol Chem*. 2003;278(37):35354-35361.

72. Overton MC, Blumer KJ. The extracellular N-terminal domain and transmembrane domains 1 and 2 mediate oligomerization of a yeast G protein-coupled receptor. *J Biol Chem*. 2002;277(44):41463-41472.

73. Issafras H, Angers S, Bulenger S, et al. Constitutive agonist-independent CCR5 oligomerization and antibody-mediated clustering occurring at physiological levels of receptors. *J Biol Chem*. 2002;277(38):34666-34673.

74. Rankovic Z, Brust TF, Bohn LM. Biased agonism: An emerging paradigm in GPCR drug discovery. *Bioorg Med Chem Lett*. 2016;26(2):241-250.

75. Wurch T, Matsumoto A, Pauwels PJ. Agonist-independent and -dependent oligomerization of dopamine D2 receptors by fusion to fluorescent proteins. *FEBS Lett*. 2001;507(1):109-113.

76. Hillion J, Canals M, Torvinen M, et al. Coaggregation, cointernalization, and codesensitization of adenosine A2A receptors and dopamine D2 receptors. *J Biol Chem*. 2002;277(20):18091-18097.

77. Ginés S, Hillion J, Torvinen M, et al. Dopamine D1 and adenosine A1 receptors form functionally interacting heteromeric complexes. *Proc Natl Acad Sci U S A*. 2000;97(15):8606-8611.

78. Mellado M, Rodríguez-Frade JM, Vila-Coro AJ, et al. Chemokine receptor homo- or heterodimerization activates distinct signaling pathways. *EMBO J*. 2001;20(10):2497-2507.

79. Zhu W-, Chakir K, Zhang S, et al. Heterodimerization of ß1- and ß2-adrenergic receptor subtypes optimizes ß-adrenergic modulation of cardiac contractility. *Circ Res*. 2005;97(3):244-251.

80. Wei S-, Zhang Z-, Yu Y, Weiss RM, Felder RB. Central actions of the chemokine stromal cell-derived factor 1 contribute to neurohumoral excitation in heart failure rats. *Hypertension*. 2012;59(5):991-998.

81. Chu P-, Zatta A, Kiriazis H, et al. CXCR4 antagonism attenuates the cardiorenal consequences of mineralocorticoid excess. *Circ Heart Fail*. 2011;4(5):651-658.

82. Albee LJ, Eby JM, Tripathi A, et al. A1-adrenoceptors function within hetero-oligomeric complexes with chemokine receptors ACKR3 and CXCR4 in vascular smooth muscle cells. *Journal of the American Heart Association*. 2017.

83. Evans AE, Tripathi A, LaPorte HM, et al. New insights into mechanisms and functions of chemokine (C-X-C motif) receptor 4 heteromerization in vascular smooth muscle. *Int J Mol Sci*. 2016;17(6).

84. Tripathi A, Vana PG, Chavan TS, et al. Heteromerization of chemokine (C-X-C motif) receptor 4 with a1A/B -adrenergic receptors controls adrenergic a1 receptor function. *Proc Natl Acad Sci U S A*. 2015;112(13):E1659-E1668.

85. AbdAlla S, Lother H, Quitterer U. AT1-receptor heterodimers show enhanced G-protein activation and altered receptor sequestration. *Nature*. 2000;407(6800):94-98.

86. Wang ER, Jarrah AA, Benard L, et al. Deletion of CXCR4 in cardiomyocytes exacerbates cardiac dysfunction following isoproterenol administration. *Gene Ther*. 2014;21(5):496-506.

87. Stanasila L, Perez J-, Vogel H, Cotecchia S. Oligomerization of the a1a- and a 1b-adrenergic receptor subtypes. potential implications in receptor internalization. *J Biol Chem*. 2003;278(41):40239-40251.

88. Jordan BA, Gomes I, Rios C, Filipovska J, Devi LA. Functional interactions between μ opioid and a 2A-adrenergic receptors. *Mol Pharmacol*. 2003;64(6):1317-1324.

89. Terrillon S, Barberis C, Bouvier M. Heterodimerization of V1a and V2 vasopressin receptors determines the interaction with ß-arrestin and their trafficking patterns. *Proc Natl Acad Sci U S A*. 2004;101(6):1548-1553.

90. Miller WE, Lefkowitz RJ. Expanding roles for ß-arrestins as scaffolds and adapters in GPCR signaling and trafficking. *Curr Opin Cell Biol*. 2001;13(2):139-145.

91. Berggård T, Linse S, James P. Methods for the detection and analysis of protein-protein interactions. *Proteomics*. 2007;7(16):2833-2842.

92. Söderberg O, Gullberg M, Jarvius M, et al. Direct observation of individual endogenous protein complexes in situ by proximity ligation. *Nat Methods*. 2006;3(12):995-1000.

93. Baba K, Benleulmi-Chaachoua A, Journé A-, et al. Heteromeric MT1/MT2 melatonin receptors modulate photoreceptor function. *Sci Signal*. 2013;6(296).

94. Bach IV HH, Saini V, Baker TA, Tripathi A, Gamelli RL, Majetschak M. Initial assessment of the role of CXC chemokine receptor 4 after polytrauma. *Mol Med*. 2012;18(7):1056-1066.

95. Saini V, Marchese A, Majetschak M. CXC chemokine receptor 4 is a cell surface receptor for extracellular ubiquitin. *J Biol Chem*. 2010;285(20):15566-15576.

96. Tripathi A, Davis JD, Staren DM, Volkman BF, Majetschak M. CXC chemokine receptor 4 signaling upon co-activation with stromal cell-derived factor-1a and ubiquitin. *Cytokine*. 2014;65(2):121-125.

97. Balabanian K, Lagane B, Infantino S, et al. The chemokine SDF-1/CXCL12 binds to and signals through the orphan receptor RDC1 in T lymphocytes. *J Biol Chem*. 2005;280(42):35760-35766.

98. Busillo JM, Benovic JL. Regulation of CXCR4 signaling. *Biochim Biophys Acta Biomembr*. 2007;1768(4):952-963.

99. Callewaere C, Banisadr G, Desarménien MG, et al. The chemokine SDF-1/CXCL12 modulates the firing pattern of vasopression neurons and counteracts induced vasopressin release through CXCR. *Proc Natl Acad Sci U S A*. 2006;103(21):8221-8226.

100. Agarwal U, Ghalayini W, Dong F, et al. Role of cardiac myocyte CXCR4 expression in development and left ventricular remodeling after acute myocardial infarction. *Circ Res*. 2010;107(5):667-676.

101. Eby JM, Abdelkarim H, Albee LJ, et al. Functional and structural consequences of chemokine (C-X-C motif) receptor 4 activation with cognate and non-cognate agonists. *Mol Cell Biochem*. 2017;434(1-2):143-151.

102. Naumann U, Cameroni E, Pruenster M, et al. CXCR7 functions as a scavenger for CXCL12 and CXCL11. *PLoS ONE*. 2010;5(2).

103. Ödemis V, Boosmann K, Heinen A, Küry P, Engele J. CXCR7 is an active component of SDF-1 signalling in astrocytes and schwann cells. *J Cell Sci*. 2010;123(7):1081-1088.

104. Bach HH, Wong YM, LaPorte HM, Gamelli RL, Majetschak M. Pharmacological targeting of chemokine (C-X-C motif) receptor 4 in porcine polytrauma and hemorrhage models. *J Trauma Acute Care Surg*. 2016;80(1):102-110.

105. Dai S, Yuan F, Mu J, et al. Chronic AMD3100 antagonism of SDF-1a-CXCR4 exacerbates cardiac dysfunction and remodeling after myocardial infarction. *J Mol Cell Cardiol*. 2010;49(4):587-597.

106. Martin C, Bridger GJ, Rankin SM. Structural analogues of AMD3100 mobilise haematopoietic progenitor cells from bone marrow in vivo according to their ability to inhibit CXCL12 binding to CXCR4 in vitro. *Br J Haematol*. 2006;134(3):326-329.

107. Hawkins OE, Richmond A. The dynamic yin-yang interaction of CXCR4 and CXCR7 in breast cancer metastasis. *Breast Cancer Res*. 2012;14(1).

108. Wang J, He L, Combs CA, Roderiquez G, Norcross MA. Dimerization of CXCR4 in living malignant cells: Control of cell migration by a synthetic peptide that reduces homologous CXCR4 interactions. *Mol Cancer Ther*. 2006;5(10):2474-2483.

109. Tunc T, Cekmez F, Cetinkaya M, et al. Diagnostic value of elevated CXCR4 and CXCL12 in neonatal sepsis. *J Matern -Fetal Neonatal Med*. 2015;28(3):356-361.

110. Wu Y, Zhu Y, Chen X-, Liu L-, Li T. Diversity of vascular reactivity and the treatment response in diabetic, hypertensive, hyperlipidemic, and healthy rats subjected to hemorrhagic shock. *Shock*. 2016;45(2):174-183.

111. Russell JA. Management of sepsis. *New Engl J Med*. 2006;355(16):1699-1713.

112. Lesur O, Roussy J-, Chagnon F, et al. Proven infection-related sepsis induces a differential stress response early after ICU admission. *Crit Care*. 2010;14(4).

113. Franchini S, Marcianò T, Sorlini C, et al. Serum CXCL12 levels on hospital admission predict mortality in patients with severe sepsis/septic shock. *Am J Emerg Med*. 2015;33(12):1802-1804.

114. Bach HH, Wong YM, Tripathi A, Gamelli RL, Majetschak M. Chemokine (C-X-C motif) receptor 4 and atypical chemokine receptor 3 regulate vascular a1-adrenergic receptor function. *Mol Med*. 2014;20(JULY-DECEMBER 2014):435-447.

115. Guo W, Shi L, Filizola M, Weinstein H, Javitch JA. Crosstalk in G protein-coupled receptors: Changes at the transmembrane homodimer interface determine activation. *Proc Natl Acad Sci U S A*. 2005;102(48):17495-17500.

116. Rodríguez D, Gutiérrez-de-Terán H. Characterization of the homodimerization interface and functional hotspots of the CXCR4 chemokine receptor. *Proteins Struct Funct Bioinformatics*. 2012;80(8):1919-1928.

117. Chen J, Chemaly E, Liang L, et al. Effects of CXCR4 gene transfer on cardiac function after ischemia-reperfusion injury. *Am J Pathol*. 2010;176(4):1705-1715.

118. LaRocca TJ, Jeong D, Kohlbrenner E, et al. CXCR4 gene transfer prevents pressure overload induced heart failure. *J Mol Cell Cardiol*. 2012;53(2):223-232.

119. Décaillot FM, Kazmi MA, Lin Y, Ray-Saha S, Sakmar TP, Sachdev P. CXCR7/CXCR4 heterodimer constitutively recruits ß-arrestin to enhance cell migration. *J Biol Chem*. 2011;286(37):32188-32197.

120. Watts AO, Van Lipzig MMH, Jaeger WC, et al. Identification and profiling of CXCR3-CXCR4 chemokine receptor heteromer complexes. *Br J Pharmacol*. 2013;168(7):1662-1674.

121. Sohy D, Yano H, de Nadai P, et al. Hetero-oligomerization of CCR2, CCR5, and CXCR4 and the protean effects of "selective" antagonists. *J Biol Chem*. 2009;284(45):31270-31279.

122. Pello OM, Martínez-Muñoz L, Parrillas V, et al. Ligand stabilization of CXCR4/d-opioid receptor heterodimers reveals a mechanism for immune response regulation. *Eur J Immunol*. 2008;38(2):537-549.

123. Levoye A, Balabanian K, Baleux F, Bachelerie F, Lagane B. CXCR7 heterodimerizes with CXCR4 and regulates CXCL12-mediated G protein signaling. *Blood*. 2009;113(24):6085-6093.

124. Bachelerie F, Ben-Baruch A, Burkhardt AM, et al. International union of pharmacology. LXXXIX. update on the extended family of chemokine receptors and introducing a new nomenclature for atypical chemokine receptors. *Pharmacol Rev*. 2014;66(1):1-79.

125. Pawig L, Klasen C, Weber C, Bernhagen J, Noels H. Diversity and inter-connections in the CXCR4 chemokine receptor/ligand family: Molecular perspectives. *Front Immunol*. 2015;6(AUG).

126. Hausdorff WP, Hnatowich M, O'Dowd BF, Caron MG, Lefkowitz RJ. A mutation of the ß2-adrenergic receptor impairs agonist activation of adenylyl cyclase without affecting high affinity agonist binding: Distinct molecular determinants of the receptor are involved in physical coupling to and functional activation of gs. *J Biol Chem*. 1990;265(3):1388-1393.

127. Randle J.C.R., Mazurek M., Kneifel D., Dufresne J., Renaud L.P. A1-adrenergic receptor activation releases vasopressin and oxytocin from perfused rat hypothalamic explants. *Neurosci Lett*. 1986;65(2):219-223.

128. Hanson KM, Post JA, Desiderio MA. Alpha-adrenergic blocking agents and the cardiovascular response to pharmacological doses of vasopressin. *Pharmacology*. 1980;21(1):16-28.

129. Cotecchia S, ed. *Constitutive activity and inverse agonism at the a1a and a1b adrenergic receptor subtypes.* ; 2010Methods in Enzymology; No. 485.

130. Kong J-, Taylor DA, Fleming WW. Functional distribution and role of alpha-1 adrenoceptor subtypes in the mesenteric vasculature of the rat. *J Pharmacol Exp Ther*. 1994;268(3):1153-1159.

131. Buckner SA, Oheim KW, Morse PA, Knepper SM, Hancock AA. A1-adrenoceptor-induced contractility in rat aorta is mediated by the a1D subtype. *Eur J Pharmacol*. 1996;297(3):241-248.

132. Ziolkowski N, Grover AK. Functional linkage as a direction for studies in oxidative stress: A-adrenergic receptors. *Can J Physiol Pharmacol*. 2010;88(3):220-232.

133. Bristow MR, Ginsburg R, Minobe W, et al. Decreased catecholamine sensitivity and ß-adrenergic-receptor density in failing human hearts. *N Engl J Med*. 1982;307(4):205-211.

134. Cavalli A, Lattion A-, Hummler E, et al. Decreased blood pressure response in mice deficient of the a1b-adrenergic receptor. *Proc Natl Acad Sci U S A*. 1997;94(21):11589-11594.

135. Cotecchia S, Stanasila L, Diviani D. Protein-protein interactions at the adrenergic receptors. *Curr Drug Targets*. 2012;13(1):15-27.

136. Cummings S., Seybold V. Relationship of alpha-1- and alpha-2-adrenergic-binding sites to regions of the paraventricular nucleus of the hypothalamus containing corticotropin-releasing factor and vasopressin neurons. *Neuroendocrinology*. 1988;47(6):523-532.

137. Gericke A, Kordasz ML, Steege A, et al. Functional role of a 1-adrenoceptor subtypes in murine ophthalmic arteries. *Invest Ophthalmol Vis Sci*. 2011;52(7):4795-4799.

138. Rokosh DG, Simpson PC. Knockout of the a1A/C-adrenergic receptor subtype: The a1A/C is expressed in resistance arteries and is required to maintain arterial blood pressure. *Proc Natl Acad Sci U S A*. 2002;99(14):9474-9479.

139. Muramatsu I, Murata S, Isaka M, et al. A1-adrenoceptor subtypes and two receptor systems in vascular tissues. *Life Sci*. 1998;62(17-18):1461-1465.

140. Saussy Jr. DL, Goetz AS, Queen KL, King HK, Lutz MW, Rimele TJ. Structure activity relationships of a series of buspirone analogs at alpha-1 adrenoceptors: Further evidence that rat aorta alpha-1 adrenoceptors are of the alpha-1D-subtype. *J Pharmacol Exp Ther*. 1996;278(1):136-144.

141. Milligan G. The role of dimerisation in the cellular trafficking of G-protein-coupled receptors. *Curr Opin Pharmacol*. 2010;10(1):23-29.

142. Bylund DB, Eikenberg DC, Hieble JP, et al. International union of pharmacology nomenclature of adrenoceptors. *Pharmacol Rev*. 1994;46(2):121-136.

143. Uberti MA, Hall RA, Minneman KP. Subtype-specific dimerization of a1-adrenoceptors: Effects on receptor expression and pharmacological properties. *Mol Pharmacol*. 2003;64(6):1379-1390.

144. Mustafa S, See HB, Seeber RM, et al. Identification and profiling of novel a 1A-adrenoceptor-CXC chemokine receptor 2 heteromer. *J Biol Chem*. 2012;287(16):12952-12965.

145. BARTELSTONE HJ, NASMYTH PA. Vasopressin potentiation of catecholamine actions in dog, rat, cat, and. *Am J Physiol*. 1965;208:754-762.

146. Derad I, Pauschinger P, Born J. Norepinephrine amplifies effects of vasopressin on the isolated rat heart. *Regul Pept*. 1992;39(1):35-41.

147. Harada S, Imaizumi T, Momohara M, Masaki H, Ando S-, Takeshita A. Arginine vasopressin attenuates phenylephrine-induced forearm vasoconstriction in men. *Clin Sci*. 1991;81(6):733-737.

148. Heineman A, Horina G, Stauber RE, Pertl C, Holzer P, Peskar BA. Lack of effect of a selective vasopressin V(1A) receptor antagonist, SR 49,059, on potentiation by vasopressin of adrenoceptor-mediated presser responses in the rat mesenteric arterial bed. *Br J Pharmacol*. 1998;125(6):1120-1127.

149. Medina P, Noguera I, Aldasoro M, Vila JM, Flor B, Lluch S. Enhancement by vasopressin of adrenergic responses in human mesenteric arteries. *Am J Physiol Heart Circ Physiol*. 1997;272(3 41-3):H1087-H1093.

150. Noguera I, Medina P, Segarra G, et al. Potentiation by vasopressin of adrenergic vasoconstriction in the rat isolated mesenteric artery. *Br J Pharmacol*. 1997;122(3):431-438.

151. Segarra G, Medina P, Vila JM, Chuan P, Domenech C, Lluch S. Increased contraction to noradrenaline by vasopressin in human renal arteries. *J Hypertens*. 2002;20(7):1373-1379.

152. Steppan J, Nyhan SM, Sikka G, et al. Vasopressin-mediated enhancement of adrenergic vasoconstriction involves both the tyrosine kinase and the protein kinase C pathways. *Anesth Analg*. 2012;115(6):1290-1295.

153. Streefkerk JO, Pfaffendorf M, Van Zwieten PA. Vasopressin-induced facilitation of adrenergic responses in the rat mesenteric artery is V1-receptor dependent. *Auton Autacoid Pharmacol*. 2003;23(1):35-41.

154. Vincent J-, Su F. Physiology and pathophysiology of the vasopressinergic system. *Best Pract Res Clin Anaesthesiol*. 2008;22(2):243-252.

155. Cottet M, Albizu L, Perkovska S, et al. Past, present and future of vasopressin and oxytocin receptor oligomers, prototypical GPCR models to study dimerization processes. *Curr Opin Pharmacol*. 2010;10(1):59-66.

156. Thibonnier M, Kilani A, Rahman M, et al. Effects of the nonpeptide V1vasopressin receptor antagonist SR49059 in hypertensive patients. *Hypertension*. 1999;34(6):1293-1300.

157. Loison S, Cottet M, Orcel H, et al. Selective fluorescent nonpeptidic antagonists for vasopressin V2 GPCR: Application to ligand screening and oligomerization assays. *J Med Chem*. 2012;55(20):8588-8602.

158. Terrillon S, Durroux T, Mouillac B, et al. Oxytocin and vasopressin V1a and V2 receptors form constitutive homo- and heterodimers during biosynthesis. *Mol Endocrinol*. 2003;17(4):677-691.

159. Chang Y-, Yang C-, Wang S-, Kao M-, Tsai P-, Huang C-. Vasopressin inhibits endotoxin binding in activated macrophages. *J Surg Res*. 2015;197(2):412-418.

160. Szmydynger-Chodobska J, Fox LM, Lynch KM, Zink BJ, Chodobski A. Vasopressin amplifies the production of proinflammatory mediators in traumatic brain injury. *J Neurotrauma*. 2010;27(8):1449-1461.

161. Michel MC, Wieland T, Tsujimoto G. How reliable are G-protein-coupled receptor antibodies? *Naunyn-Schmiedeberg's Arch Pharmacol*. 2009;379(4):385-388.

162. Berahovich RD, Penfold MET, Schall TJ. Nonspecific CXCR7 antibodies. *Immunol Lett*. 2010;133(2):112-114.

163. Böhmer T, Pfeiffer N, Gericke A. Three commercial antibodies against a1-adrenergic receptor subtypes lack specificity in paraffin-embedded sections of murine tissues. *Naunyn-Schmiedeberg's Arch Pharmacol*. 2014;387(7):703-706.

164. Hamdani N, Van Der Velden J. Lack of specificity of antibodies directed against human beta-adrenergic receptors. *Naunyn-Schmiedeberg's Arch Pharmacol*. 2009;379(4):403-407.

165. Jensen BC, Swigart PM, Simpson PC. Ten commercial antibodies for alpha-1-adrenergic receptor subtypes are nonspecific. *Naunyn-Schmiedeberg's Arch Pharmacol*. 2009;379(4):409-412.

166. Pradidarcheep W, Stallen J, Labruyère WT, Dabhoiwala NF, Michel MC, Lamers WH. Lack of specificity of commercially available antisera against muscarinergic and adrenergic receptors. *Naunyn-Schmiedeberg's Arch Pharmacol*. 2009;379(4):397-402.

167. Talmont F, Moulédous L, Boué J, Mollereau C, Dietrich G. Denatured G-protein coupled receptors as immunogens to generate highly specific antibodies. *PLoS ONE*. 2012;7(9).

168. Tripathi A, Gaponenko V, Majetschak M. Commercially available antibodies directed against a-adrenergic receptor subtypes and other G protein-coupled receptors with acceptable selectivity in flow cytometry experiments. *Naunyn-Schmiedeberg's Arch Pharmacol*. 2016;389(2):243-248.

169. Gambaryan N, Perros F, Montani D, et al. Targeting of c-kit+ haematopoietic progenitor cells prevents hypoxic pulmonary hypertension. *Eur Respir J*. 2011;37(6):1392-1399.

170. Sartina E, Suguihara C, Ramchandran S, et al. Antagonism of CXCR7 attenuates chronic hypoxia-induced pulmonary hypertension. *Pediatr Res*. 2012;71(6):682-688.

171. Kroeze WK, Sassano MF, Huang X-, et al. PRESTO-tango as an open-source resource for interrogation of the druggable human GPCRome. *Nat Struct Mol Biol*. 2015;22(5):362-369.

172. Hussain MB, Marshall I. Characterization of a1-adrenoceptor subtypes mediating contractions to phenylephrine in rat thoracic aorta, mesenteric artery and pulmonary artery. *Br J Pharmacol*. 1997;122(5):849-858.

173. Hussain MB, Marshall I. A1-adrenoceptor subtypes mediating contractions of the rat mesenteric artery. *Eur J Pharmacol*. 2000;395(1):69-76.

174. Tarasov SG, Gaponenko V, Howard OMZ, et al. Structural plasticity of a transmembrane peptide allows self-assembly into biologically active nanoparticles. *Proc Natl Acad Sci U S A*. 2011;108(24):9798-9803.

175. Hebert TE, Moffett S, Morello J-, et al. A peptide derived from a ß 2-adrenergic receptor transmembrane domain inhibits both receptor dimerization and activation. *J Biol Chem*. 1996;271(27):16384-16392.

176. Tarasova NI, Rice WG, Michejda CJ. Inhibition of G-protein-coupled receptor function by disruption of transmembrane domain interactions. *J Biol Chem*. 1999;274(49):34911-34915.

177. Proost P, Schutyser E, Menten P, et al. Amino-terminal truncation of CXCR3 agonists impairs receptor signaling and lymphocyte chemotaxis, while preserving antiangiogenic properties. *Blood*. 2001;98(13):3554-3561.

178. Proost P, Mortier A, Loos T, et al. Proteolytic processing of CXCL11 by CD13/aminopeptidase N impairs CXCR3 and CXCR7 binding and signaling and reduces lymphocyte and endothelial cell migration. *Blood*. 2007;110(1):37-44.

179. Milligan G, Bouvier M. Methods to monitor the quaternary structure of G protein-coupled receptors. *FEBS J*. 2005;272(12):2914-2925.

180. Martinez-Pinilla E, Rodriguez-Perez AI, Navarro G, et al. Dopamine D2 and angiotensin II type 1 receptors form functional heteromers in rat striatum. *Biochem Pharmacol*. 2015;96(2):131-142.

181. Pfeiffer M, Kirscht S, Stumm R, et al. Heterodimerization of substance P and mu-opioid receptors regulates receptor trafficking and resensitization. *J Biol Chem*. 2003;278(51):51630-51637.

182. Chernow B, Rainey TG, Lake CR. Endogenous and exogenous catecholamines in critical care medicine. *Crit Care Med*. 1982;10(6):409-416.

183. Altara R, Manca M, Brandão RD, Zeidan A, Booz GW, Zouein FA. Emerging importance of chemokine receptor CXCR3 and its ligands in cardiovascular diseases. *Clin Sci*. 2016;130(7):463-478.

184. Cai X, Bai B, Zhang R, Wang C, Chen J. Apelin receptor homodimeroligomers revealed by singlemolecule imaging and novel G protein-dependent signaling. *Sci Rep*. 2017;7.

185. Gaitonde SA, González-Maeso J. Contribution of heteromerization to G protein-coupled receptor function. *Curr Opin Pharmacol*. 2017;32:23-31.

186. Kasai RS, Suzuki KGN, Prossnitz ER, et al. Full characterization of GPCR monomer-dimer dynamic equilibrium by single molecule imaging. *J Cell Biol*. 2011;192(3):463-480.

187. Vischer HF, Castro M, Pin J-. G protein-coupled receptor multimers: A question still open despite the use of novel approaches. *Mol Pharmacol*. 2015;88(3):561-571.

188. Bouvier M. Oligomerization of G-protein-coupled transmitter receptors. *Nat Rev Neurosci*. 2001;2(4):274-286.

189. Ciruela F, Burgueño J, Casadó V, et al. Combining mass spectrometry and pull-down techniques for the study of receptor heteromerization. direct epitope-epitope electrostatic interactions between adenosine A2A and dopamine D2 receptors. *Anal Chem*. 2004;76(18):5354-5363.

190. Filizola M, Weinstein H. The study of G-protein coupled receptor oligomerization with computational modeling and bioinformatics. *FEBS J*. 2005;272(12):2926-2938.

191. Hern JA, Baig AH, Mashanov GI, et al. Formation and dissociation of M1 muscarinic receptor dimers seen by total internal reflection fluorescence imaging of single molecules. *Proc Natl Acad Sci U S A*. 2010;107(6):2693-2698.

192. Watanabe K, Penfold MET, Matsuda A, et al. Pathogenic role of CXCR7 in rheumatoid arthritis. *Arthritis Rheum*. 2010;62(11):3211-3220.

193. Cao Y, Xie K-, Zhu X-. The enhancement of dopamine D1 receptor desensitization by adenosine A1 receptor activation. *Eur J Pharmacol*. 2007;562(1-2):34-38.

194. Yabuuchi K, Kuroiwa M, Shuto T, et al. Role of adenosine A1 receptors in the modulation of dopamine D1 and adenosine A2A receptor signaling in the neostriatum. *Neuroscience*. 2006;141(1):19-25.

195. Le Crom S, Prou D, Vernier P. Autocrine activation of adenosine A1 receptors blocks D1A but not D1B dopamine receptor desensitization. *J Neurochem*. 2002;82(6):1549-1552.

196. Zhang YQ, Limbird LE. Hetero-oligomers of a2A-adrenergic and μ-opioid receptors do not lead to transactivation of G-proteins or altered endocytosis profiles. *Biochem Soc Trans*. 2004;32(5):856-860.

197. Wigdor S, Wilcox GL. Central and systemic morphine-induced antinociception in mice: Contribution of descending serotonergic and noradrenergic pathways. *J Pharmacol Exp Ther*. 1987;242(1):90-95.

198. Stone LS, MacMillan LB, Kitto KF, Limbird LE, Wilcox GL. The a(2a) adrenergic receptor subtype mediates spinal analgesia evoked by a2 agonists and is necessary for spinal adrenergic-opioid synergy. *J Neurosci*. 1997;17(18):7157-7165.

199. Kent T, McAlpine C, Sabetnia S, Presland J. G-protein-coupled receptor heterodimerization: Assay technologies to clinical significance. *Curr Opin Drug Discov Dev*. 2007;10(5):580-589.

200. González S, Rangel-Barajas C, Peper M, et al. Dopamine D 4 receptor, but not the ADHD-associated D 4.7 variant, forms functional heteromers with the dopamine D 2S receptor in the brain. *Mol Psychiatry*. 2012;17(6):650-662.

201. Ballesteros JA, Jensen AD, Liapakis G, et al. Activation of the ß2-adrenergic receptor involves disruption of an ionic lock between the cytoplasmic ends of transmembrane segments 3 and 6. *J Biol Chem*. 2001;276(31):29171-29177.

202. Jastrzebska B, Chen Y, Orban T, Jin H, Hofmann L, Palczewski K. Disruption of rhodopsin dimerization with synthetic peptides targeting an interaction interface. *J Biol Chem*. 2015;290(42):25728-25744.

203. Gurevich VV, Gurevich EV. How and why do GPCRs dimerize? *Trends Pharmacol Sci*. 2008;29(5):234-240.

204. Panetta R, Greenwood MT. Physiological relevance of GPCR oligomerization and its impact on drug discovery. *Drug Discov Today*. 2008;13(23-24):1059-1066.

205. Cotecchia S, Fanelli F, Costa T. Constitutively active G protein-coupled receptor mutants: Implications on receptor function and drug action. *Assay Drug Dev Technol*. 2003;1(2):311-316.

206. Jordan BA, Trapaidze N, Gomes I, Nivarthi R, Devi LA. Oligomerization of opioid receptors with ß2-adrenergic receptors: A role in trafficking and mitogen-activated protein kinase activation. *Proc Natl Acad Sci U S A*. 2001;98(1):343-348.

207. Griffiths PD, Sambrook MA, Perry R, Crossman AR. Changes in benzodiazepine and acetylcholine receptors in the globus pallidus in parkinson's disease. *J Neurol Sci*. 1990;100(1-2):131-136.

208. Jansen KLR, Faull RLM, Dragunow M, Synek BL. Alzheimer's disease: Changes in hippocampal N-methyl-d-aspartate, quisqualate, neurotensin, adenosine, benzodiazepine, serotonin and opioid receptors-an autoradiographic study. *Neuroscience*. 1990;39(3):613-627.

209. Rajput PS, Kharmate G, Norman M, et al. Somatostatin receptor 1 and 5 double knockout mice mimic neurochemical changes of huntington's disease transgenic mice. *PLoS ONE*. 2011;6(9).

210. Simón AM, De Maturana RL, Ricobaraza A, et al. Early changes in hippocampal eph receptors precede the onset of memory decline in mouse models of alzheimer's disease. *J Alzheimer's Dis*. 2009;17(4):773-786.

211. Takekoshi T, Ziarek JJ, Volkman BF, Hwang ST. A locked, dimeric CXCL12 variant effectively inhibits pulmonary metastasis of CXCR4-expressing melanoma cells due to enhanced serum stability. *Mol Cancer Ther*. 2012;11(11):2516-2525.

212. Veldkamp CT, Seibert C, Peterson FC, et al. Structural basis of CXCR4 sulfotyrosine recognition by the chemokine SDF-1/CXCL12. *Sci Signal*. 2008;1(37).

VITA

Lauren J. Albee was born in Chicago, IL on November 20, 1983. She attended Bradley University in Peoria, IL where she earned her Bachelor of Science, *cum laude*, in Cellular and Molecular Biology in May 2008. Following her graduation from Bradley University, Lauren moved to London, UK to start her postgraduate studied in Human and Applied Physiology at King's College London. She earned her Masters of Science with Merit in October 2009. After completion of her M.Sc., she returned to Chicago, IL to work and continue her education.

Lauren entered the Integrated Program in Biomedical Sciences at Loyola University Chicago, Stritch School of Medicine in August 2013. In the fall of her second year at Loyola, Lauren joined the Integrative Cell Biology track.

Lauren's work on G protein-coupled receptor heteromerization identified and validated two native hetero-oligomeric complexes that exist in vascular smooth muscle cells. She published multiple manuscripts and presented her work at international conferences during this period. After completion of her graduate studies, Lauren and her beloved dogs, Coco Chanel and Kate Spade, will move back to London, UK to pursue a postdoctoral fellowship in the laboratory of Professor Michael Shattock at King's College London. She will study the role of the Na^+/K^+ ATPase in heart failure and hypertension.